USGS
science for a changing world

# Hydrologic Monitoring and Selected Hydrologic and Environmental Studies by the U.S. Geological Survey in Georgia, 2011–2013

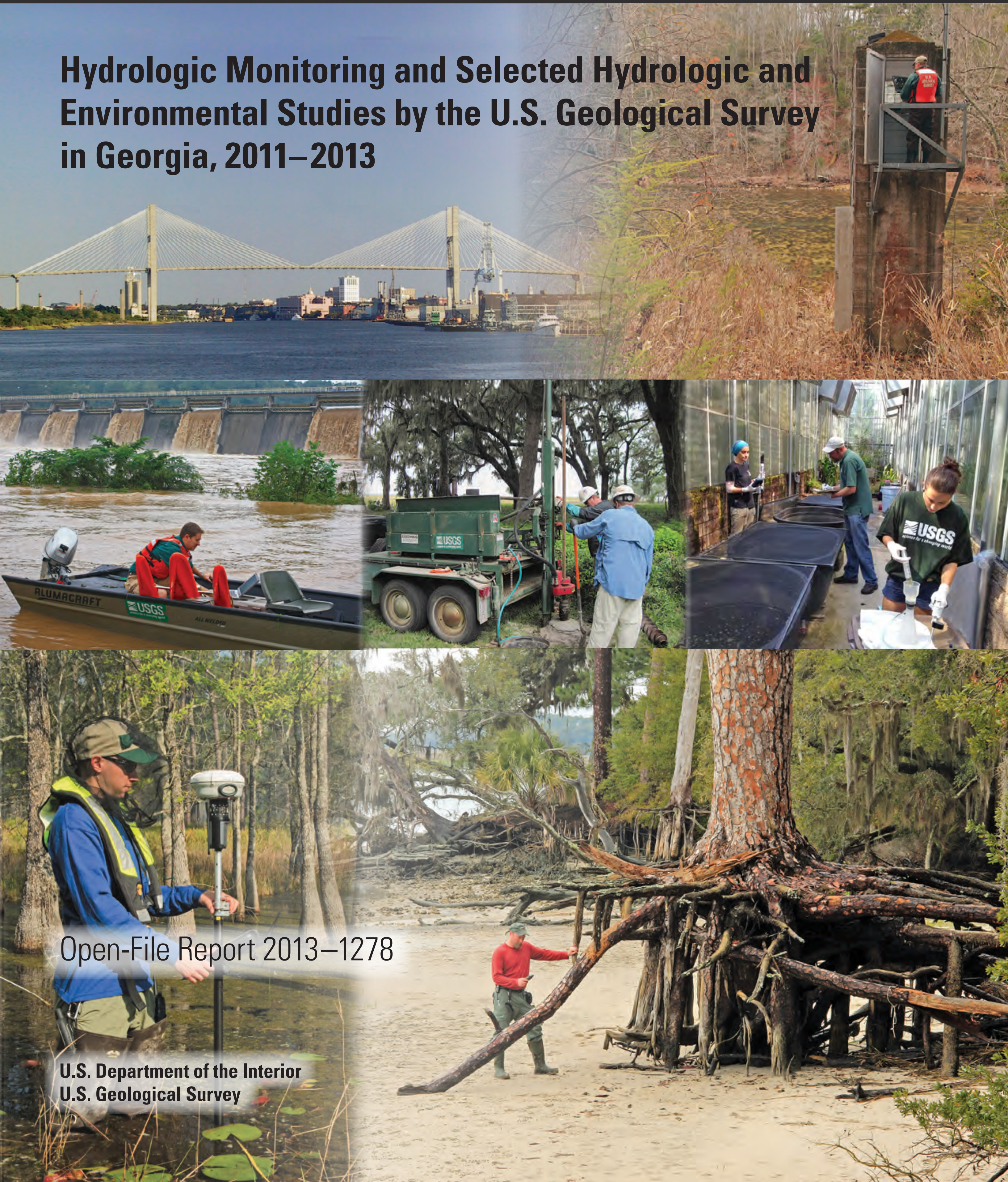


Open-File Report 2013–1278

U.S. Department of the Interior
U.S. Geological Survey

## Foreword

This compendium of papers describes results of hydrologic monitoring and hydrologic and environmental studies completed by the U.S. Geological Survey (USGS) in Georgia during 2011–2013. The USGS addresses a wide variety of water issues in the State of Georgia working with local, State, and Federal partners. As the primary Federal science agency for water resource information, the USGS monitors the quantity and quality of water in the Nation's rivers and aquifers, assesses the sources and fate of contaminants in aquatic systems, collects and analyzes data on aquatic ecosystems, develops tools to improve the application of hydrologic information, and ensures that its information and tools are available to all potential users.

During 2011–2013, the USGS continued a long-term program of monitoring stream and groundwater resources, including flow, water quality, and water use. In addition, a variety of hydrologic and environmental studies were completed to assess water availability, hydrologic hazards, and the impact of development on water resources. Information on USGS activities in Georgia is available online at *http://ga.water.usgs.gov/*.

**Cover.** All photographs by Alan M. Cressler, USGS, unless noted otherwise.

Top row: left, Talmadge Memorial Bridge, Savannah, Georgia (Edward H. Martin, USGS); right, USGS gaging station, Chattooga National Wild and Scenic River, Chattahoochee and Sumter National Forests, Georgia and South Carolina.

Middle row: left, Morgan Falls Dam, Chattahoochee River, Fulton and Cobb Counties, Georgia; middle, hydrologic technicians installing a well into the surficial aquifer, Jekyll Island, Glynn County, Georgia (John S. Clarke, USGS); right, collecting water samples from *Lithobates capito* tadpole-rearing tanks at the Atlanta Botanical Gardens, Atlanta, Georgia.

Bottom row: left, Global positioning system (GPS) surveying, Talpoideum Pond, St. Marks National Wildlife Refuge, Wakulla County, Florida; right, coastal erosion, Brickhill Bluff, Brickhill River, Cumberland Island National Seashore, Camden County, Georgia.

# Hydrologic Monitoring and Selected Hydrologic and Environmental Studies by the U.S. Geological Survey in Georgia, 2011–2013

By John S. Clarke and Melinda J. Dalton, compilers

Open-File Report 2013–1278

**U.S. Department of the Interior**
**U.S. Geological Survey**

**U.S. Department of the Interior**
SALLY JEWELL, Secretary

**U.S. Geological Survey**
Suzette M. Kimball, Acting Director

U.S. Geological Survey, Reston, Virginia: 2013

For more information on the USGS—the Federal source for science about the Earth, its natural and living resources, natural hazards, and the environment, visit http://www.usgs.gov or call 1–888–ASK–USGS.

For an overview of USGS information products, including maps, imagery, and publications, visit http://www.usgs.gov/pubprod

To order this and other USGS information products, visit http://store.usgs.gov



Suggested citation:
Clarke, J.S., and Dalton, M.J., compilers, Hydrologic monitoring and selected hydrologic and environmental studies by the U.S. Geological Survey in Georgia, 2011–2013: U.S. Geological Survey Open-File Report 2013–1278, 73 p., *http://dx.doi.org/10.3133/ofr20131278*.

ISSN 2331-1258 (online)

# Contents

# Conversion Factors

Inch/Pound to SI

| Multiply | By | To obtain |
|---|---|---|
| | Length | |
| inch | 2.54 | centimeter (cm) |
| inch | 25.4 | millimeter (mm) |
| foot (ft) | 0.3048 | meter (m) |
| mile (mi) | 1.609 | kilometer (km) |
| | Area | |
| square mile ($mi^2$) | 259.0 | hectare (ha) |
| square mile ($mi^2$) | 2.590 | square kilometer ($km^2$) |
| | Volume | |
| gallon (gal) | 3.785 | liter (L) |
| gallon (gal) | 0.003785 | cubic meter ($m^3$) |
| gallon (gal) | 3.785 | cubic decimeter ($dm^3$) |
| | Flow rate | |
| cubic foot per second ($ft^3/s$) | 0.02832 | cubic meter per second ($m^3/s$) |
| gallon per minute (gal/min) | 0.06309 | liter per second (L/s) |
| gallon per day (gal/d) | 0.003785 | cubic meter per day ($m^3/d$) |
| million gallons per day (Mgal/d) | 0.04381 | cubic meter per second ($m^3/s$) |
| | Transmissivity* | |
| foot squared per day ($ft^2/d$) | 0.09290 | meter squared per day ($m^2/d$) |

SI to Inch/Pound

| Multiply | By | To obtain |
|---|---|---|
| | Length | |
| micometer (µm) | 0.00003937 | inch (in.) |
| millimeter (mm) | 0.03937 | inch (in.) |
| meter (m) | 3.281 | foot (ft) |
| | Pressure | |
| hectopascal (hPa) | 0.0009869 | atmosphere, standard (atm) |
| hectopascal (hPa) | 0.01450 | pound-force per inch (lbf/in) |
| hectopascal (hPa) | 0.001 | bar |

Temperature in degrees Celsius (°C) may be converted to degrees Fahrenheit (°F) as follows:

$$°F = (1.8 \times °C) + 32$$

Temperature in degrees Fahrenheit (°F) may be converted to degrees Celsius (°C) as follows:

$$°C = (°F - 32) / 1.8$$

Vertical coordinate information is referenced to the North American Vertical Datum of 1988 (NAVD 88) or National Geodetic Vertical Datum of 1928 (NGVD 29)

*Transmissivity: The standard unit for transmissivity is cubic foot per day per square foot times foot of aquifer thickness [($ft^3/d$)/$ft^2$]ft. In this report, the mathematically reduced form, foot squared per day ($ft^2/d$), is used for convenience.

Specific conductance is given in microsiemens per centimeter at 25 degrees Celsius (µS/cm at 25 °C).

Concentrations of chemical constituents in water are given either in milligrams per liter (mg/L) or micrograms per liter (µg/L).

## Abbreviations

| | |
|---|---|
| ACF | Apalachicola–Chattahoochee–Flint |
| AHPS | Advanced Hydrologic Prediction Service |
| ASO | Aucilla–Suwannee–Ochlockonee |
| CCSM3 | Community Climate System Model version 3 |
| CSC | Climate Science Center |
| DEM | digital elevation model |
| DNA | deoxyribonucleic acid |
| DO | dissolved oxygen |
| eDNA | environmental deoxyribonucleic acid |
| FIM | Flood-Inundation Mapper |
| GaWSC | Georgia Water Science Center |
| GaEPD | Georgia Department of Natural Resources Environmental Protection Division |
| GCM | Global Climate Model |
| GDP | Geo Data Portal |
| GFDL | Geophysical Fluid Dynamics Laboratory |
| GPS | global positioning system |
| HAAF | Hunter Army Airfield |
| HRU | hydrologic response unit |
| Lidar | light-detection and ranging |
| LFA | Lower Floridan aquifer |
| LFCU | Lower Floridan confining unit |
| MBES | multibeam echosounder |
| NCCWSC | National Climate Change and Wildlife Science Center |
| NWI | National Wetland Inventory |
| NWIS | National Water Information System |
| NWS | National Weather Service |
| PCM | Parallel Climate Model |
| PEEP | photoelectric bank pin |
| PRMS | Precipitation-Runoff Modeling System |
| qPCR | quantitative polymerase chain reaction |
| RTK | real-time kinematic |
| SBES | single beam echo sounder |
| SERAP | Southeast Regional Assessment Project |
| SHEP | Savannah Harbor Expansion Project |
| SMNWR | St. Marks National Wildlife Refuge |
| SNTemp | Stream Network Temperature model |
| TPI | Topographic Position Index |
| UFA | Upper Floridan aquifer |
| USACE | U.S. Army Corps of Engineers |
| USGS | U.S. Geological Survey |
| WY | water year |

# USGS Long-Term Hydrologic Monitoring in Support of the Savannah Harbor Expansion Project

By Brian E. McCallum

## Abstract

The U.S. Geological Survey (USGS) has been requested by the U.S. Army Corps of Engineers (USACE)-Savannah District to install and operate a hydrologic and water-quality monitoring network within the Savannah River estuary starting in October 2013 in support of the expected Savannah Harbor Expansion Project (SHEP). The intent of the SHEP is to deepen the shipping channel by 5 feet to a new depth of 47 feet, which would allow super-cargo container ships to use the Port of Savannah. After years of monitoring and analyses by a diverse group of Federal, State, and local stakeholders, the primary concern about the project is the consequent potential for increased salinity encroachment, which may damage fragile ecosystems, threaten public water intakes, and decrease the dissolved oxygen levels within the Savannah River.

The SHEP hydrologic and water-quality monitoring network would involve the installation of five new stations with tidal discharge and continuous water-quality instruments and the upgrade of eight existing stations to an equivalent data instrument array (fig. 1).

The hydrologic monitoring is designed to occur in three phases of channel construction: a 1-year pre-construction phase, a 4-year construction phase, and a 10-year post-construction phase. A subset of the proposed locations would continue to be operated well beyond the project timeframe. Additionally, a chloride warning network will be installed to protect the public drinking-water intakes in the upper Savannah River estuary. All data will be available in real-time on the USGS National Water Information System Web Interface (NWISWeb; *http://waterdata.usgs.gov*) and will also be provided to the SHEP database managed by the USACE for frequent modeling updates.

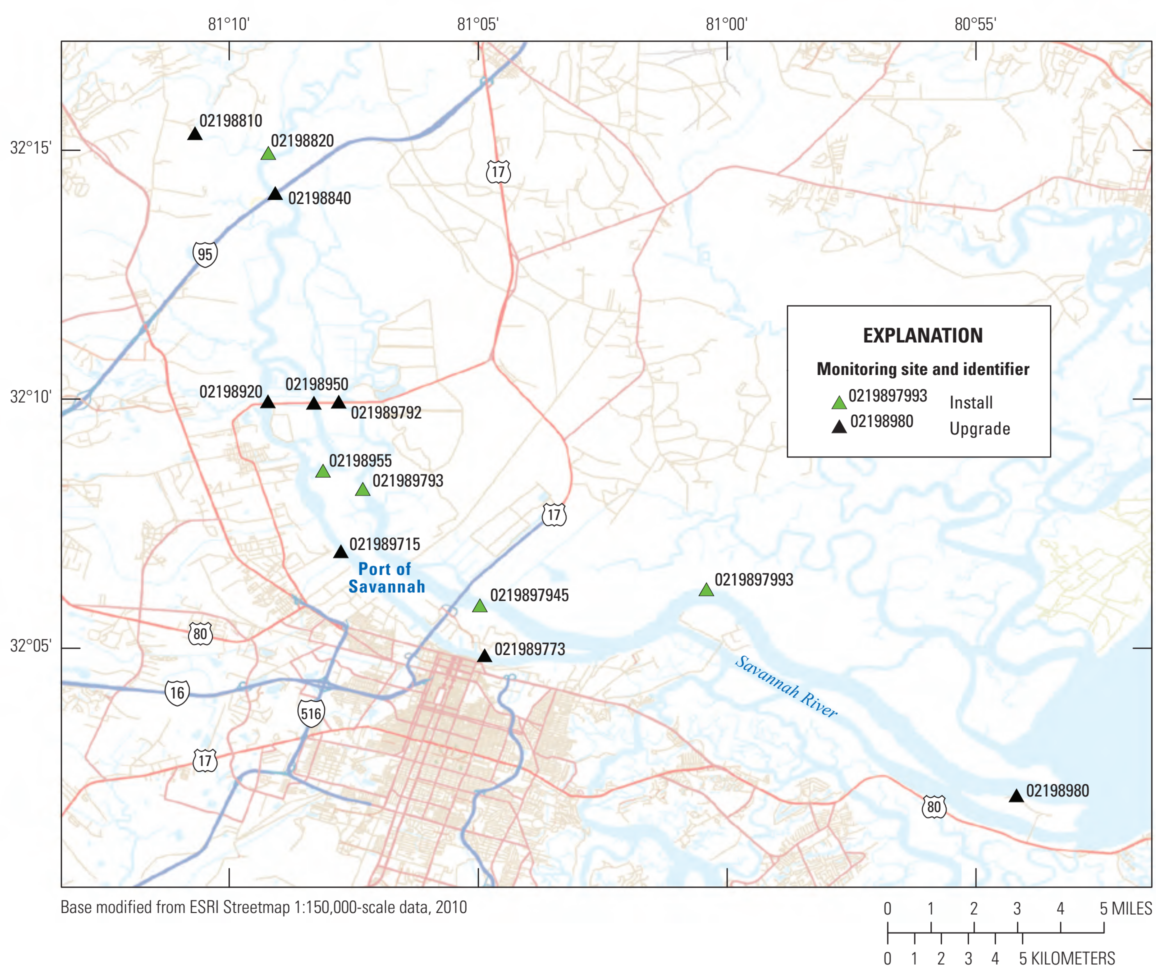


**Figure 1.** The Savannah Harbor Expansion Project (SHEP) Monitoring Network.

# Access to Flood-Inundation Information for Georgia Using Interactive Websites

By Jonathan W. Musser

## Abstract

Interactive websites and digital maps of flood inundation for select areas in Georgia are available on sites hosted by the U.S. Geological Survey (USGS) and the National Weather Service (NWS). The USGS Georgia Water Science Center (GaWSC) has been modeling and mapping flood inundation in Georgia since 1994. The mapped and modeled areas to date include the Flint River in Albany, Peachtree Creek in Atlanta, Sweetwater Creek in Cobb and Douglas Counties, and Suwanee Creek in Gwinnett County (fig. 1). Flood-inundation maps are posted on the NWS Advanced Hydrologic Prediction Service (AHPS) website (*http://water.weather.gov/ahps/forecasts.php*) and on the USGS Flood-Inundation Mapper (FIM) website (*http://wim.usgs.gov/FIMI/FloodInundationMapper.html*). The inundation maps provide water-surface elevations in relation to the North American Vertical Datum of 1988 (NAVD 88) and show flood extent and water depths so emergency managers and the public can see and prepare for potential flooding.

The NWS AHPS flood-inundation website has background map images obtained from the Google Maps satellite with multiple zoom levels. Water depth is color coded in shades of blue, and the transparency level can be modified. Additional gage information, such as flood categories, flood-impact statements, and forecasts can be obtained at this site. Other tabbed information available at this website include Hydrograph, River at a Glance, Download, Weekly Chance of Exceeding Levels, and Chance of Exceeding Levels During Entire Period.

The USGS FIM website shows flood-inundated areas on a choice of backgrounds (street map, satellite imagery with labels, or topography) as well as additional information about the streamgaging location and the area(s) of inundation. Once a streamgage is selected, an information window is displayed that includes additional tabbed information the user may find helpful. The first tab is Flood Tools, which include one or two slide bars to set the gage height and elevation at the streamgage(s). The inundated area changes based on the streamgage heights. The second tab displays recent hydrograph(s) for the streamgage(s). The third tab provides access to the NWS prediction for the streamgage. The fourth tab provides access to the Federal Emergency Management Agency Hazus data for the site if it exists. The next two tabs show images from webcams, if they exist, and the final tab provides information about the site, including published reports. Other tools included with the FIM mapper are zoom history, latitude and longitude connected to the mouse pointer, a search engine, and additional layers which can be displayed, such as NWS radar, flood watches and (or) warnings, and AHPS forecast sites.

For the Flint River flood-inundation maps in Albany, users can view potential impacts of floods from modeled streamflow ranges from 52,500 cubic feet per second ($ft^3/s$) at a stage of 30.0 feet (ft) to 123,000 $ft^3/s$ at a stage of 43.0 ft (USGS streamgage 02352500; Musser and Dyar, 2007). This corresponds to water-surface elevations from 179.5 to 192.5 ft above NAVD 88. The stage of 30.0 ft is 1 ft below moderate flood stage (as established by the NWS), and the 43.0-ft stage is the peak measured stage, which resulted from rainfall associated with Tropical Storm Alberto in 1994. The information for the Flint River at Albany site is on the NWS AHPS website (fig. 2) and the USGS FIM website.

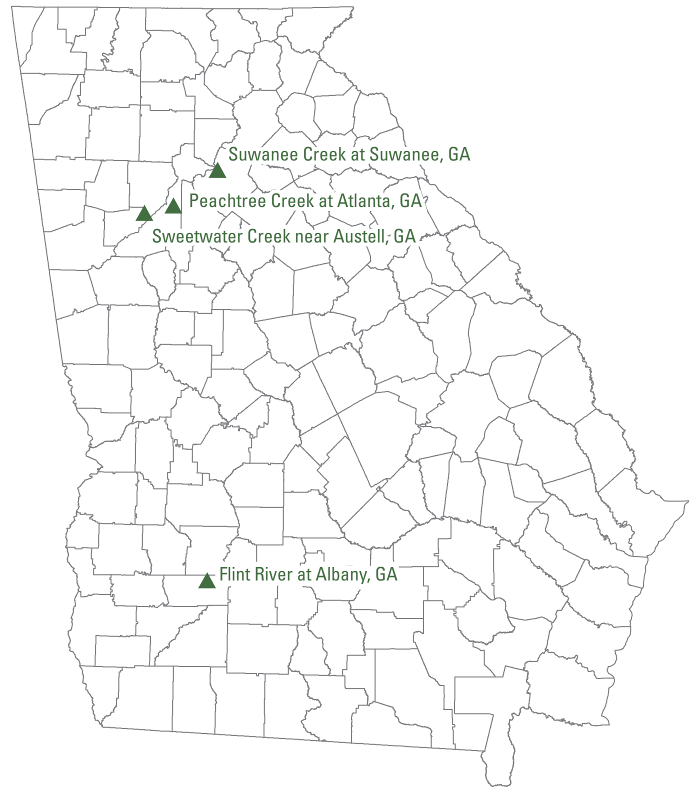


**Figure 1.** Locations of gages in Georgia with flood-inundation mapping.

For the Sweetwater Creek flood-inundation maps in Cobb and Douglas Counties, potential floods from modeled streamflow ranges from 4,430 $ft^3/s$ at a stage of 12.0 ft to 34,000 $ft^3/s$ at a stage of 32.0 ft near Austell (USGS streamgage 02337000; Musser, 2012c). This corresponds to water-surface elevations from 869.3 to 889.3 ft above NAVD 88. The 12.0-ft stage is 1 ft below moderate flood stage listed on the AHPS website. The peak discharge in September 2009 was estimated to be about 31,500 $ft^3/s$ at a stage of about 30.82 ft. Information for the streamgage at Sweetwater Creek near Austell is available on both the NWS AHPS and the USGS FIM websites.

For the Suwanee Creek flood-inundation maps in Gwinnett County, potential floods from modeled streamflow ranges from 800 $ft^3/s$ at a stage of 7.0 ft to 11,300 $ft^3/s$ at a stage of 16.0 ft at Suwanee (USGS streamgage 02334885; Musser, 2012b). This corresponds to water-surface elevations from 916.9 to 925.9 ft above NAVD 88. Flood stage at this streamgage is 8.0 ft. The maximum recorded discharge occurred in September 2009 at 7,870 $ft^3/s$ at a stage of about 14.30 ft. Information for the streamgage at Suwanee Creek at Suwanee is available on both the NWS AHPS and the USGS FIM websites.

For the Peachtree Creek flood-inundation maps in Atlanta, potential floods from modeled streamflow ranges from 5,000 $ft^3/s$ at a stage of 15.0 ft to 21,000 $ft^3/s$ at a stage of 24.0 ft (USGS streamgage 02336300). The 5,000-$ft^3/s$ flow corresponds to a water-surface elevation of 779.2 ft above NAVD 88 without backwater effects from the Chattahoochee River; this is the first flooding effect listed on the AHPS website that affects roads or homes. The 21,000-$ft^3/s$ streamflow is the maximum recorded and occurred in 1919; the corresponding water-surface elevation was 788.2 ft above NAVD 88 without backwater effects (Musser, 2012a). Inundation maps during periods of backwater effects from the Chattahoochee River are produced using a matrix of modeling results based on the water-surface elevation at the Chattahoochee River at GA 280, near Atlanta (USGS streamgage 02336490) and selected streamflows along Peachtree Creek. Because of the backwater effect, the Peachtree Creek at Atlanta site is available only on the USGS FIM website (fig. 3), which has two separate slide bars that allow the user to select the gage heights for Peachtree Creek and the Chattahoochee River.

## References

Musser, J.W., 2012a, Flood-inundation maps for Peachtree Creek from the Norfolk Southern Railway bridge to the Moores Mill Road NW bridge, Atlanta, Georgia: U.S. Geological Survey Scientific Investigations Map 3189, 9 p., 50 sheets, available online at *http://pubs.usgs.gov/sim/3189/*.

Musser, J.W., 2012b, Flood-inundation maps for Suwanee Creek from the confluence of Ivy Creek to the Noblin Ridge Drive bridge, Gwinnett County, Georgia: U.S. Geological Survey Scientific Investigations Map 3226, 8 p. pamphlet, 19 sheets; available online at *http://pubs.usgs.gov/sim/3226/*.

Musser, J.W., 2012c, Flood-inundation maps for Sweetwater Creek from above the confluence of Powder Springs Creek to the Interstate 20 bridge, Cobb and Douglas Counties, Georgia: U.S. Geological Survey Scientific Investigations Map 3220, 10 p. pamphlet, 21 sheets, available online at *http://pubs.usgs.gov/sim/3220/*.

Musser, J.W., and Dyar, T.R., 2007, Two-dimensional flood-inundation model of the Flint River at Albany, Georgia: U.S. Geological Survey Scientific Investigations Report 2007–5107, 49 p., available online at *http://pubs.usgs.gov/sir/2007/5107/sir2007-5107.pdf*.

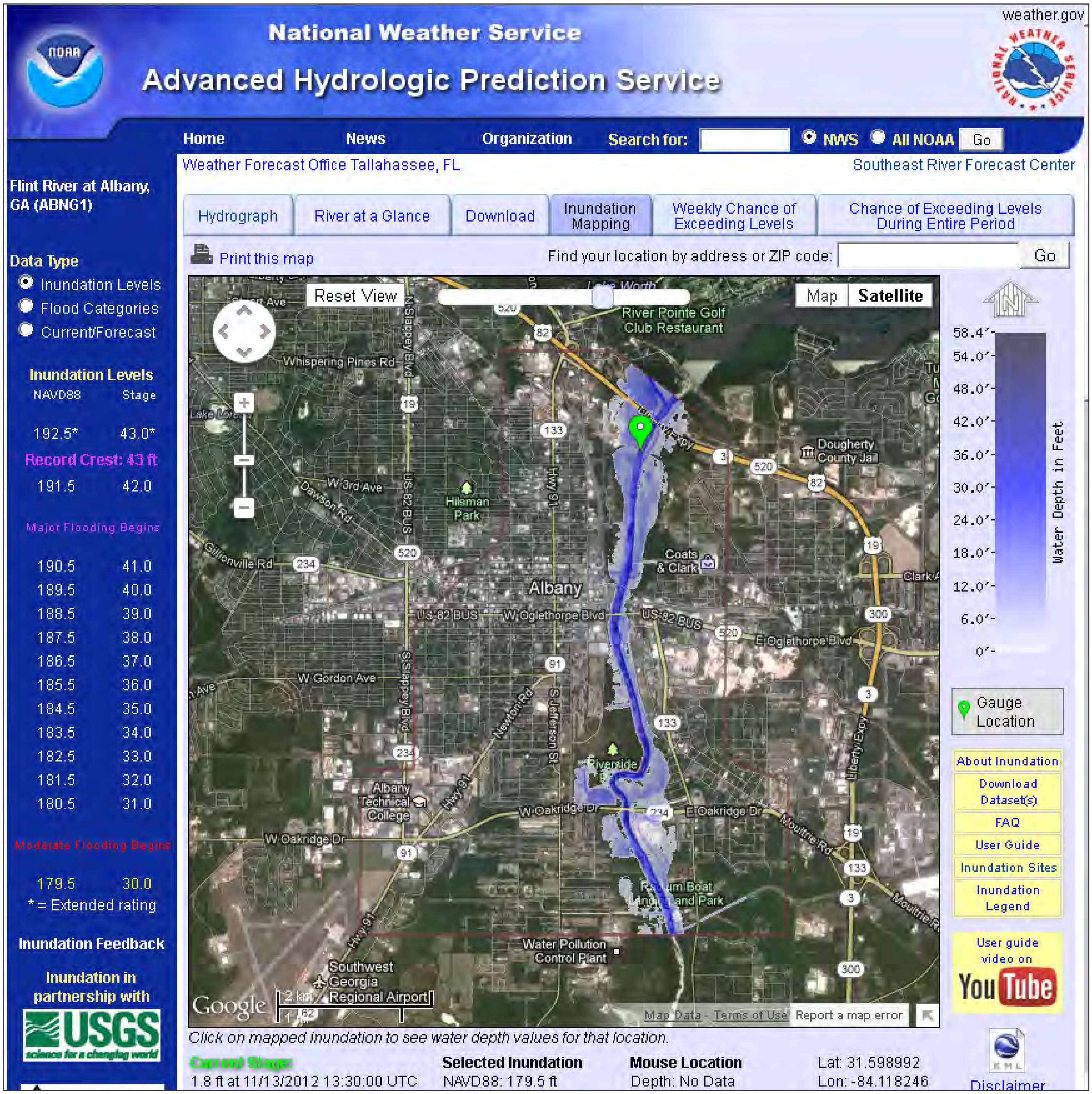


**Figure 2.** Screen capture of the National Weather Service Advanced Hydrologic Prediction Service website for Flint River at Albany, GA (ABNG1).

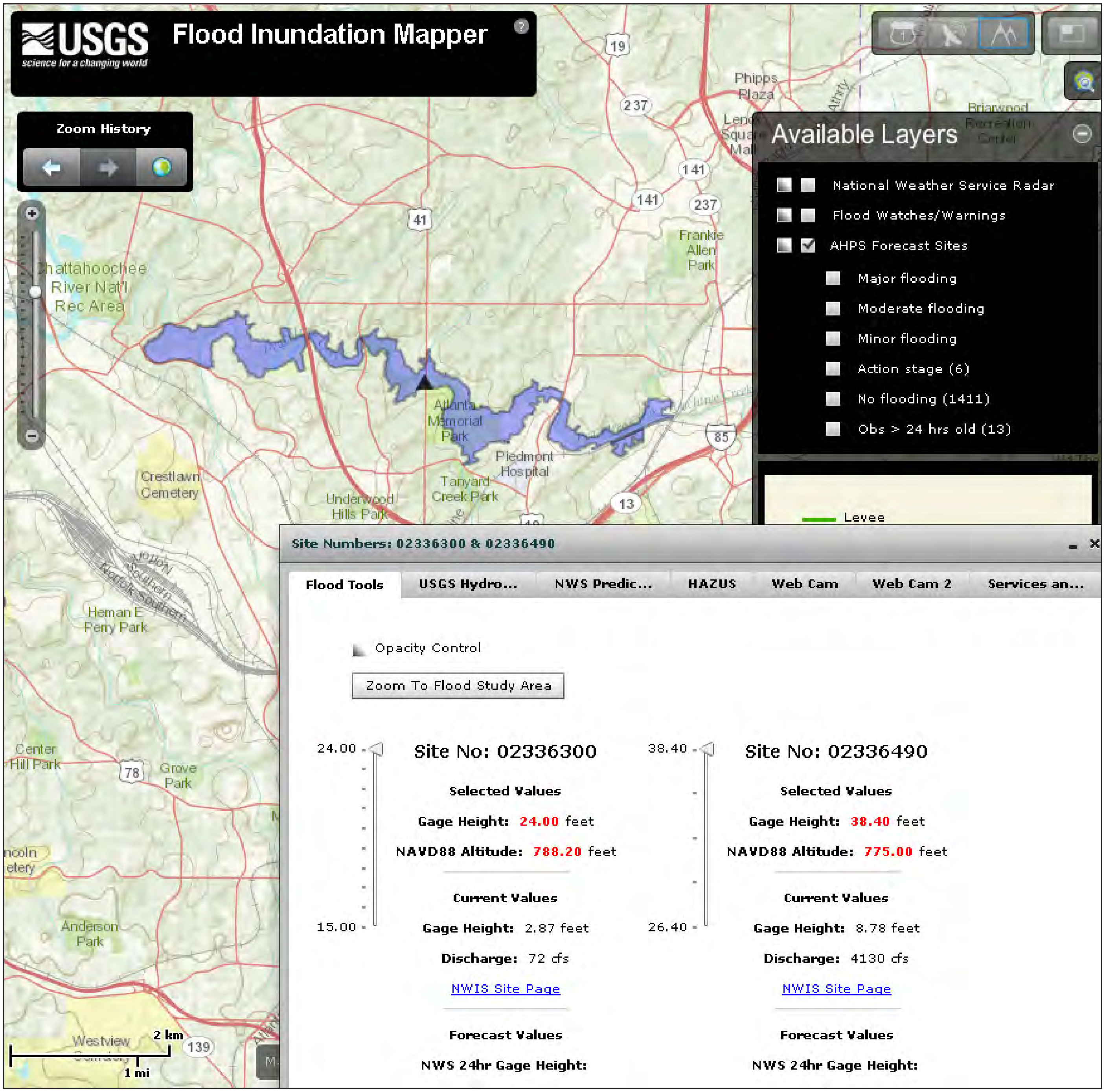


**Figure 3.** Screen capture of the USGS Flood-Inundation Mapper website for Peachtree Creek at Atlanta, GA (USGS streamgage 02336300).

# StreamStats—A Web-Based Tool for Estimating Streamflow Characteristics in Georgia

By Jaime A. Painter, Jonathan W. Musser, Anthony J. Gotvald

## Abstract

StreamStats is a Web-based geographic information system application developed by the U.S. Geological Survey (USGS), in cooperation with Environmental Systems Research Institute, Inc., to provide access to analytical tools for water-resources planning and management. StreamStats enables users to easily obtain streamflow statistics, basin characteristics, and descriptive information for USGS data-collection sites and selected ungaged sites (table 1). Users also can interactively select sites and receive information related to stream reaches upstream and downstream from a specified location, as well as potential activities within the basin that can affect streamflow conditions (fig. 1). These features are available through a map-based Web interface. StreamStats for each State is implemented as a separate application, relying on local partnerships for funding. The USGS is cooperating with the Georgia Department of Transportation and Georgia Environmental Protection Division to implement StreamStats for the State of Georgia.

**Table 1.** Basin characteristics and streamflow statistics available in StreamStats.

| Basin characteristics | Streamflow statistics |
|---|---|
| Drainage area (square mile) | 0.2-, 0.5-, 1-, 2-, 4-, 10-, 20-, 50- percent annual exceedance probability flood, determined through regression equations developed for both rural and urban basins by Gotvald and others (2009) and Gotvald and Knaak (2011) |
| Mean basin elevation (feet) | |
| Mean basin slope (percent) | |
| Mean channel slope (percent) | |
| Percent developed land | |
| Percent impervious | |
| Percent forested | |
| Mean annual precipitation (inches) | |
| Soil drainage index | |
| Hydrologic soils index | |

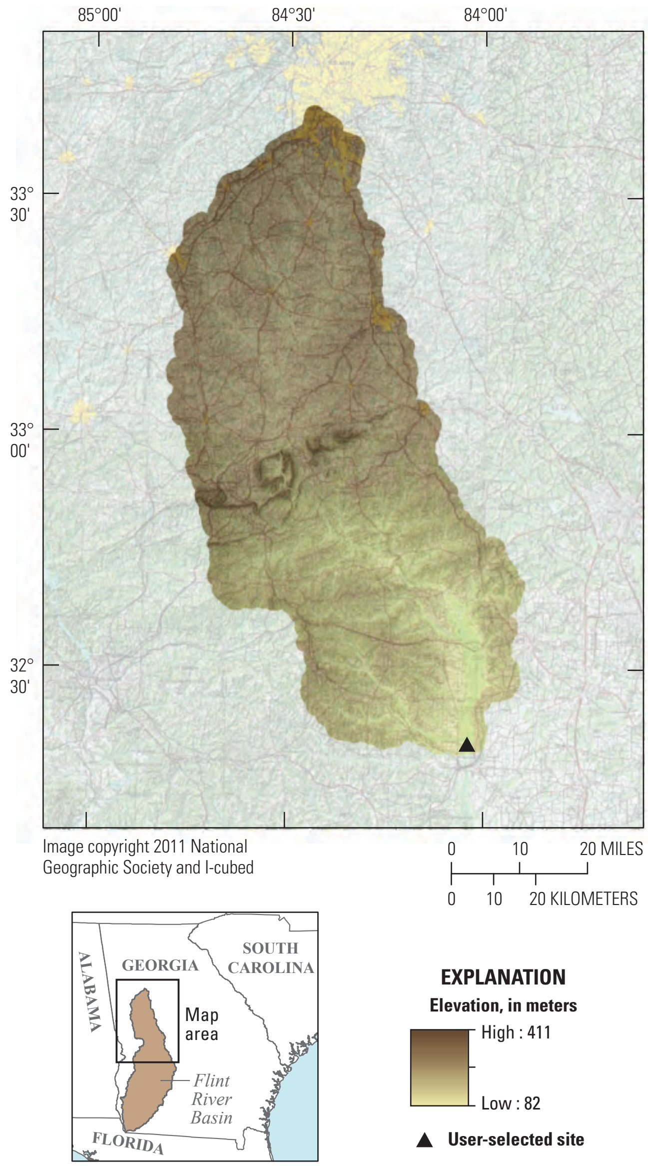


**Figure 1.** Identification of stream reaches upstream from a user-selected site in the Upper Flint River basin, Georgia.

## References

Gotvald, A.J., Feaster, T.D., and Weaver, J.C., 2009, Magnitude and frequency of rural floods in the southeastern United States, 2006—Volume 1, Georgia: U.S. Geological Survey Scientific Investigations Report 2009–5043, 120 p.

Gotvald, A.J., and Knaak, A.E., 2011, Magnitude and frequency of floods for urban and small rural streams in Georgia, 2008: U.S. Geological Survey Scientific Investigations Report 2011–5042, 39 p.

# Hydrologic Conditions in Georgia During the Extreme Drought of 2011

By Andrew E. Knaak, Eric R. Frantz, and Michael F. Peck

## Abstract

The United States Geological Survey (USGS) in cooperation with State, local, and other Federal agencies maintains a long-term hydrologic monitoring network of more than 320 real-time streamgages, including 10 real-time lake-level monitoring stations and 63 real-time water-quality monitors in Georgia. Additionally, the USGS operates more than 180 groundwater wells, 35 of which are real-time. Hydrologic conditions during water year (WY) 2011, a period of extreme drought, were determined by comparing the results of statistical analyses of the data collected during the current year to historical data collected over the long term. During 2011, several streamgages with 20 or more years of record experienced record low flows. Unconfined aquifers in the Georgia Climate Response Network also reflected dryer conditions as water levels generally remained below the historic median for most of the water year.

## Hydrologic Conditions During 2011

On August 31, 2011, the Office of the State Climatologist reported extreme drought conditions in almost all areas of Georgia south of the north Georgia mountains and that all counties in Georgia were classified as being in moderate, severe or extreme drought (Stooksbury, 2011). These drought conditions resulted in record low streamflow and groundwater levels throughout much of Georgia.

### Streamflow

Quarterly hydrologic conditions during the 2011 WY were summarized by comparing current to available historical data. The colors represent runoff (flow per unit area) as a percentile of long-term averages. Runoff was calculated for each basin and assumed to be uniform over the entire basin area. Only streamflow stations with a complete daily-flow dataset for the 2011 WY were used (U.S. Geological Survey, 2012b). For the first quarter of the 2011 WY (October–December 2010), much of the State was observing “below normal” and “much below normal” runoff conditions as a result of extreme temperatures and lack of precipitation during the preceding summer months of the 2010 WY (fig. 1*A*). Little to no precipitation kept the majority of the State in drought during the second and third quarter of the 2011 WY (figs. 1*B, C*). After receiving 50–75 percent of normal precipitation from central Georgia to Florida during the 2011 WY, the majority of the State was in an extreme drought during the fourth quarter as runoff was “much below normal,” and large areas of the State observed some of the lowest runoff conditions on record. (fig. 1*D*).

In 2011, new record-low monthly discharge occurred at 52 of 113 streamgages that have 20 or more years of data (fig. 2). These 52 streamgages are located throughout Georgia. Most of the State received lower-than-normal precipitation; from central Georgia to Florida the State received 50–75 percent of normal precipitation. Normal is defined as a 30-year average for 1971–2000. New record-low 7-day average discharge occurred at 24 of 113 streamgages that have 20 or more years of data in 2011. The majority of these streamgages were located in southern Georgia.

In south-central Georgia, the Ocmulgee River flows out of Jackson Lake and joins the Oconee River to form the Altamaha River (U.S. Geological Survey, 1975). The 7-day average streamflows were mostly in the normal range from October through March at streamgage 02213000 near Macon (fig. 3). After an extended period of lower-than-normal precipitation, streamflows were “much below normal” for the

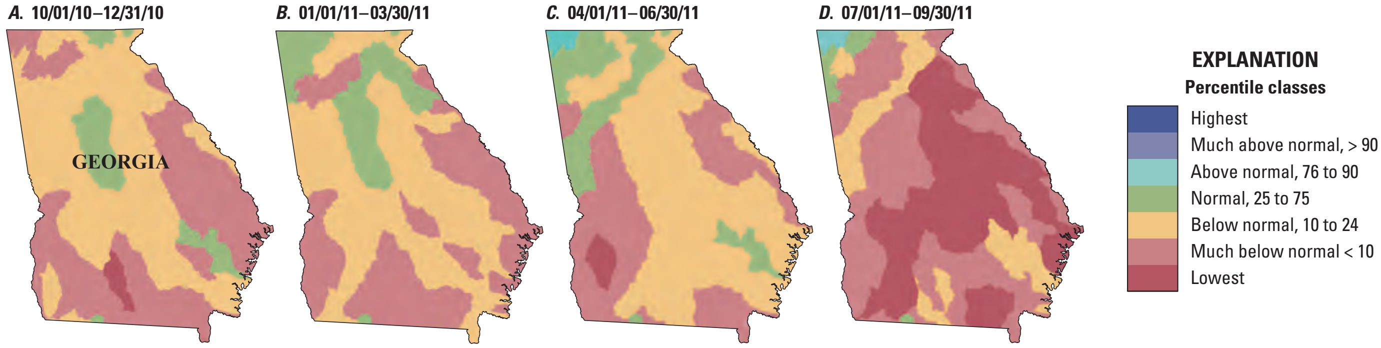


**Figure 1.** Quarterly hydrologic conditions in Georgia for 2011 WY, based on drainage basin runoff (modified from Knaak and others, 2013).

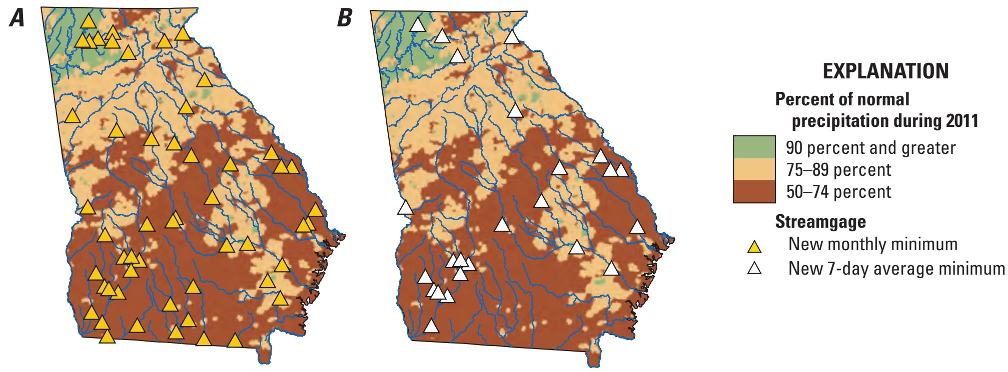


**Figure 2.** Percent of normal precipitation maps showing streamgaging sites with *(A)* new record-low monthly discharges and *(B)* new record-low 7-day discharges in Georgia streams during the 2011 WY (modified from Knaak and others, 2013).

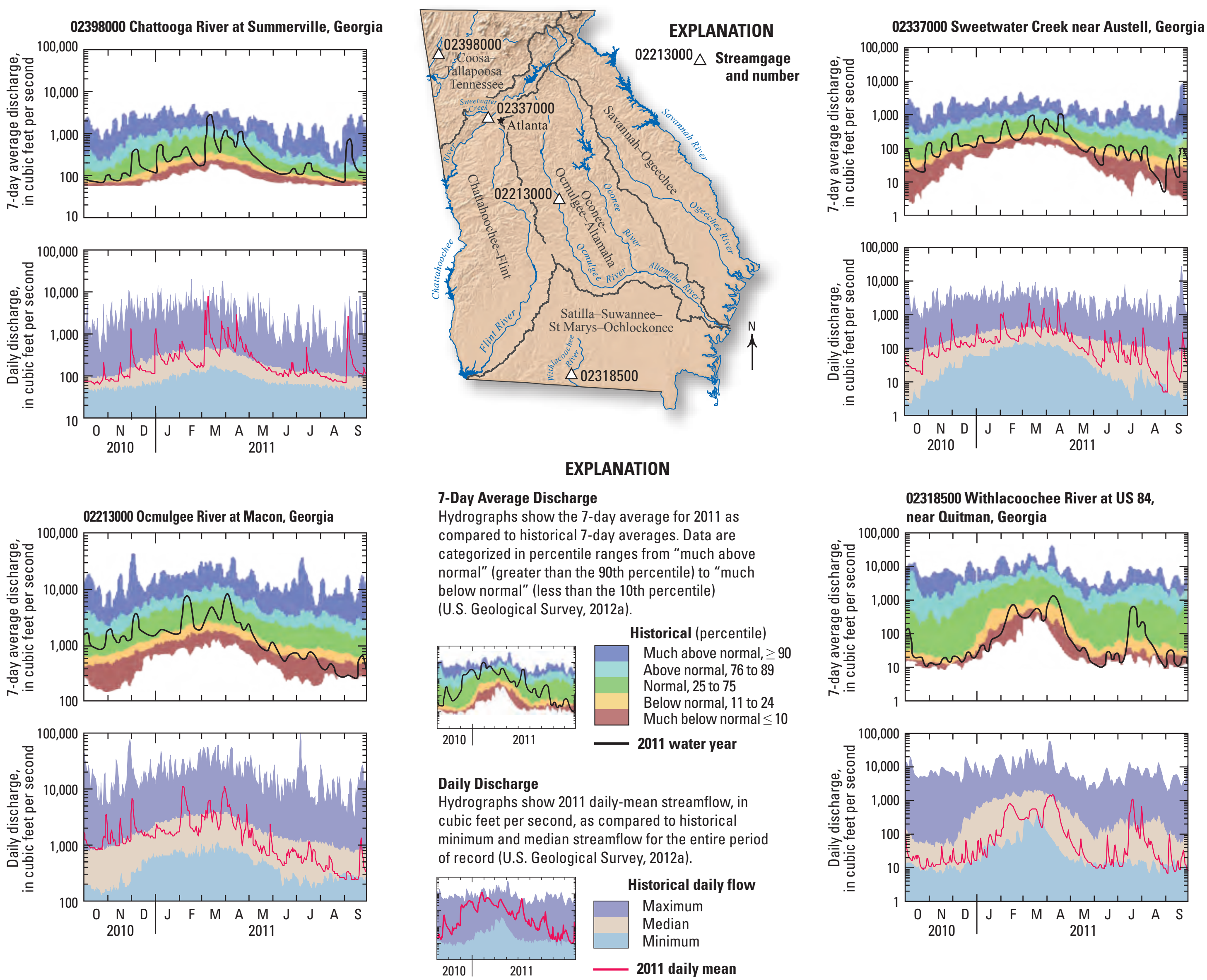


**Figure 3.** Daily discharge and 7-day average streamflow conditions, 2011 WY (modified from Knaak and others, 2013).

remainder of the 2011 WY and came close to setting new record lows. Daily discharge remained near historical median flows for most of the 2011 water year. Further south, the Withlacoochee River flows in the Ochlockonee River basin in the southern coastal plain of Georgia (U.S. Geological Survey, 1975). For most of the 2011 WY, 7-day average streamflow conditions at streamgage 02318500 near Quitman were "below normal" to "much below normal" and came close to the record low recorded in 1940. Several daily discharges reached new record lows during the months of January, May, June, July, August, and September.

In northern Georgia, Sweetwater Creek is a major tributary of the Chattahoochee River in the Atlanta metropolitan area (U.S. Geological Survey, 1975). The 7-day average streamflow at streamgage 02337000 near Austell fluctuated between "normal" and "much below normal" from October through April gradually declining to "much below normal" during the latter part of the 2011 WY as the area received 10–20 percent below-normal precipitation (fig. 3). Several daily discharges reached new record lows during the months of August and September. To the northwest, the Chattooga River flows in the northwestern corner of Georgia and into Alabama where it flows into Weiss Lake (U.S. Geological Survey, 1975). The northwestern corner of Georgia received 90–110 percent of normal precipitation in the 2011 WY. Daily discharge and 7-day average streamflow for the 2011 WY at station 02398000 near Summerville was predominately in the "normal" range.

## Groundwater

The USGS maintains a network of groundwater wells to monitor the effects of droughts and other climate variability on groundwater levels. These wells are part of the Climate Response Network, which is designed to measure the effects of climate on groundwater levels in unconfined aquifers or near-surface confined aquifers where pumping or other human influences on groundwater levels are minimal (U.S. Geological Survey, 2007, 2012a). Hydrographs for selected wells in the Climate Response Network with at least 5 years of continuous data demonstrate variations in groundwater levels during the year in different parts of the State (fig. 4). In the unconfined surficial aquifer of the Coastal Plain, well 07H003 demonstrates water levels in the southwestern part of the State and well 37P116 shows water levels in the southeastern part of the State. In northern Georgia, well 16MM03 shows water levels in the crystalline rock aquifer of the Blue Ridge and well 03PP01 shows water levels in the Paleozoic rock aquifer of the Valley and Ridge.

In the southwestern part of the State, the water level in well 07H003 generally rises rapidly during wet periods and declines slowly during dry periods in a similar manner as streamflow at the nearby streamgage on Ichawaynochaway Creek at Milford, Ga. (02353500). In the 2011 WY, water levels in well 07H003 were below the historical daily median for much of the year. For a brief period in January 2011, the daily mean water level fell below the historical daily minimum water level. To the southeast, along the coast, water levels in well 37P116 generally rise rapidly during wet periods and decline slowly during dry periods in a similar manner as streamflow at the nearby streamgage on Peacock Creek near McIntosh, Ga. (02203559). The water level in well 37P116 fluctuated above and below the historical daily minimum for most of the 2011 WY.

In the crystalline rock aquifer of northeastern Georgia groundwater is stored in the regolith and fractures, and the water level is affected by precipitation and evapotranspiration (Cressler and others, 1983). Precipitation can cause a rapid water-level rise in wells tapping aquifers overlain by thin regolith (Peck and others, 2011). The water level in well 16MM03 responds to seasonal change similarly to streamflow at the nearby streamgage on Chattahoochee River at Helen, Ga. (02330450), which indicates atmospheric, surface-water, and groundwater interactions. The water level in well 16MM03 remained below the historical daily median for much of the 2011 WY. To the northwest in the Paleozoic rock aquifer, groundwater storage is in the regolith, primary openings, and secondary fractures and solution openings in rock (Peck and others, 2011). Water levels are influenced mainly by precipitation and local pumping (Cressler, 1964). The water level in well 03PP01 responds to seasonal change similarly to stream-flow at the nearby streamgage on Lookout Creek near New England, Ga. (03568933), which indicates atmospheric, surface-water, and groundwater interactions. The water level in well 03PP01 was near the historical daily median for much of the 2011 WY.

## Lakes and Reservoirs

Major lakes and reservoirs throughout Georgia are managed primarily by the U.S. Army Corps of Engineers and Georgia Power Company to provide water for public and industrial use, flood protection, power generation, wildlife management, and recreation. Graphs showing lake stage, and water inflows and outflows from selected reservoirs in the northern half of Georgia demonstrate the effects of drought on reservoir storage (fig. 5).

Lake Sidney Lanier on the Chattahoochee River is the primary drinking-water source for the Atlanta metropolitan area. Lake Sidney Lanier is the most upstream reservoir in a series of reservoirs that include West Point Lake, Walter F. George Lake, and Lake Seminole. Lake Lanier had 24 percent more outflow than inflow during the 2011 WY, and the lake elevation fell nearly 10 feet from April through September. West Point Dam provides flood protection and hydroelectric power to Troup County. The water-level elevation of West Point Lake remained near the top of conservation pool until May when the lake level dropped nearly 6 feet during the remainder of the WY.

Hartwell Lake, on the border between Georgia and South Carolina on the Savannah and Tugaloo Rivers is the most upstream major reservoir, on the Savannah River. Water is released to the downstream reservoirs, Richard B. Russell and

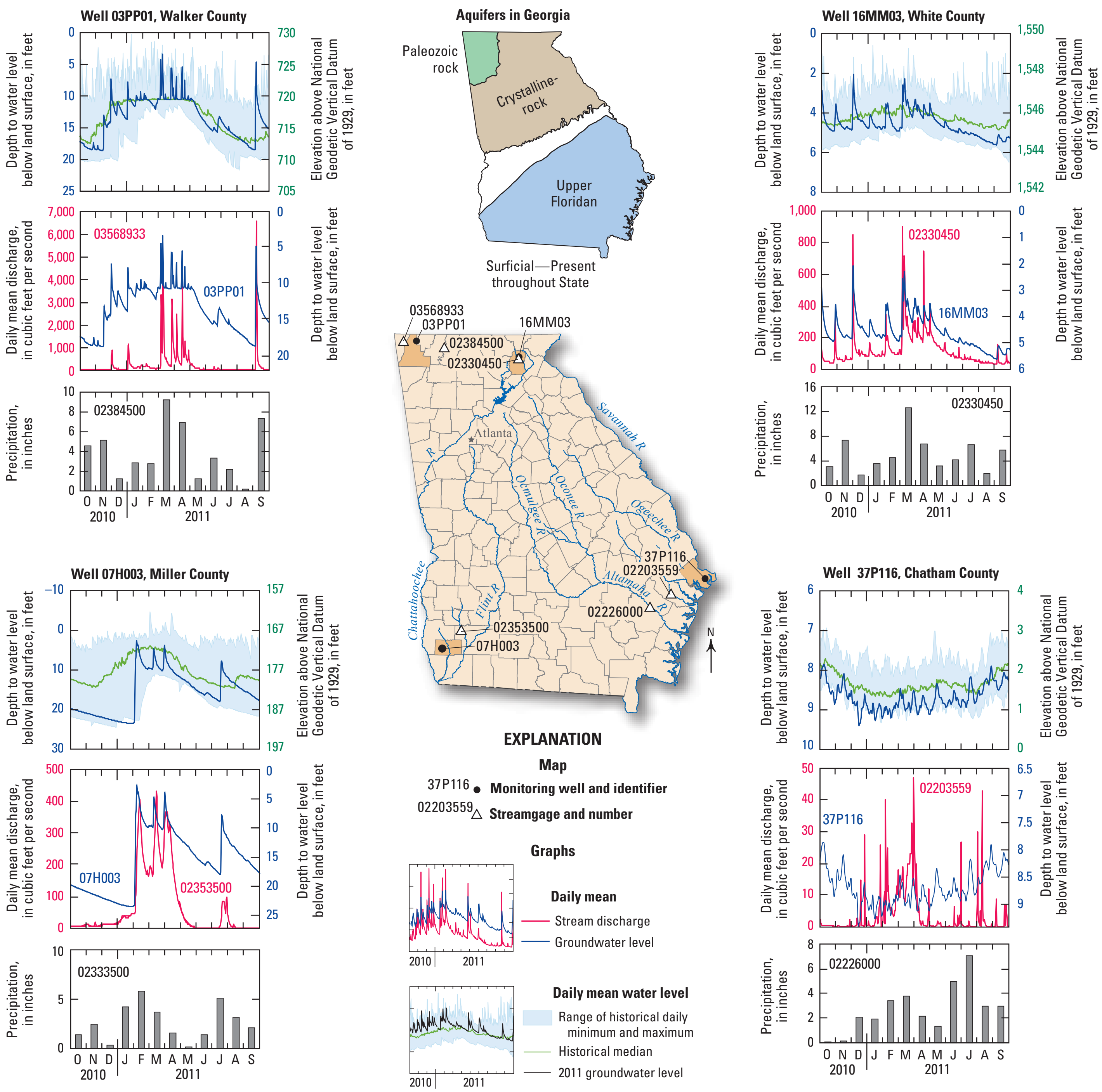


**Figure 4.** Groundwater levels, streamflow, and precipitation at selected sites in Georgia during 2011 WY (modified from Knaak and others, 2013).

J. Strom Thurmond. These three lakes on the Savannah River are managed by the U.S. Army Corps of Engineers for water supply, power generation, and water-quality needs of the Savannah River. Hartwell Lake reached full pool after having nearly 2.4 times more in-flow than outflow in March but then dropped nearly 8 feet from May through September as outflow was 1.7 times greater than inflow.

Allatoona Lake is on the Etowah River and is managed by the U.S. Army Corps of Engineers. During the 2011 WY, Allatoona Lake remained above or just below the top of conservation pool from October through June. By the end of the 2011 WY, the lake level was nearly 7 feet below the top of conservation pool, as outflow was 2.4 times greater than inflow from July through September.

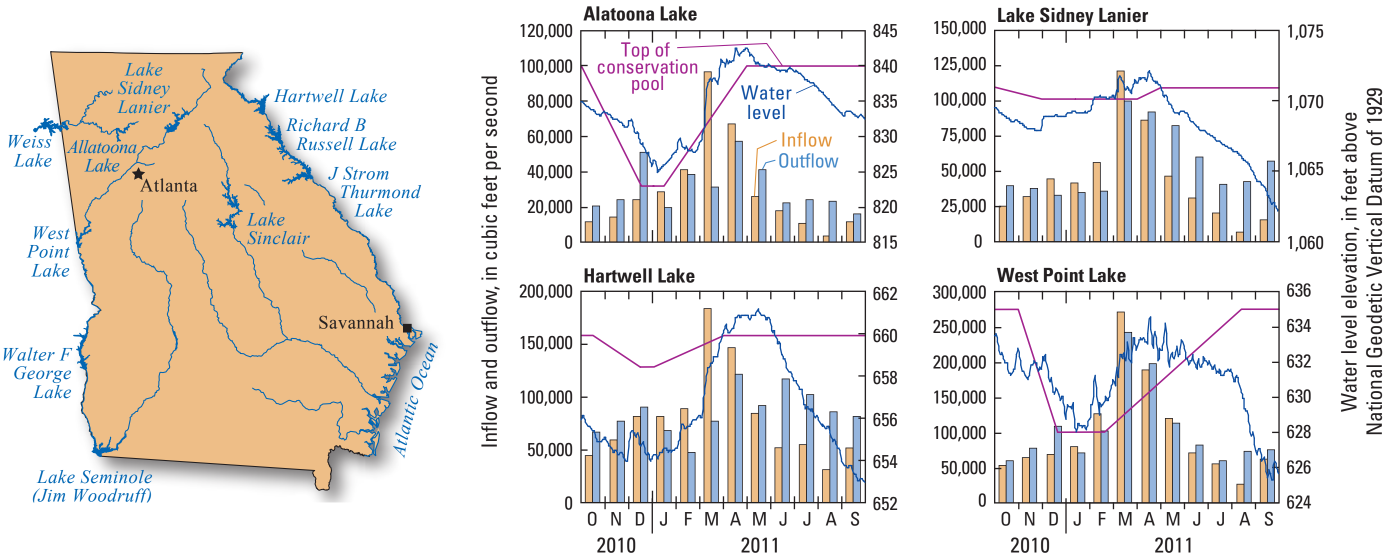


**Figure 5.** Water level, inflow, and outflow to selected lakes and reservoirs in Georgia, 2011 WY (modified from Knaak and others, 2013).

## Water-Quality Monitoring in Georgia in Cooperation With the Georgia Department of Natural Resources Environmental Protection Division

The USGS, in cooperation with the Georgia Department of Natural Resources Environmental Protection Division (GaEPD), collects nearly 1,000 monthly chemical and nutrient samples and about 800 fecal coliform samples at 49 long-term monitoring stations across the State in addition to data from 3 continuous water-quality monitors (fig. 6). Four fecal coliform samples typically are collected within 30 days twice during the May-to-October period when the standard for water contact applies, and then twice during the November-to-April period when the alternate standard applies, which provides the basis for computing the geometric mean fecal coliform density once-quarterly each calendar year. In addition, about 200 quality-assurance samples for all constituents are collected concurrently to verify the accuracy of sampling techniques and analytical methods.

The USGS provides the GaEPD and the public a relevant, nationally consistent database of long-term water-quality data, which assists the GaEPD in meeting its responsibilities under the Clean Water Act, including, (1) identifying the beneficial uses of surface waters within the State, (2) establishing water-quality standards to maintain the full beneficial uses of surface waters, and (3) identifying water bodies where stream standards are not met and beneficial uses are impaired (Grams, 2011). Water-quality data for Georgia streams are available on a publicly accessible Web site at *http://waterdata.usgs.gov/ga/nwis/qw/*.

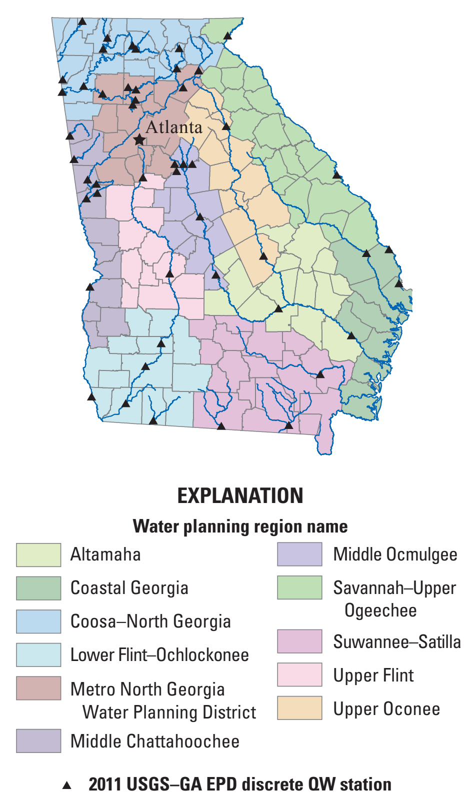


**Figure 6.** USGS-GaEPD discrete water-quality sample station locations and watershed basins (from Knaak and others, 2013).

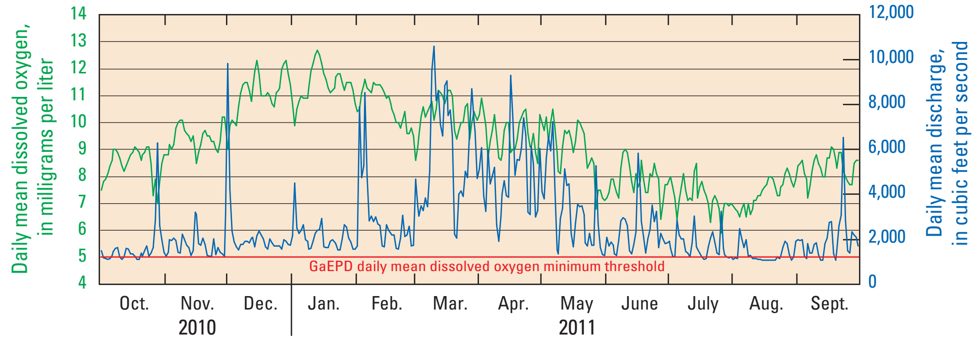


**Figure 7.** The daily mean dissolved oxygen and daily mean discharge for the Chattahoochee River near Fairburn, Ga. (from Knaak and others, 2013).

The USGS–GaEPD cooperative program collects continuous water-quality data at three sites in Georgia, including USGS station 02337170 Chattahoochee River near Fairburn, Ga. This stream reach is classified as "Fishing" under Georgia Code 391-3-6-.03 "Water Use Classifications and Water Quality Standards," which requires that the daily mean dissolved oxygen (DO) concentrations in the stream remain at or above 5.0 milligrams per liter (Georgia Environmental Protection Division, 2011). The daily mean DO and daily mean discharge for the Chattahoochee River near Fairburn, Ga., is shown in graph (fig. 7) for the 2011 WY. No daily mean DO levels fell below the "Fishing" criteria in Georgia streams during the 2011 WY.

## References

Cressler, C.W., 1964, Geology and groundwater resources of Walker County, Georgia: Georgia Geologic Survey Information Circular 63, 144 p.

Cressler, C.W., Thurmond, C.J., and Hester, W.G., 1983, Groundwater in the greater Atlanta region, Georgia: Georgia Geological Survey Information Circular 63, 15 p.

Georgia Department of Natural Resource, Environmental Protection Division, 2011, Existing rules and corresponding laws, 391-3-6 Water quality control: Accessed July 16, 2012, at *http://www.gaepd.org/Documents/rules_exist.html*.

Grams, S.C., 2011, Benefits of long-term water-quality monitoring in Georgia [abs.], *in* Carroll, G.D., ed., Proceedings of the 2011 Georgia Water Resources Conference, April 11–13, 2011, Athens, Georgia: Georgia Water Resources Institute, 6. Water informatics, 6.1 Watershed data, 1 p.

Knaak, A.E., Frantz, E.R., and Peck, M.F., 2013, Extreme drought—Summary of hydrologic conditions in Georgia, 2011: U.S. Geological Survey Fact Sheet 2013–3002, 6 p., available online at *http://pubs.usgs.gov/fs/2013/3002/*.

National Oceanic and Atmospheric Administration, 2011, National Weather Service advanced hydrologic prediction service, 2011 precipitation maps for Georgia: Accessed June 1, 2012, at *http://water.weather.gov*.

Peck, M.F., Painter, J.A., and Leeth, D.C., 2011, Ground-water conditions and studies in Georgia, 2009–2010: U.S. Geological Survey Scientific Investigations Report 2009–5048, 83 p., available at *http://pubs.usgs.gov/sir/2011/5048/*.

Stooksbury, D.E., 2011, Extreme drought spreads into north Georgia, *in* News to use about Georgia family, agricultural consumer & environmental sciences, August 31, 2011: University of Georgia, accessed June 26, 2012, at *http://georgiafaces.caes.uga.edu/index.cfm?public=viewStory&pk_id=4207*.

U.S. Army Corps of Engineers, 2012, Lake elevations, inflows and outflows: Accessed June 1, 2012, at *http://www.sas.usace.army.mil/*.

U.S. Geological Survey, 1975, Hydrologic unit map 1974, State of Georgia: U.S. Geological Survey, scale 1:500,000, 1 sheet.

U.S. Geological Survey, 2007, U.S. Geological Survey Ground-Water Climate Response Network: U.S. Geological Survey Fact Sheet 2007–3003, 4 p., accessed July 1, 2009, at *http://pubs.usgs.gov/fs/2007/3003/*.

U.S. Geological Survey, 2012a, U.S. Geological Survey annual data report for Georgia, water year 2011: Accessed June 1, 2012, at *http://ga.water.usgs.gov/publications/pubswdr.html*.

U.S. Geological Survey, 2012b, U.S. Geological Survey groundwater watch, Climate Response Network: Accessed June 1, 2012, at *http://groundwaterwatch.usgs.gov/*.

U.S. Geological Survey, 2012c, WaterWatch–Current water resources in Georgia: Accessed June 1, 2011, at *http://waterwatch.usgs.gov/*.

# Analysis of Trends in Annual Minimum 7-Day Average Flows for the Lower Apalachicola–Chattahoochee–Flint River Basin, Georgia, 1903–2011

By Anthony J. Gotvald

## Abstract

Streamflow at U.S. Geological Survey streamgages in the lower Apalachicola–Chattahoochee–Flint River basin was evaluated to determine whether significant changes in annual minimum 7-day average flows have occurred since 1903. Monotonic trends in annual minimum 7-day average flows were evaluated at gages in the basin with more than 60 years of data using a nonparametric test (Kendall's tau). Seven of the eight streamgages indicated significant negative trends in annual minimum 7-day average flows.

## Introduction

In 2010, the U.S. Department of the Interior launched a sustainable water strategy known as WaterSMART, which stands for "Sustain and Manage America's Resources for Tomorrow." As part of WaterSMART, the U.S. Geological Survey (USGS) is studying availability and use of water in various areas across the country, including the Apalachicola–Chattahoochee–Flint (ACF) River basin in Alabama, Florida, and Georgia. WaterSMART focuses on improving water conservation and helping water-resource managers make sound decisions about water use (U.S. Department of the Interior, 2010).

The USGS has been operating streamgages in Georgia for more than 100 years. Low-flow frequency statistics of streamflow, such as the annual minimum 7-day average flow that occurs, on average, once every 10 years (7Q10), are an important part of assessing water resources in a watershed. These frequency statistics can be used by water-resource managers to determine water availability, water assimilative capacities of streams, and aquatic habitat needs.

The results of frequency statistics may be adversely affected if the annual low-flow time-series data are not random, independent, and stationary over time, as is assumed in frequency analyses. Annual low-flow time series data need to be closely examined for possible trends and any indications of regulation, local diversions of flow (discharges and withdrawals), and possible sustained changes in streamflows because of changes in the prevailing climate. This paper documents the trends in annual minimum 7-day average flows for long-term USGS streamgages in the lower ACF River basin in Georgia but does not include any assessments that address the cause(s) of the trends.

## Description of Study Area

The ACF basin includes three major rivers—the Apalachicola, Chattahoochee, and Flint Rivers (fig. 1). The Chattahoochee River begins in the mountains of northeast Georgia and flows southwest through Metropolitan Atlanta to the Alabama-Georgia border, where the river flows south to Lake Seminole on the Florida-Georgia State line. The Flint River begins in north-central Georgia, just south of Atlanta, and flows south to Lake Seminole. The Apalachicola River begins at Lake Seminole, which is the confluence of the Chattahoochee and Flint Rivers, and flows south through Florida to the Gulf of Mexico. The Chattahoochee River is regulated by four U.S. Army Corps of Engineers (USACE) projects and nine run-of-river dams, while the Flint River is relatively unregulated with just two run-of-river dams (U.S. Army Corps of Engineers, 1997). The study area is in the lower portion of the ACF in southwestern Georgia (fig. 1), where streams are in close connection with the Upper Floridan aquifer, and streamflow is affected by agricultural withdrawals from the aquifer. In this area, there currently (2012) are eight USGS streamgages with 60 or more years of daily-mean flow record.

## Methods

The trend analysis used in this study is based on the commonly used nonparametric Kendall's tau statistical test to detect monotonic trends in annual minimum 7-day average flows with time (Helsel and Hirsch, 2002). The annual minimum 7-day average flow is the lowest daily mean discharge during 7 consecutive days in a given climatic year. (A climatic year is defined as the 12-month period from April 1 to March 31 and is designated by the year in which it ends.) A positive tau indicates an upward monotonic streamflow trend; conversely, a negative tau indicates a downward monotonic streamflow trend. The trend is considered to be significant if the probability value (p-value) is less than or equal to 0.05. The trend analysis reported in this study is limited to direction and not magnitude of streamflow change (Barbie and others, 2012).

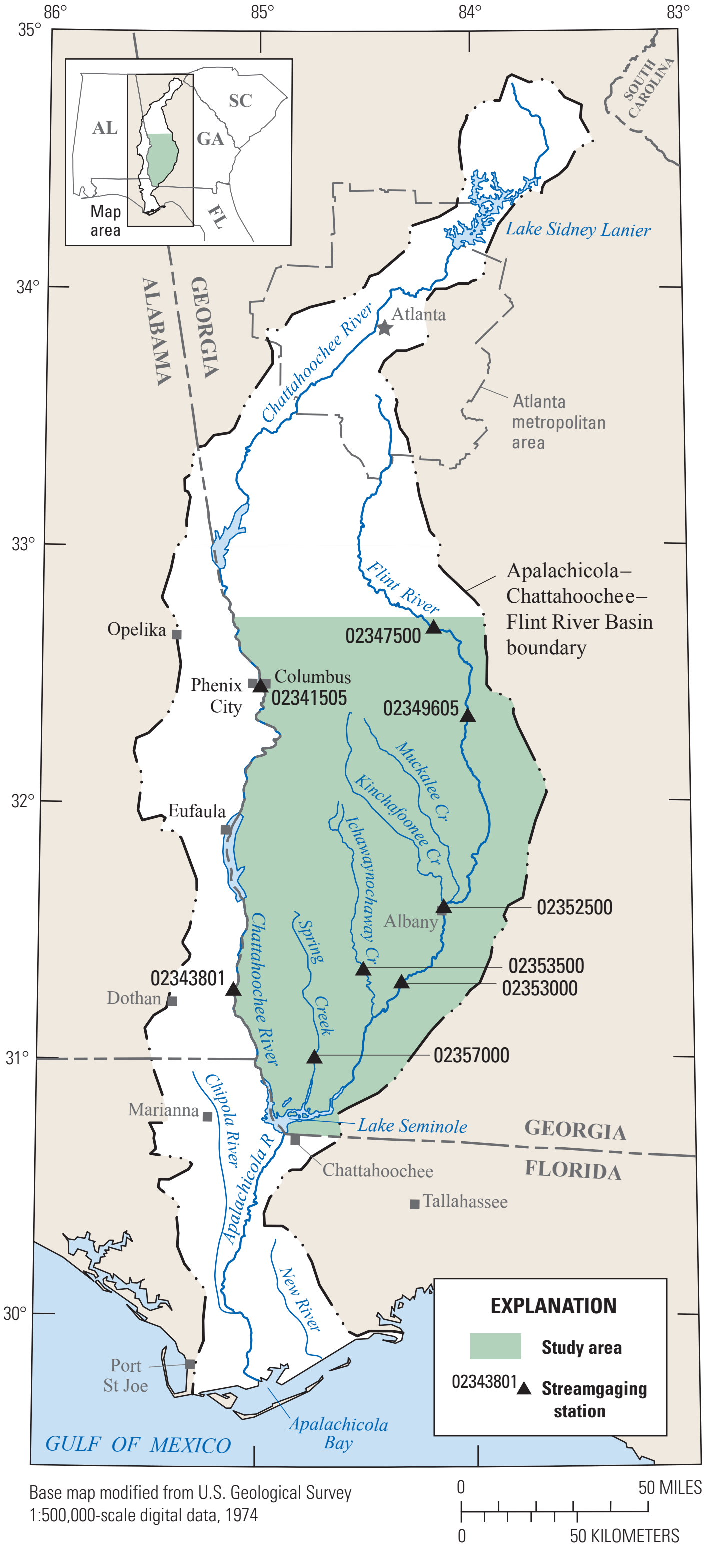


**Figure 1.** Location of Apalachicola–Chattahoochee–Flint River basin and selected USGS streamgages.

## Results and Discussion

The trend analysis was performed on eight currently operating USGS streamgages in the study area with 60 or more years of daily mean flow record. The results of the trend analyses are listed in table 1. The annual minimum 7-day average flows and resulting Kendall's tau trend lines are plotted in figure 2. Analyses indicated significant negative (downward) trends for seven of the streamgages. The streamgage on the Chattahoochee River near Columbus, Georgia, showed a slight negative trend, however, the trend is statistically insignificant .

To illustrate the effect of a significant trend in annual minimum 7-day average flow on the 7Q10, the 7Q10 for streamgage 02352500 (Flint River at Albany, GA) was computed beginning with the first 10 years of record after the Lake Worth and Warkwick Reservoir impoundments (April 1930–March 1940) and then computed on a 10-year accumulated basis through climatic year 2010. Figure 3 shows the annual minimum 7-day average flow by climatic year along with the computed 7Q10. By climatic year 1980, the 7Q10 was 1,040 cubic feet per second ($ft^3/s$), which is close to the 1,000 $ft^3/s$ 7Q10 value computed by Carter and Putnam (1978) for this streamgage. After 1980, the 7Q10 decreased every 10 years and was 848 $ft^3/s$ using record from April 1930 to March 2010.

The scope of this paper does not include analyses of the causes of trends, such as how possible changes in regulation, precipitation, land use, or groundwater withdrawals might have affected streamflow trends. Further detailed analyses, such as land use changes, trends in precipitation, and water use are needed in order to determine the causes of the trends.

## References Cited

Barbie, D.L., Wehmeyer, L.L., and May, J.E., 2012, Analysis of trends in selected streamflow statistics for the Concho River Basin, Texas, 1916–2009: U.S. Geological Survey Scientific Investigations Report 2012–5193, 15 p.

Carter, R.F. and Putnam, S.A., 1978, Low-flow frequency of Georgia streams: U.S. Geological Survey Water-Resources Investigations Open File Report 77–127, 104 p.

Helsel, D.R., and Hirsch, R.M., 2002, Statistical methods in water resources: U.S. Geological Survey Techniques of Water-Resources Investigations book 4, chap. A3, 522 p. (Also available at *http://pubs.usgs.gov/twri/twri4a3*.)

U.S. Army Corps of Engineers, 1997, ACT/ACF comprehensive water resources study, surface water availability, Volume I, unimpaired flow: USACE report 96, p. 701–711.

U.S. Department of the Interior, 2010, WaterSMART Program, accessed on September 27, 2012, at *http://www.doi.gov/watersmart/html/about.html*.

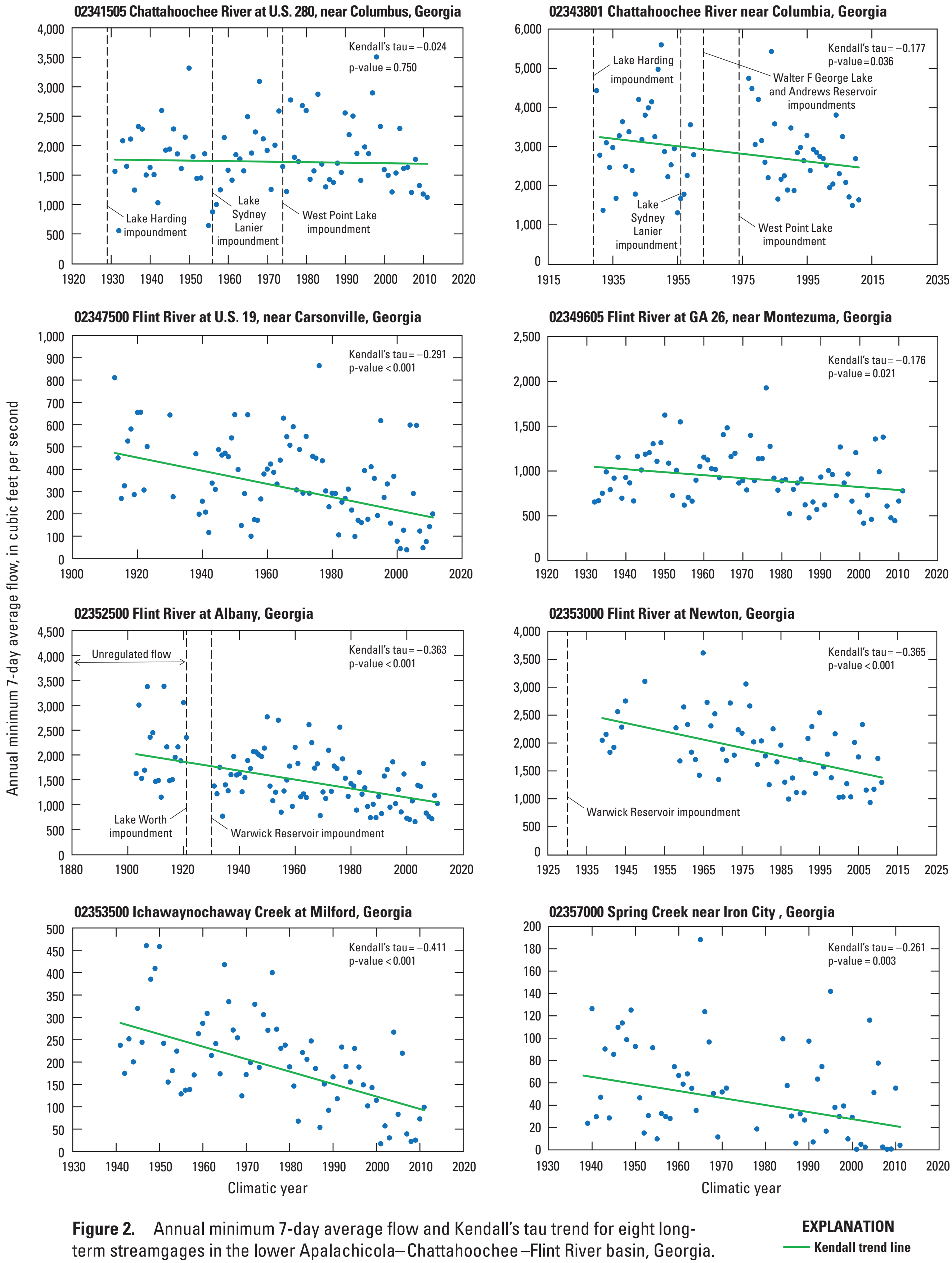


**Figure 2.** Annual minimum 7-day average flow and Kendall's tau trend for eight long-term streamgages in the lower Apalachicola–Chattahoochee–Flint River basin, Georgia.

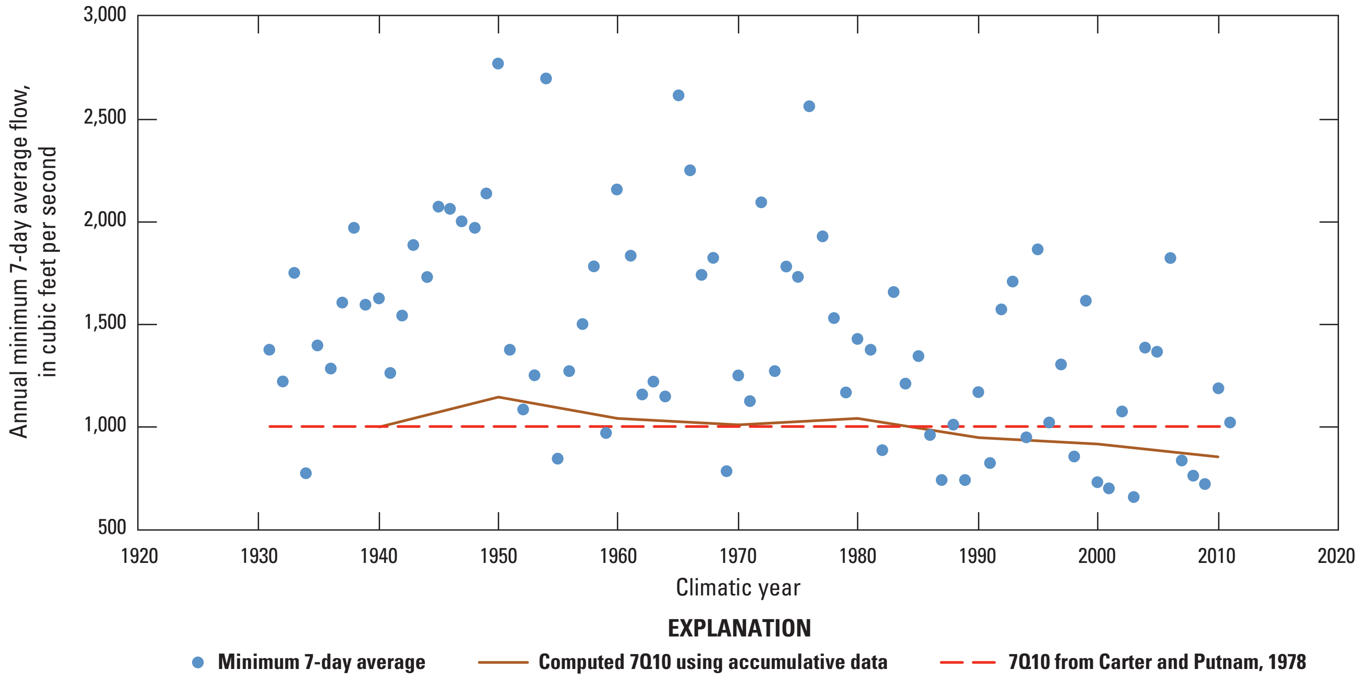


**Figure 3.** The annual minimum 7-day average flows and 7Q10 estimates at USGS streamgage 02352500, Flint River at Albany, Georgia.

**Table 1.** Results of Kendall's tau statistical test for detection of monotonic trends in annual minimum 7-day average flows for U.S. Geological Survey (USGS) streamgages that have more than 60 years of flow data in the lower Apalachicola–Chattahoochee–Flint River basin, Georgia.

[<, less than]

| USGS station number | USGS station name | Climatic years analyzed | Kendall's tau | p-value | Trend |
|---|---|---|---|---|---|
| 02341505 | Chattahoochee River at US 280, near Columbus, Georgia | 1931–2011 | −0.024 | 0.750 | Not significant |
| 02343801 | Chattahoochee River near Columbia, Georgia | 1930–1960, 1977–2011 | −0.177 | 0.036 | Downward |
| 02347500 | Flint River at US 19, near Carsonville, Georgia | 1913–1923, 1930–1931, 1938–2011 | −0.291 | <0.001 | Downward |
| 02349605 | Flint River at GA 26, near Montezuma, Georgia | 1932–2011 | −0.176 | 0.021 | Downward |
| 02352500 | Flint River at Albany, Georgia | 1903–1921, 1932–2011 | −0.363 | <0.001 | Downward |
| 02353000 | Flint River at Newton, Georgia | 1939–1945, 1950, 1958–2011 | −0.365 | <0.001 | Downward |
| 02353500 | Ichawaynochaway Creek at Milford, Georgia | 1941–2011 | −0.411 | <0.001 | Downward |
| 02357000 | Spring Creek near Iron City, Georgia | 1939–1971, 1978, 1984–2011 | −0.261 | 0.003 | Downward |

# Hydrologic Conditions in the Lower Apalachicola–Chattahoochee–Flint and Parts of the Aucilla–Suwannee–Ochlockonee River Basins in Georgia, Florida, and Alabama, During Drought Conditions, July 2011

By Debbie W. Gordon, Michael F. Peck, and Jaime A. Painter

## Abstract

As part of the U.S. Department of the Interior's Water SMART program for sustainable water, the U.S. Geological Survey documented hydrologic conditions in the lower Apalachicola–Chattahoochee–Flint and western and central Aucilla–Suwanee–Ochlockonee River basins in Alabama, Florida, and Georgia during low-flow conditions in July 2011. Moderate drought conditions prevailed in these areas during early 2011, and worsened to exceptional drought conditions by June. Cumulative rainfall totals were below the 1981–2010 climate normal, with deficits ranging from 17 to 27 inches. As a result, groundwater levels and stream discharges were below median daily levels throughout most of 2011.

## Introduction

In 2010, the U.S. Department of the Interior (DOI) launched a sustainable water initiative known as the WaterSMART (Sustain and Manage America's Resources for Tomorrow) program to address a simple reality: "America's demands for water are quickly out-growing our supplies of water" (*http://www.doi.gov/news/video/Interior-Launches-WaterSMART-Initiative.cfm/index.cfm*). As part of the WaterSMART program, the U.S. Geological Survey (USGS) is studying water availability and use in several focus areas across the country, including the Apalachicola–Chattahoochee–Flint (ACF) River basin in Alabama, Florida, and Georgia (fig. 1; *http://www.usgs.gov/conferences/watersmart-acf/about.html*). WaterSMART focuses on improving water conservation, helping water-resource managers make sound decisions about water use, and identifying adaptive measures to address climate change and its effect on future water availability (U.S. Department of the Interior WaterSMART Clearinghouse, accessed January 4, 2012, at *http://www.doi.gov/watersmart/html/about.html*) .

Severe drought during 2011 in the Southeastern United States resulted in record-low groundwater levels and streamflow in the lower ACF and western and central Aucilla–Suwannee–Ochlockonee (ASO) River basins. Documenting historic hydrologic conditions through measurements of groundwater levels, streamflow, and springflow provides essential data to help evaluate the effects of climatic extremes on the water resources of these basins and to further understand the exchange of water between the Upper Floridan karst aquifer and overlying streams. These data will provide a basis for detailed calibrations of groundwater-flow models used to simulate water-management scenarios for the area while also directly supporting WaterSMART.

Groundwater levels, streamflow, and springflow were measured simultaneously for low-flow conditions during July 18–24, 2011. Groundwater levels were measured in wells completed in the Upper Floridan and surficial aquifers. Streamflow measurements were coordinated with appropriate dam regulators to minimize variations in the streamflow data caused by releases for power generation and other purposes.

## Study Area

The study area is located in the Coastal Plain Physiographic Province in southwestern Georgia, southeastern Alabama (Houston County), and north-central Florida (fig. 1). The study area includes the lower ACF River basin, and the western and central parts of the ASO River basin. The flow system and stream-aquifer connection in the study area are controlled by geology, hydraulic properties of the Upper Floridan aquifer and its confining units, precipitation, and groundwater withdrawals. The study area extends through the Gulf Trough–Apalachicola Embayment, a northeast-southwest trending geologic feature composed of fine-grained, dense, low-permeability limestone overlain by a thick sequence of Oligocene to Miocene sediments, which forms a barrier to groundwater flow southeastward in the Upper Floridan aquifer (Torak, and others, 2010).

The hydrologic connection between the streams, the overburden sediments of the upper semiconfining unit and the Upper Floridan aquifer in the ACF and ASO River basins are quite different. During the wet season when winter and spring rains recharge the aquifer and irrigation pumping is inactive, the water table is close to land surface in the overburden and water flows from the Upper Floridan aquifer into the Flint River and other streams in the basin. Some of the water also discharges from the overburden sediments into the streams in the ASO River basin (fig. 2*A*). During the dry, summer growing season when rainfall is sporadic and irrigation pumping is fully active, the water level of the Flint River drops and the water table drops in the overburden causing many of the streams to go dry, especially in the ASO River basin. As a result, some of the water that was originally discharged into the Flint River and other streams in the basins is pumped out of the aquifer to irrigate crops during the summer growing season (fig. 2*B*).

**Figure 1.** Location of the study area, physiographic provinces, basin boundaries, and weather stations in the lower Apalachicola–Chattahoochee–Flint (ACF) River basin and in western and central parts of the Aucilla–Suwannee–Ochlockonee (ASO) River basin, Alabama, Florida, and Georgia (modified from Gordon and others, 2012).

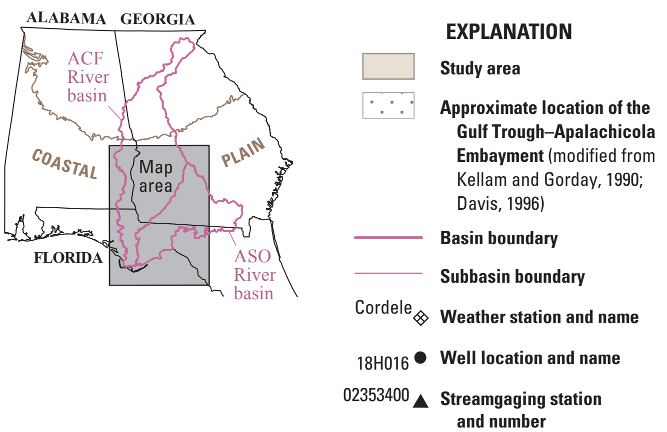


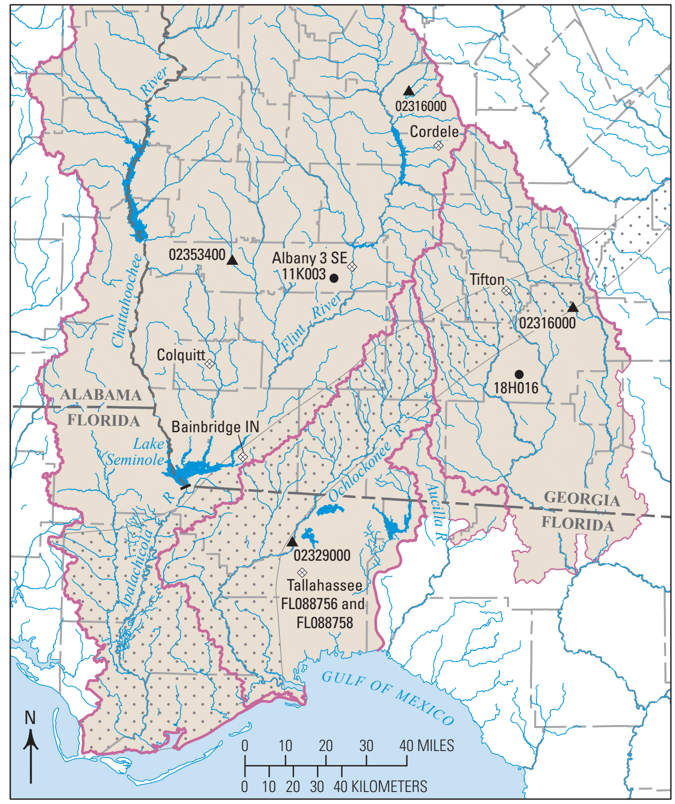


Base modified from U.S. Geological Survey 1:100,000-scale digital data

**Figure 2.** Schematic cross sections showing the hydrologic connection between the Flint River, the overburden sediments of the upper semiconfining unit, and the Upper Floridan aquifer in Georgia. *A*, During the wet season when winter and spring rains recharge the aquifer and irrigation pumping ceases, the water table is close to land surface in the overburden, and water flows from the Upper Floridan aquifer into the Flint River and other streams in the basin. Some of the rainfall also discharges from the aquifer into the streams in the Aucilla–Suwanee–Ochlockonee River basin. *B*, During the dry, summer growing season, rainfall is sporadic and irrigation pumping is at its peak, which causes the water table to decline in the overburden and streams to go dry in the Suwannee River basin. The water level of the Flint River drops, and some of the water that would have discharged into the river is now being pumped out of the aquifer to irrigate crops (modified from Gordon and others, 2012).

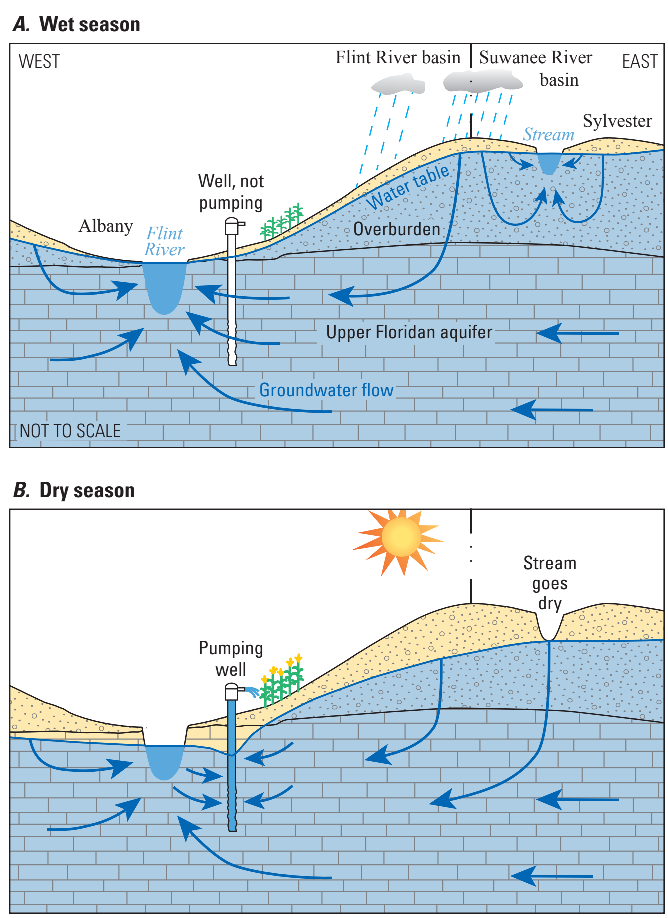

## Hydrologic Conditions During July 2011

Cumulative departures from normal precipitation during 2008–2011 indicate a long-term precipitation deficit ranging from 17 to 27 inches in July 2011 (fig. 3). Flow was below median levels in many of the streams measured during July 2011 (fig. 4). Ground-water levels were below normal throughout most of 2011 (fig. 5), and record-low water levels were recorded at 128 wells tapping the Upper Floridan aquifer in Georgia during July (fig. 6).

A potentiometric-surface map of the Upper Floridan aquifer was constructed using water-level measurements collected in 312 wells in Alabama, Florida, and Georgia (fig. 6). The potentiometric surface indicates that groundwater in the study area generally flows to the south and toward streams except where stream reaches discharge to the Upper Floridan aquifer. One of the most prominent features observed in the potentiometric surface is in the area of the Gulf Trough, where hydraulic properties of the aquifer change and the hydraulic gradient abruptly steepens. The lesser degree of connection between the Upper Floridan aquifer and streams on the east side of the Flint River is a result of the thicker layer of overburden in that area (fig. 2). The reduced connection is evident from stream-stage altitudes measured in July 2011 east of the Flint River, which were as much as 160 feet higher than water-level altitudes measured nearby in the Upper Floridan aquifer. In this area, a large number of streams were dry during the July measurement period (fig. 7).

Streamflow consists of surface runoff, interflow, and base flow. Stream base flow is the portion of stream-flow contributed by groundwater discharge. During periods of low precipitation, all or most of streamflow is base flow. Near base-flow conditions were assumed to prevail when measurements were made during July 2011. Although some rainfall occurred during the 7 days prior to the measurement period, measurements were collected after the peak discharge subsided and discharge was below the median daily value (fig. 6). Of the 2,122 stream miles represented by discharge measurements, 1,230 miles were in gaining-stream conditions, 286 stream miles were in losing-stream conditions, and 606 stream miles had no flow (fig. 7).

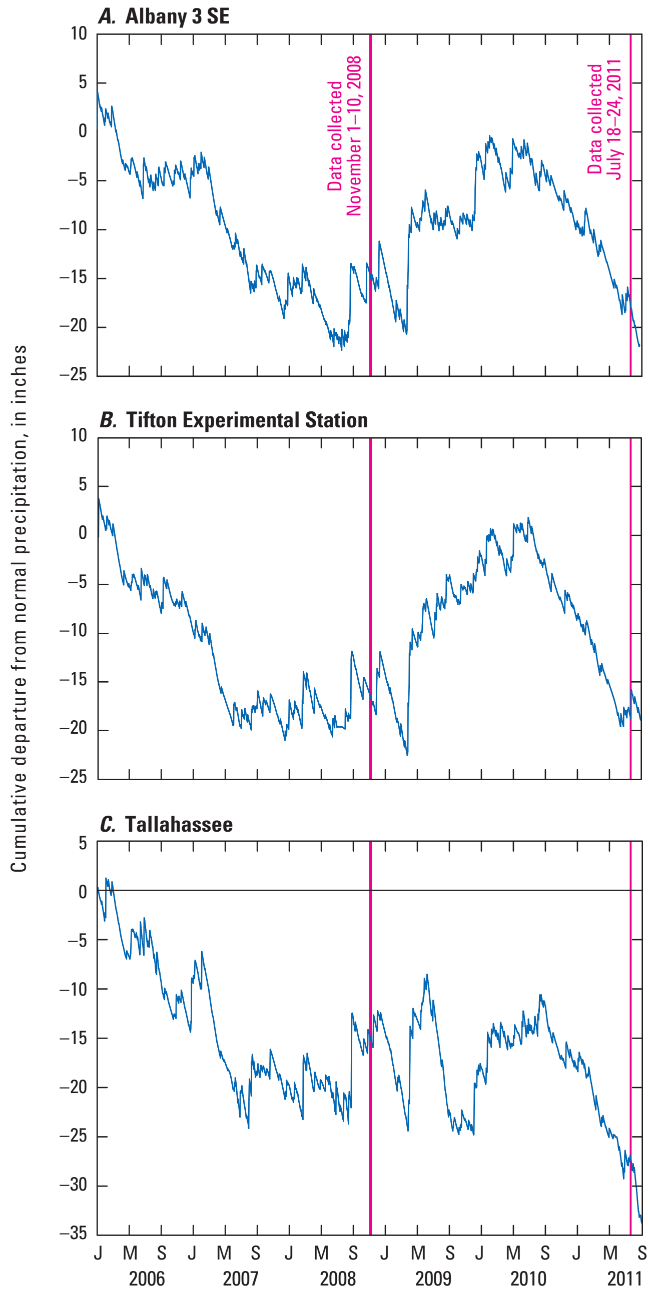


**Figure 3.** Cumulative departure from normal (1981–2010) precipitation at National Oceanic and Atmospheric Administration Georgia weather stations *(A)* Albany 3 SE, *(B)* Tifton Experimental Station, and *(C)* Tallahassee, 2006–2011. (See figure 1 for locations; modified from Gordon and others, 2012.)

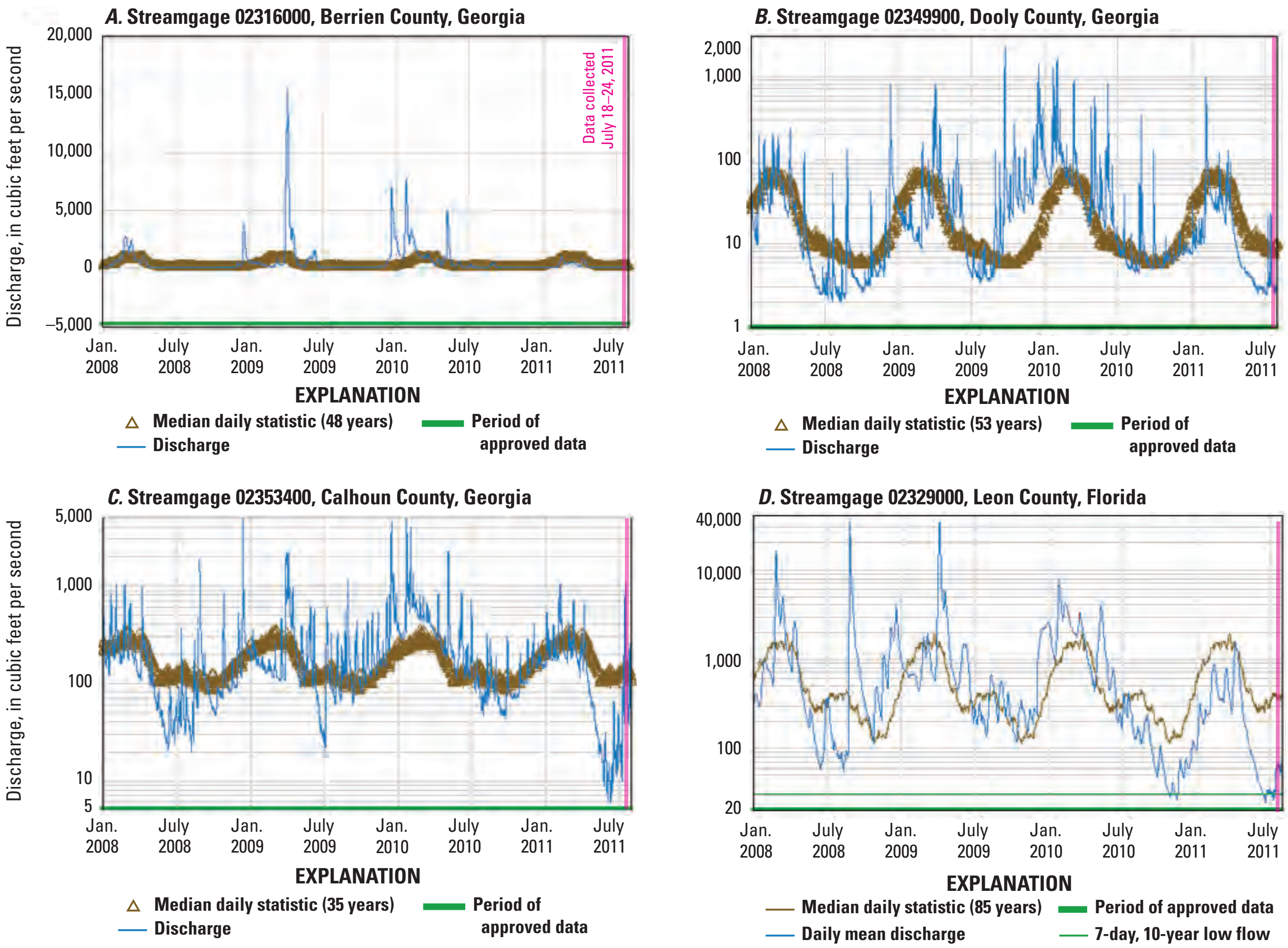


**Figure 4.** Discharge for U.S. Geological Survey streamgages *(A)* 02316000, *(B)* 02349900, *(C)* 02353400, and *(D)* 02329000, 2008–2011. (See figure 1 for locations; modified from Gordon and others, 2012).

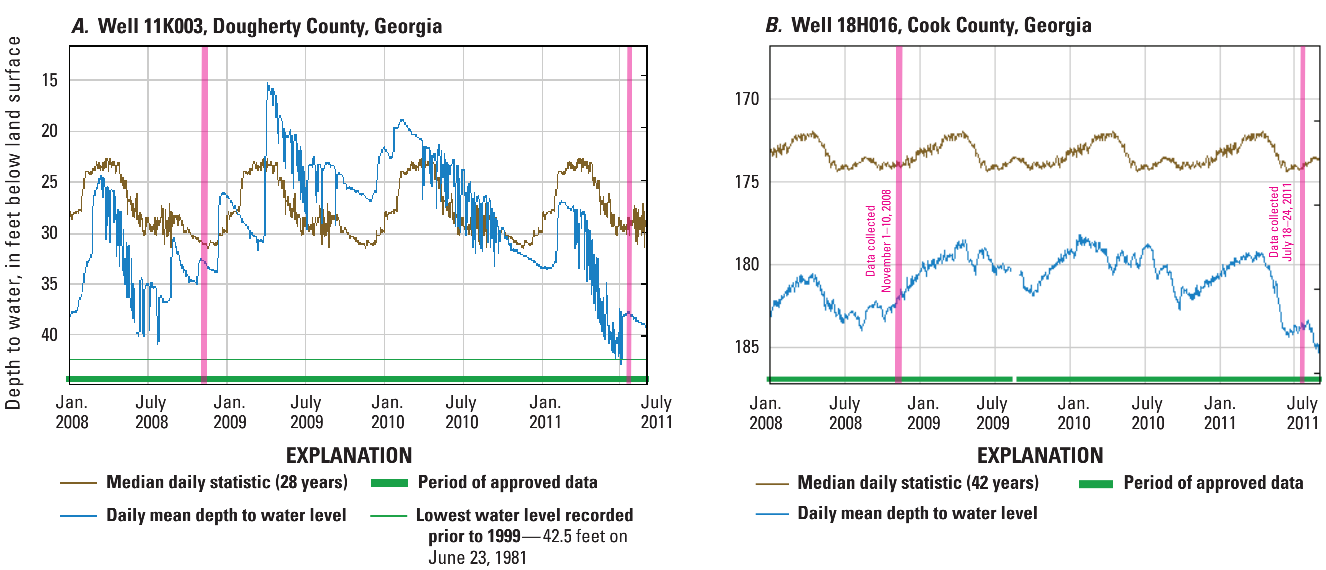


**Figure 5.** Water levels and long-term daily median statistics for *(A)* well 11K003 and *(B)* well 18H016. (See figure 1 for locations; modified from Gordon and others, 2012.)

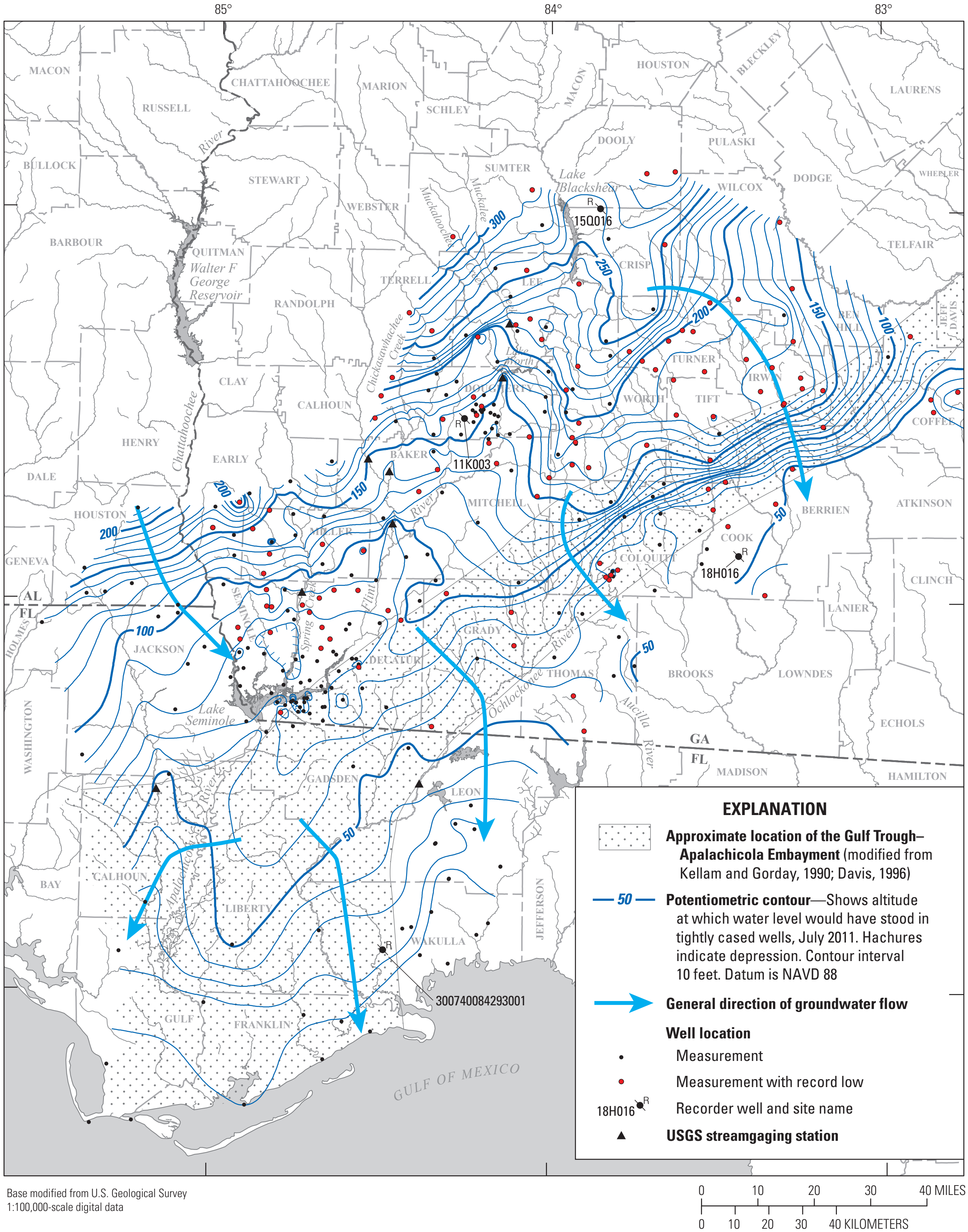


**Figure 6.** Potentiometric surface and record low water levels of the Upper Floridan aquifer in the lower Apalachicola–Chattahoochee–Flint River basin and western and central parts of the Aucilla–Suwanee–Ochlockonee River basin, Alabama, Florida, and Georgia, July 2011 (modified from Gordon and others, 2012).

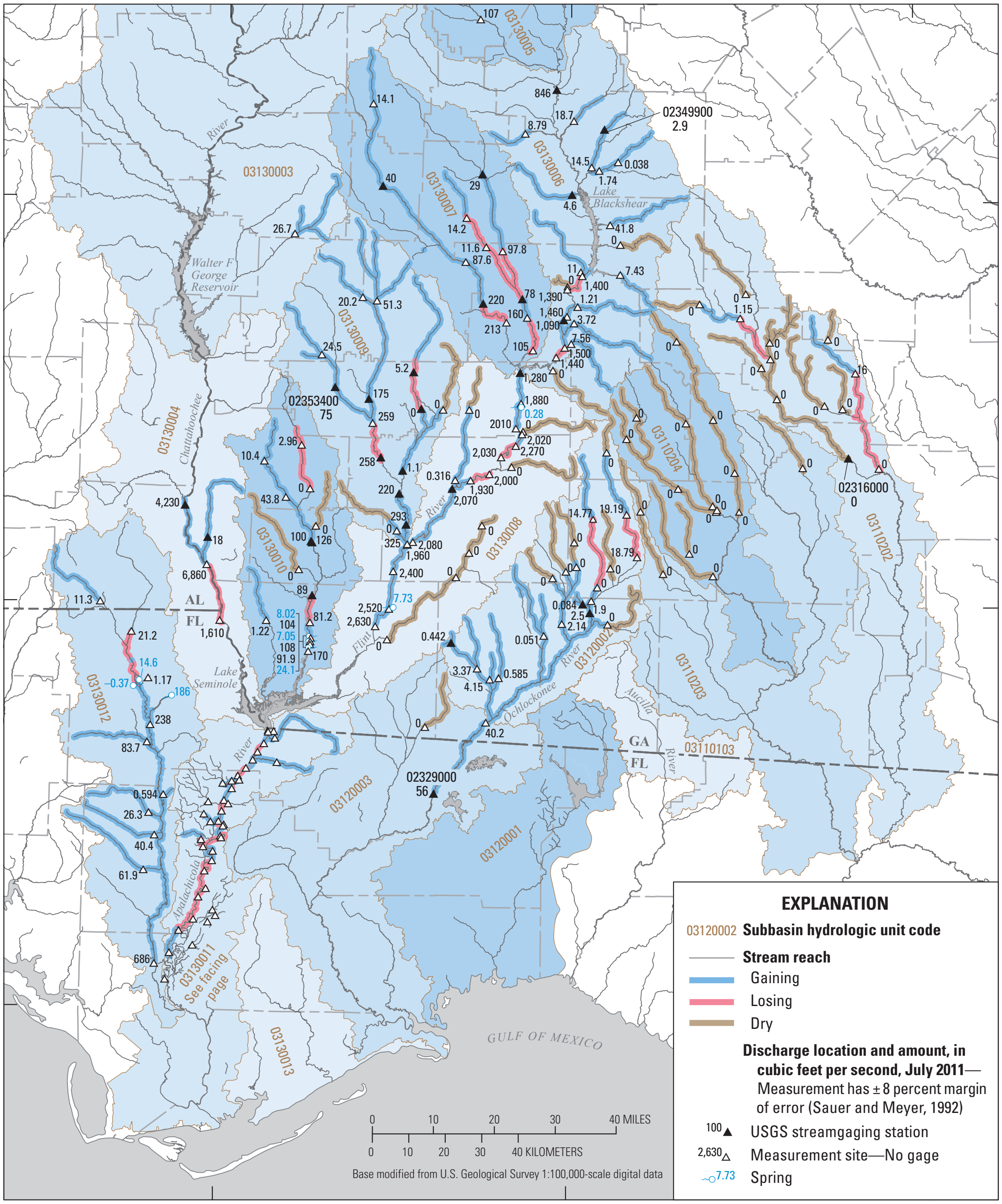


**Figure 7.** Discharge measurements made in the lower Apalachicola–Chattahoochee–Flint River basin and western and central parts of the Aucilla–Suwanee–Ochlockonee River basin, Alabama, Florida, and Georgia, showing gaining, losing, and dry stream reaches during July 2011 (modified from Gordon and others, 2012).

## References


Davis, J.H., 1996, Hydrogeologic investigation and simulation of ground-water flow in the Upper Floridan aquifer of north-central Florida and southwestern Georgia and delinea-tion of contributing areas for selected City of Tallahassee, Florida, water-supply wells: U.S. Geological Survey Water-Resources Investigations Report 95–4296, 55 p.

Gordon, D.W., Peck, M.F., and Painter, J.A., 2012, Hydrologic and water-quality conditions in the lower Apalachicola–Chattahoochee–Flint and parts of the Aucilla–Suwanee–Ochlockonee River basins in Georgia and adjacent parts of Florida and Alabama during drought conditions, July 2011: U.S. Geological Survey Scientific Investigations Report 2012–5179, 69 p., 1 sheet, available online at *http://pubs.usgs.gov/sir/2012/5179/*.

Kellam, M.F., and Gorday, L.L., 1990, Hydrogeology of the Gulf Trough–Apalachicola Embayment area, Georgia: Georgia Geologic Survey Bulletin 94, 74 p.

Sauer V.B., and Meyer R.W., 1992, Determination of error in individual discharge measurements: U.S. Geological Survey Open-File Report 92–144, 21 p.

Torak, L.J., Painter, J.A., and Peck, M.F., 2010, Geohydrology of the Aucilla–Suwannee–Ochlockonee River Basin, south-central Georgia and adjacent parts of Florida: U.S. Geological Survey Scientific Investigations Report 2010–5072, 78 p., available online at *http://pubs.usgs.gov/sir/2010/5072/*.

# A Comparison of Groundwater Conditions in the Clayton and Claiborne Aquifers, Southwest Georgia, 1994 to 2011

By Michael F. Peck and Debbie W. Gordon

## Abstract

The Clayton and Claiborne aquifers are heavily pumped as sources of water for irrigation, public supply, and industrial purposes in southwestern Georgia. This pumping has led to water-level declines of as much as 1.64 feet per year during 1979–2009 in the Clayton aquifer and 1.1 feet per year during 1978–2009 in the Claiborne aquifer (Peck and others, 2011). To help diminish the rate of groundwater level decline in the Clayton aquifer, the Georgia Environmental Protection Division imposed a moratorium on new withdrawal permits in the Clayton aquifer in the early 1990s; however, there are no restrictions on new permits in the Claiborne aquifer.

To provide data to support water-management decisions, the U.S. Geological Survey, in cooperation with State and local agencies, operates a continuous water-level monitoring network that includes 11 wells in the Clayton aquifer and 10 wells in the Claiborne aquifer (Peck and others, 2011). Although these data provide an indication of water-level fluctuations and trends in parts of the area, periodic water-level measurements in an expanded network of existing wells provides additional information that can be used to map potentiometric surfaces of the aquifers and determine areas of recharge, discharge, and groundwater pumping. The last time an area-wide effort to measure groundwater levels in the aquifers and map their potentiometric surfaces was October/November 1994 (Barber, 1997). To determine the current groundwater conditions in southwestern Georgia, water levels were measured in 54 wells completed in the Clayton aquifer and 50 wells completed in the Claiborne aquifer during November 7–18, 2011. These data were used to construct water-level change maps for each aquifer (fig. 1).

A comparison of groundwater levels measured in the Clayton aquifer for November 2011 and October/November 1994 (Barber, 1997) indicates that water levels declined over most of the area. The water-level declines ranged from 2.51 to 75.8 feet (ft), with declines exceeding 30 ft in much of the area west of Albany, Dougherty County. The greatest declines, exceeding 50 ft, were measured in eastern Clay County, and a narrow band extending from southeastern Randolph to northwestern Dougherty County. Water levels rose 2.24 to 3.67 ft in eastern Dougherty County and 3.71 ft in a well in west-central Terrell County.

A comparison of groundwater levels measured in the Claiborne aquifer for November 2011 and October/November 1994 (Barber, 1997) indicates that water levels declined from 1.65 to 42.3 ft during 1994–2011. The greatest declines of 32.8 to 42.3 ft were measured in Dooly County.

Changes in groundwater levels in the two aquifers are related to alterations in pumping patterns that result from increased irrigation demand and reduced withdrawal for public supply at Albany.

## References

Barber, N.L., 1997, Potentiometric surfaces (fall 1994) and water-level fluctuations and trends in the Clayton and Claiborne aquifers in Southwestern Georgia: Georgia Geologic Survey Hydrologic Atlas 21, 1 plate.

Peck, M.F., Leeth, D.C., and Painter, J.A., 2011, Groundwater conditions and studies in Georgia, 2008–2009: U.S. Geological Survey Scientific Investigations Report 2011–5048, 83 p., available online at *http://pubs.usgs.gov/sir/2011/5048/*.

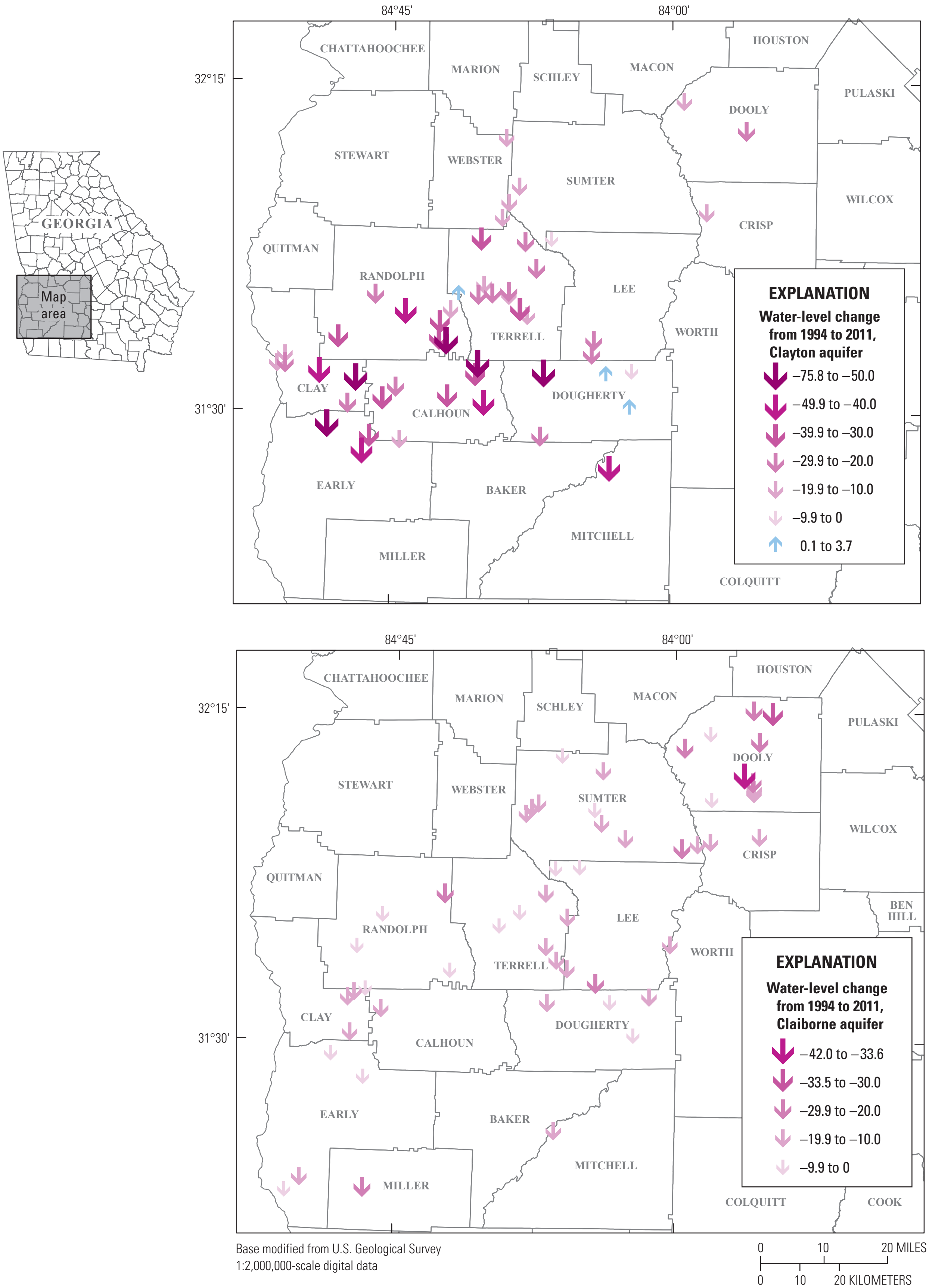


**Figure 1.** Change in water level in the Clayton and Claiborne aquifers from 1994 to 2011.

# Estimation of Reservoir Storage Capacity Using Terrestrial Lidar and Multibeam Sonar, Randy Poynter Lake, Rockdale County, Georgia

By Kathryn G. Lee

## Abstract

Randy Poynter Lake is a 650-acre reservoir that was constructed to meet the drinking-water needs of Rockdale County, Georgia. The lake formed following impoundment of Big Haynes Creek from the construction of Jack Turner Dam in Black Shoals Park about 6 miles north of Conyers (fig. 1). Suspended-sediment monitoring on Big Haynes Creek indicated excessive sediment yields upstream from the reservoir. Thus, an accurate three-dimensional model of the lake was needed to provide the current storage capacity of the lake as well as to establish a baseline for monitoring sedimentation in the future. In 2012, the U.S. Geological Survey (USGS), in cooperation with the Rockdale County Department of Water Resources, collected topographic and bathymetric data simultaneously at Randy Poynter Lake using a marine-based mobile mapping unit to estimate storage capacity. The marine-based mobile mapping unit has several components: a multibeam echo sounder (MBES), a single beam echo sounder (SBES), a light-detection and ranging (LIDAR) system, a navigation and motion-sensing system, and a data-acquisition computer.

Bathymetric data (fig. 2) were collected using the MBES and SBES. The MBES collects a wide swath of high-resolution bathymetric data by recording the intensity of sound reflected off the lake bottom (acoustic backscatter). Additional data were collected in shallow areas using the SBES to fill data gaps and verify the data collected with the MBES. Topographic data were collected using LIDAR around the perimeter of the lake (fig. 3). Elevation data were collected using a real-time kinematic (RTK) global positioning system (GPS) at various target locations to verify the topographic data. The data collected by the MBES, SBES, and LIDAR are represented accurately in three-dimensional space by using the navigation and motion-sensing system. A temporary bench mark was established, and a GPS base station was used to aid in the accuracy of the survey.

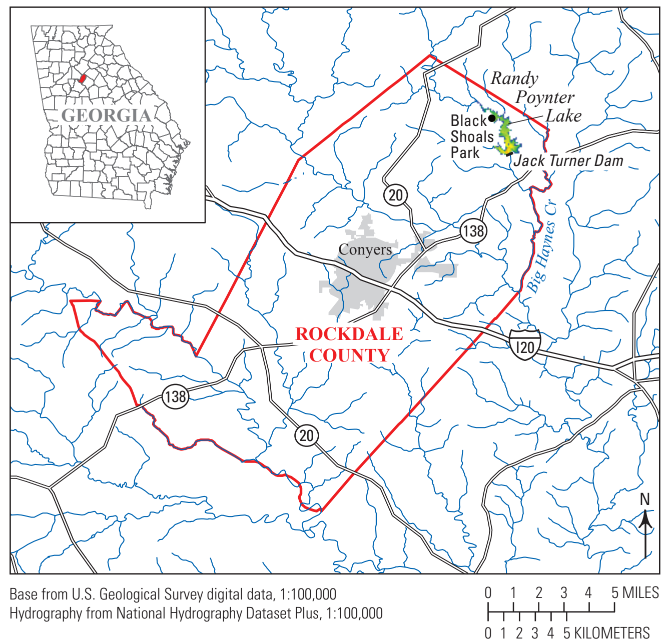


**Figure 1.** Location of Randy Poynter Lake, Rockdale County, Georgia.

The marine-based mobile mapping unit was deployed on July 16–21 and August 13–16, 2012. The MBES data were collected in longitudinal transects to provide a complete swath of the reservoir. The SBES data were collected by driving the shoreline and surveying cross sections in desired locations. The LIDAR data were collected at an equal distance from the shoreline. To fill any data gaps, RTK GPS data were collected during these same dates as well as during June 18–20, 2012. The objectives of this study are to (1) create a three-dimensional model above and below the water surface by combining bathymetry and LiDAR datasets, and (2) generate a stage-storage curve for the reservoir.

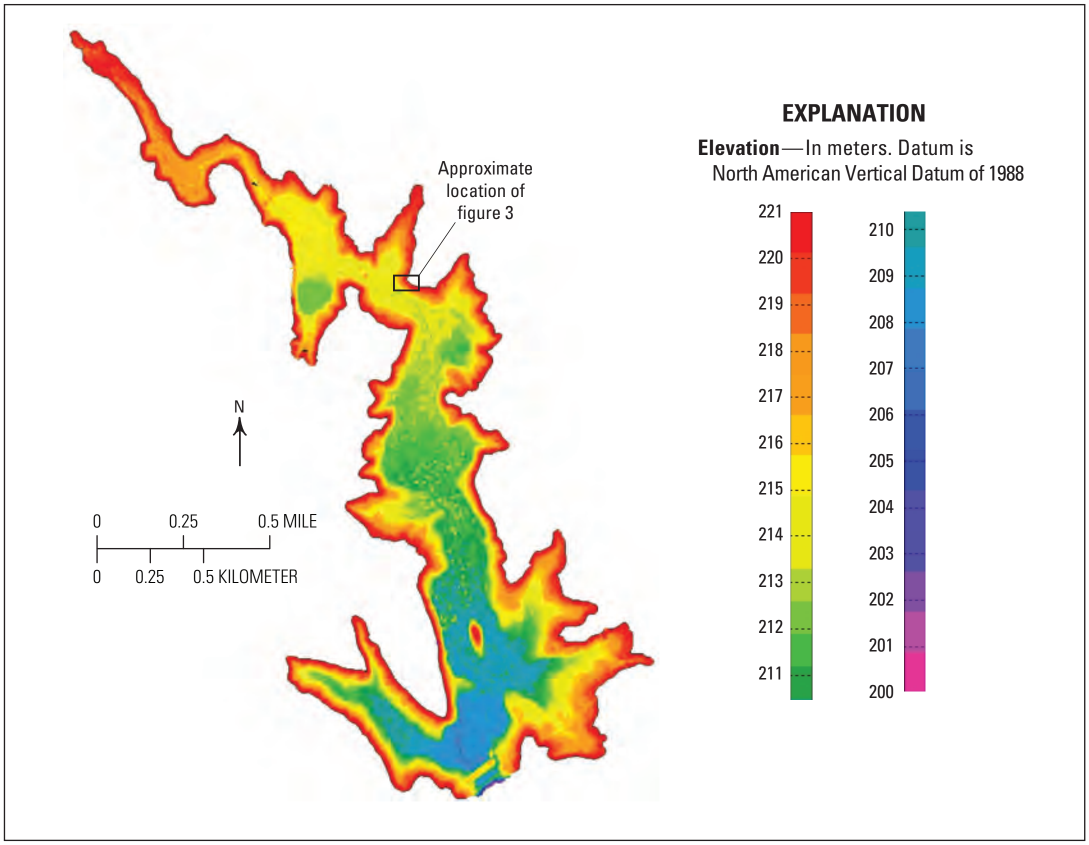


**Figure 2.** Preliminary bathymetric data collected at Randy Poynter Lake, Rockdale County, Georgia, 2012.

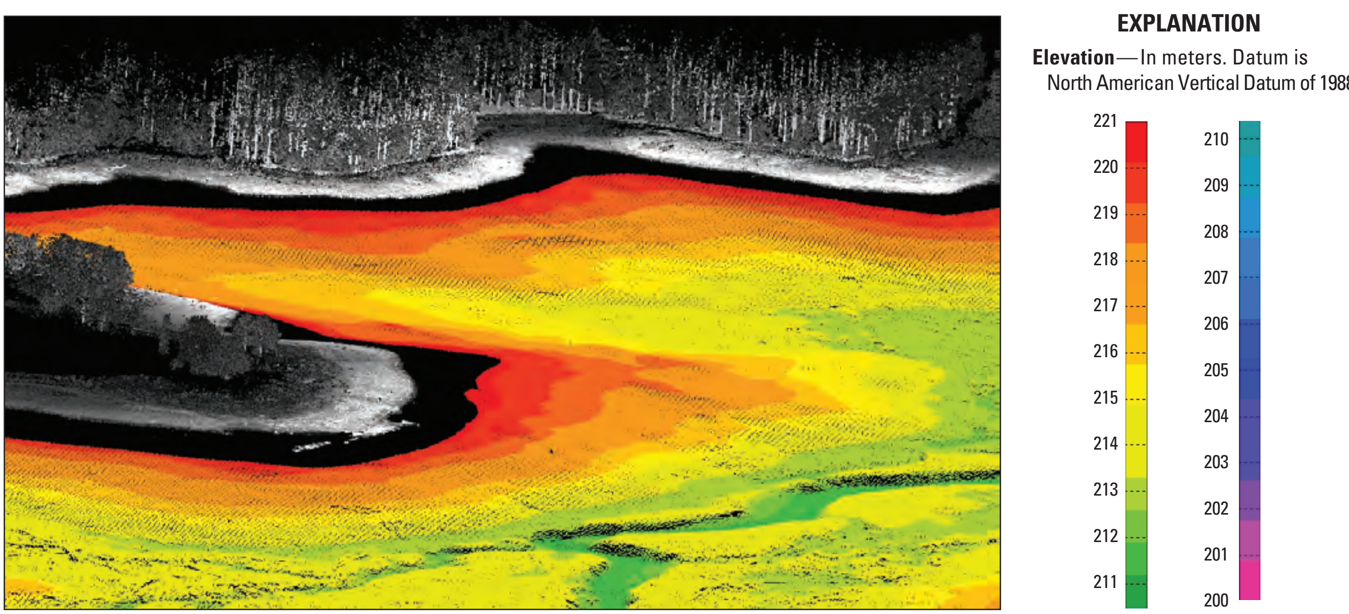


**Figure 3.** Preliminary bathymetric and topographic data collected at Randy Poynter Lake, Rockdale County, Georgia, 2012. View is looking south.

# USGS WaterSMART—Providing Information and Tools for Managing Water in the Apalachicola–Chattahoochee–Flint River Basin, Alabama, Florida, and Georgia

By W. Brian Hughes,[1] John S. Clarke,[1] Mary C. Freeman,[2] John W. Jones,[3] L. Elliott Jones,[1] Jacob H. LaFontaine,[1] Stephen J. Walsh[4]

## Abstract

During the last 50 years, the Apalachicola–Chattahoochee–Flint (ACF) River Basin in Alabama, Florida, and Georgia has undergone extensive development of water resources for municipal and industrial supplies, power generation, and agriculture. Concurrent with this development has been increasing conflict over the use of water in the ACF River Basin, resulting in legal battles over the rights to this valuable resource. The U.S. Geological Survey (USGS) is studying the ACF River Basin as part of the Department of the Interior's initiative, "Water: Sustain and Manage America's Resources for Tomorrow" (WaterSMART), to provide improved water-availability information and develop new tools to support water-management decisions. This federally funded, 3-year study has three major components that build on USGS data-collection and modeling capabilities—estimating water use, modeling surface and groundwater flow, and modeling ecosystem changes that result from flow alteration (ecological flows). The water-use component is to develop a site-specific database of water use for the ACF River Basin, develop new methods for estimating agricultural water use, and compile available water-use projections. Calculations of net water use can be improved by obtaining information on interbasin transfers, determining septic-tank return flows, and estimating consumptive use by thermoelectric plants. The hydrologic modeling component consists of the development of a surface-water model for the entire ACF River Basin using the USGS Precipitation-Runoff Modeling System (PRMS) and a MODFLOW groundwater-flow model for the lower Chattahoochee and Flint River Basins. These models can be linked to provide improved simulation of the effects of groundwater use in the lower part of the basin on streamflow. The ecological-flows component relies on the use of ecological models to predict changes in fish- and mussel-species occupancy based on variations in flow conditions associated with climate change, land-use change, and changes in water withdrawals or discharges.

## Introduction

Conflict over water resources in the Apalachicola–Chattahoochee–Flint (ACF) River Basin (fig. 1) among Alabama, Florida, and Georgia has resulted from increases in water use for municipal and industrial supplies, power generation, and agriculture as areas in the basin have grown and developed over the past 50 years. Conflict over water is not limited to States; during drought conditions, competition among different water- use sectors within States can become pronounced. A primary example of this is the legal actions arising from numerous uses of Lake Sidney Lanier near Atlanta, Georgia (U.S. Army Corps of Engineers, 2012). These uses include water supply, power generation, maintenance of water quality, supply for downstream reservoirs, and minimum flows to support aquatic species. The debate over water availability in the basin has focused on the management of water in reservoirs that are operated by the U.S. Army Corps of Engineers. In years of normal rainfall, these reservoirs have sufficient storage to meet human needs and maintain streamflows. Information for reservoir management of flows in the ACF River Basin main stem rivers is largely available. However, information on many factors that influence water availability, specifically water withdrawals and wastewater returns, groundwater pumping for irrigation, interbasin transfers, storage in unmanaged reservoirs, effects of increased impervious surfaces, and climate variability, have received less detailed study. These less-examined factors are the primary targets of the WaterSMART ACF Geographic Focus Area Study, which is designed to inform various Federal, State, and local groups involved in interstate water-supply negotiations and overall management of the ACF River Basin.

[1]U.S. Geological Survey, Georgia Water Science Center, Norcross, Georgia.

[2]Patuxent Wildlife Research Center, Institute of Ecology, University of Georgia, Athens, Georgia.

[3]U.S. Geological Survey, Eastern Geographic Science Center, Reston, Virginia.

[4]U.S. Geological Survey, Southeast Ecological Science Center, Gainesville, Florida.

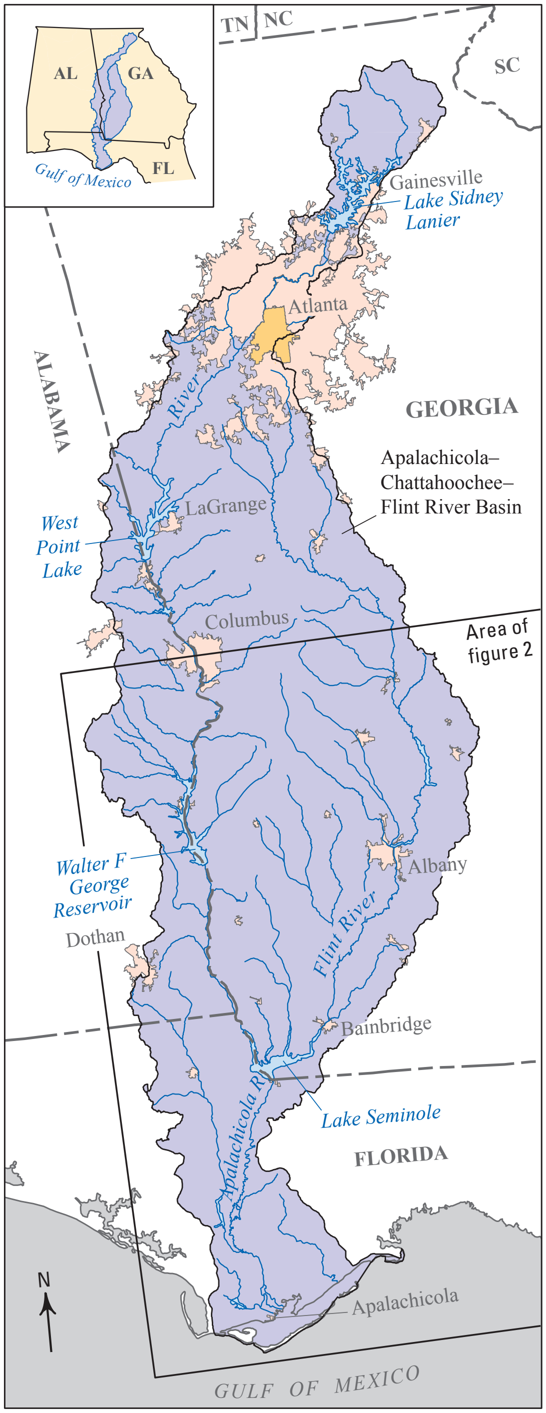


**Figure 1.** The WaterSMART Geographic Focus Area Study in the Apalachicola–Chattahoochee–Flint River Basin will build on existing USGS data collection and modeling capabilities to enhance estimates of water use, develop linked surface-water and ground models, and develop relations between streamflow and ecological conditions.

## Study Description

The Geographic Focus Area Study in the ACF River Basin is part of a much larger Department of the Interior initiative known as WaterSMART, which provides funds to support a sustainable water strategy to meet the Nation's current and future water needs (National Research Council, 2009). WaterSMART was authorized by Congress to support the National Water Census and to move toward the goals described in the SECURE Water Act of 2009. The SECURE Water Act requires the USGS to report back to Congress on progress made every 5 years. The Water Census provides for a series of studies focused on areas where competition for water has reached a level of national concern. The USGS is currently assessing water availability in three Geographic Focus Area Studies: (1) Apalachicola–Chattahoochee–Flint River Basin, (2) Colorado River Basin, and (3) Delaware River Basin.

The ACF Focus Area Study has three major components that build on ongoing USGS data-collection and modeling capabilities: (1) estimating water use, (2) modeling surface-water and groundwater flow, and (3) developing relations between streamflow and ecological conditions (ecological flows). A site-specific database of water use for the ACF River Basin and improved methods for estimating agricultural water use are being developed for the water-use component, and available water-use projections are being compiled. Calculations of net water use can be improved by obtaining information on interbasin transfers, determining septic-tank return flows, and estimating consumptive use by thermoelectric power plants. The hydrologic modeling component consists of a surface-water model for the entire ACF River Basin and a groundwater-flow model for the lower ACF River Basin. These models can be linked where agricultural pumpage of groundwater is greatest to provide improved simulation of how groundwater use affects streamflow conditions. The ecological flows component uses ecological models to predict changes in fish- and mussel-species occupancy based on variations in flow conditions associated with climate change, land-use change, and changes in water withdrawals or discharges (Freeman and others, 2012).

The enhanced water-use information and linked surface-water and groundwater models can inform water availability assessments at finer scales than information currently available for flow-regulated, main-stem rivers. Enhanced surface-water and groundwater models also provide input to the ecological models that predict changes in fish and mussel populations, including endangered and threatened species, in streams that flow into the main-stem rivers. Together, the databases and models can be used to make better decisions regarding how future growth and water use could affect water availability for diverse uses, including support of aquatic ecosystems.

The ACF Focus Area Study is complex and interdisciplinary, combining expertise from scientists that work in the Climate and Land Use Change, Ecosystems, and Water mission areas of the USGS. New data-collection activities are limited primarily to a low-flow synoptic study completed in 2011 (fig. 2; Gordon and others, 2012), data-collection for the

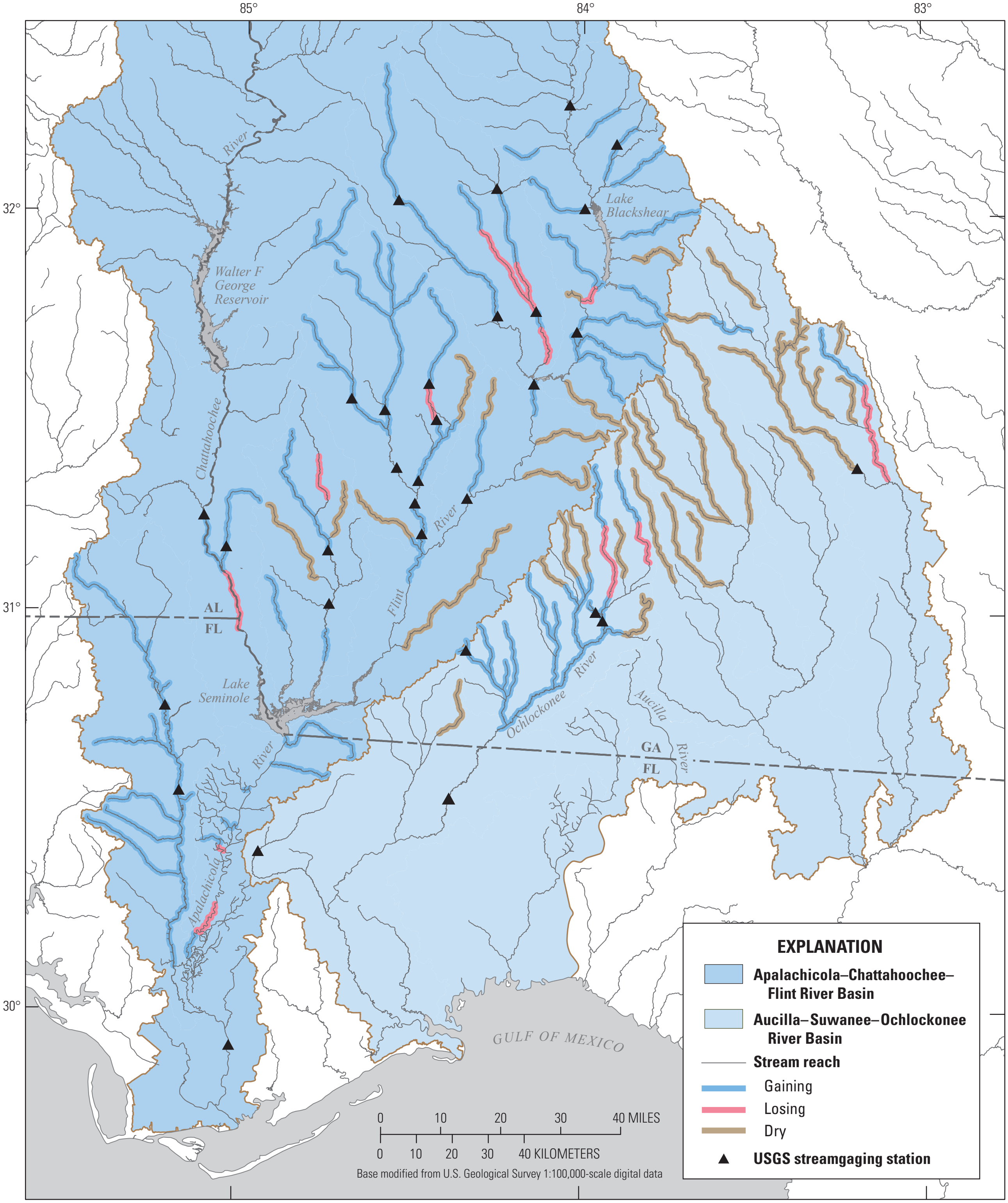


**Figure 2.** USGS measured streamflow at 267 sites in the lower Apalachicola–Chattahoochee–Flint River Basin and western and central parts of the Aucilla–Suwanee–Ochlockonee River Basin during July 2011 to measure the effects of drought and irrigation withdrawals on streamflow. In this part of the basin, water pumped from the Upper Floridan aquifer reduces flows in larger streams such as the Flint River and can completely dry out some smaller streams. For this period in July 2011, stream reaches losing water to the Upper Floridan aquifer are shown in red, those gaining water from the aquifer are blue, and dry reaches are brown (modified from Gordon and others, 2012).

septic tank return-flow study, and ecological and streamflow data collection. Project activities are closely coordinated with other Federal agencies, State agencies, and independent groups, such as the ACF Stakeholders and American Rivers. Numerous meetings and presentations have been made to obtain input from these groups, keep them involved and updated on our progress, and leverage resources where possible. Project activities began in 2011, and project completion is planned for 2014. Planned products include enhanced water-use estimates for the ACF River Basin, hydrologic models, ecological models, and reports presenting study results.

## References Cited

Freeman, M.C., Buell, G.R., Hay, L.E., Hughes, W.B, Jacobson, R.B., Jones, J.W., Jones, S.A., Lafontaine, J.H., Odom, K.R., Peterson, J.T., Riley, J.W., Schindler, J.S., Shea, C., and Weaver, J.D., 2012, Linking river management to species conservation using dynamic landscape-scale models: Wiley Online Library, River Research and Applications, published April 20, 2012, at *http://dx.doi.org/10.1002/rra.2575*.

Gordon, D.W., Peck, M.F., and Painter, J.A., 2012, Hydrologic and water-quality conditions in the lower Apalachicola–Chattahoochee–Flint and parts of the Aucilla–Suwannee–Ochlockonee River Basins in Georgia and adjacent parts of Florida and Alabama during drought conditions, July 2011: U.S. Geological Survey Scientific Investigations Report 2012–5179, 69 p., available at *http://pubs.usgs.gov/sir/2012/5179/*.

National Research Council, 2009, Toward a sustainable and secure water future: a leadership role for the U.S. Geological Survey: Washington, DC, National Academies Press, 114 p.

U.S. Army Corps of Engineers, 2012, Memorandum for the Chief of Engineers: Authority to provide for municipal and industrial water supply from the Buford Dam/Lake Lanier Project, Georgia, 48 p., accessed October 17, 2012, at *http://www.sam.usace.army.mil/2012ACF_legalopinion.pdf*.

# The Use of Downscaled Climate Data in Hydrologic and Stream Temperature Models in the Apalachicola–Chattahoochee–Flint River Basin, Southeastern USA

Jacob H. LaFontaine[1] and Lauren E. Hay[2]

## Abstract

The ability to replicate the grid-to-grid correlations of the measured environment (temperature and precipitation) using statistically downscaled Global Climate Models (GCMs) and the implications of inflated spatial correlation when downscaled results are used as input for hydrological and stream temperature models were examined in the Apalachicola–Chattahoochee–Flint River Basin. As part of the U.S. Geological Survey Southeast Regional Assessment Project, hydrologic and stream temperature models were developed as part of a portfolio of science tools to help environmental resource managers assess potential effects of climate change on ecosystems. In an effort to assess the uncertainties associated with using GCM output in basin-scale applications, inputs of measured and downscaled GCM climate data were used to drive the hydrology and water temperature models on a daily timestep for historical conditions (1960–99). Correlation matrices of climate, as well as simulations of streamflow components and stream temperature showed that downscaled GCM climate data were more highly correlated than the gridded observation dataset based on measured data for temperature, precipitation, surface runoff, and shallow subsurface runoff. The basin response between measured and GCM inputs was more similar for total streamflow, groundwater flow, and water temperature. The downscaled GCMs also simulated larger regions of wet days, drizzle days, and temperatures above 95 degrees Fahrenheit and below freezing across the basin compared to the inputs based on measured data. Despite the inflated spatial correlation in GCM grid-to-grid temperature and precipitation inputs, however, these do not transfer significant inflated spatial correlation to total streamflow or water temperature. As a result, users can have some confidence that the simulations of total streamflow and stream temperature produced using downscaled GCM inputs represent a reasonable basin-wide spatial response.

## Introduction

The U.S. Geological Survey (USGS) National Climate Change and Wildlife Science Center (NCCWSC; *http://nccwsc.usgs.gov/*), through 8 regionally based Climate Science Centers, (CSC) has undertaken a series of assessments to provide integrated science useful to resource managers for understanding the impact of climate change on a range of ecosystem responses by linking simulation models that span a broad range of scales and themes, from Global Climate Models (GCMs) to local models of hydrology and biota (fig. 1). The Southeast Regional Assessment Project (SERAP; *http://serap.er.usgs.gov*) was the first regional assessment to be funded by the NCCWSC and Southeast CSC. SERAP was

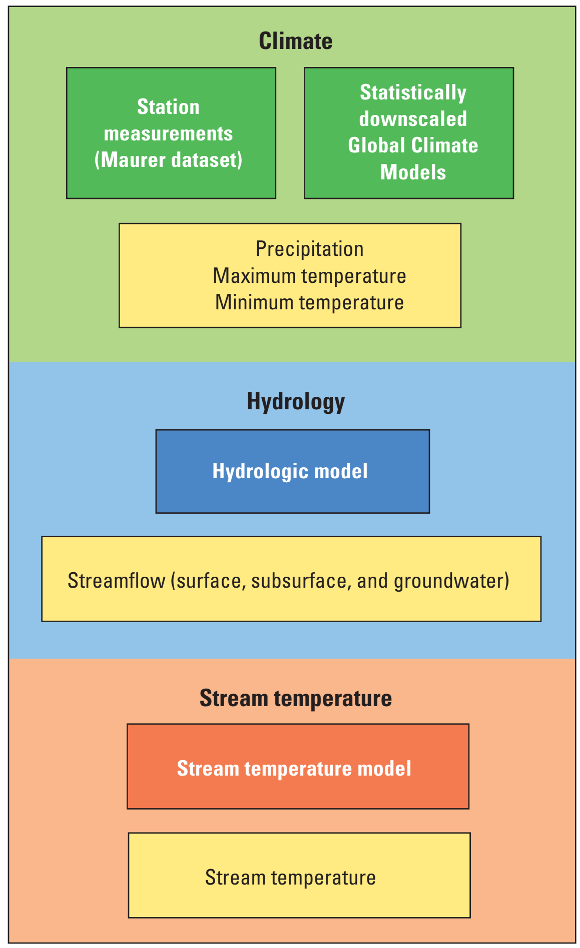


**Figure 1.** A subset of the Southeast Regional Assessment Project (SERAP; *http://serap.er.usgs.gov*) data flow focused on interactions of climate, hydrology, and stream temperature. Yellow boxes describe model outputs for climate, hydrology and stream temperature models, which are used in subsequent steps. For full SERAP data flow see LaFontaine and others (2011).

[1] U.S. Geological Survey, Georgia Water Science Center, Norcross, Georgia.

[2] U.S. Geological Survey, National Research Program, Lakewood, Colorado.

developed in close coordination with the Department of the Interior Landscape Conservation Cooperatives (*http://www.doi.gov/lcc/index.cfm*) to ensure that it meets the needs of resource managers in the southeastern United States. SERAP is developing regional models and other science tools to help environmental resource managers assess potential effects of climate change on ecosystems and priority species in the region.

Within SERAP, two important components are the development of hydrologic and stream temperature models for the Apalachicola–Chattahoochee–Flint (ACF) River Basin (fig. 2) and the corresponding climatic data sets to drive these models for historical and future conditions. In recent decades, competing demands of municipal, industrial, and agricultural water use, ecological needs of fishes and mussels, and economic development have resulted in conflict and discussions between stakeholders in Alabama, Florida, and Georgia over water allocation in the ACF River Basin. These pressures, coupled with the effects of climatic variability and potential climatic change, have stimulated research efforts to develop better water management tools, which include the use of atmospheric model output from GCMs in hydrologic and stream temperature models.

GCMs are developed by imposing a grid on the globe to divide the atmosphere into spatial units, which are then transferred to the land surface. In using this delineation at a global scale, the grid represents physiographic features much more smoothly than the real world and cannot properly resolve many atmospheric processes that have hydrologic consequences. Hydrologic modeling at the basin level requires climatological information at scales that are generally much finer than the typical grid size of even the highest resolution GCMs commonly used for climate simulations. Statistical or dynamical downscaling techniques are necessary to provide GCM climate information at the finer scales appropriate for studying the effects of climate change at the basin scale. For this study, statistical downscaling was chosen to provide climate projections for hydrologic and stream temperature simulations.

Statistical downscaling uses empirical relations between features reliably simulated by a GCM at grid box scales (e.g., 500 hectopascals (hPa) geopotential height) and surface predictands at subgrid scales (e.g., precipitation occurrence and amounts). An overview of statistical GCM downscaling techniques for hydrologic modeling is presented in Fowler and others (2007). The projections from statistical downscaling are at a finer scale than GCMs, but still have uncertainties; statistical downscaling is sensitive to the choice of predictors and GCM ability to simulate these predictors, cannot simulate any systematic changes in regional forcings, and is based on the assumption that relationships between large-scale features and local climate remain stationary under future change (Hayhoe 2010).

For the SERAP, GCM output was statistically downscaled to a 1/8-degree grid. An additional source of uncertainty therefore arises: all grid points within a single GCM grid cell will necessarily exhibit high temporal correlation, maybe more than would naturally occur. Table 1 shows that the number of

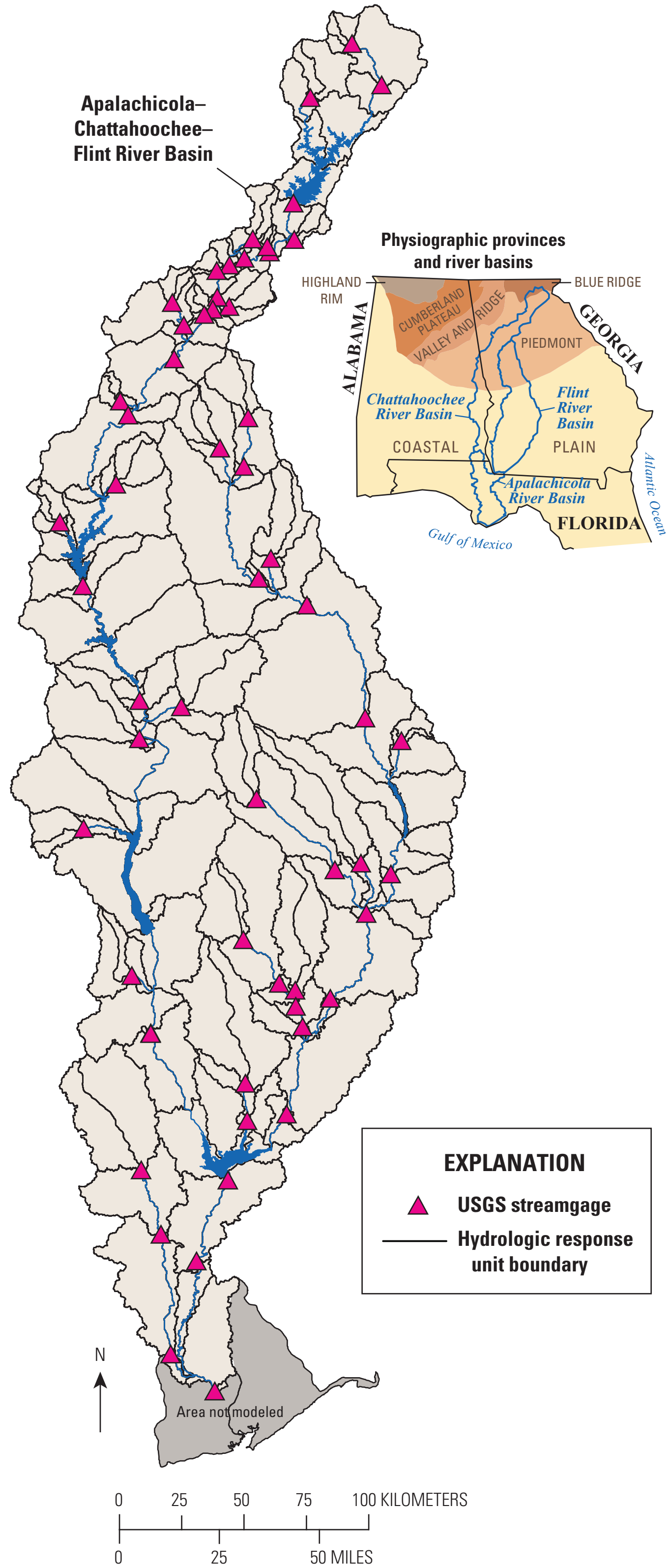


**Figure 2.** Overview map of the Apalachicola–Chattahoochee–Flint River Basin.

GCM cells needed to cover the ACF River Basin range from roughly 0.7 (Parallel Climate Model [PCM]) to 2.8 (Community Climate System Model version 3 [CCSM3])—orders of magnitude less than the 357 cells associated with the gridded observation inputs based on measured climatological data (Maurer and others, 2002). All of the temporal variability will be shared with the GCM cell and thus with each 1/8-degree grid cell within the GCM cell; for example, all 1/8-degree grids within a GCM grid cell will get unusually cold (hot) or will get wet (dry) together on any given day.

This paper examines the ability of the statistically downscaled GCMs chosen for SERAP to replicate the grid-to-grid correlations between temperatures and precipitation and the implications of inflated spatial correlation when downscaled results are used as input for hydrological and stream-temperature models. The following sections present an evaluation of statistically downscaled precipitation and maximum/minimum temperature from a set of GCMs (table 1) for historical conditions (1960–1999) and the propagation of the uncertainty from these downscaled estimates through the chain of models shown in figure 1.

**Table 1.** Global Climate Model sources and horizontal spatial resolutions.

[CCSM3, Community Climate System Model version 3; GFDL, Geophysical Fluid Dynamics Laboratory; PCM, Parallel Climate Model]

| Model name | Origin | Horizontal resolution (degrees) | Approximate number of grid cells in model by area |
|---|---|---|---|
| Maurer and others (2002) | National Oceanic and Atmospheric Administration coop station data | 0.125 × 0.125 | 357 |
| CCSM3 | National Center for Atmospheric Research, USA | 1.4 × 1.4 | 2.8 |
| GFDL | National Oceanic and Atmospheric Administration/ Geophysical Fluid Dynamics Laboratory | 2.0 × 2.5 | 1.1 |
| PCM | Department of Energy sponsored collaboration | 2.8 × 2.8 | 0.7 |

## Climate Data and Simulations

Hydrology and stream temperature models were driven with inputs derived from (1) gridded station measurements of air temperature and precipitation and (2) statistically downscaled GCMs. All climate inputs were made available through the USGS Geo Data Portal (GDP; *http://cida.usgs.gov/climate/gdp/*). The GDP was used to summarize the daily values of precipitation and maximum/minimum temperature from the station and downscaled GCM datasets to the appropriate spatial units for each model.

### Measured Data

The daily gridded precipitation and temperature dataset developed by Maurer and others (2002; referred to as the “Maurer dataset”) for the period 1950–1999 was chosen to provide a consistent framework across the project tasks in the SERAP for both historical and future climate conditions. These precipitation and maximum/minimum temperature grids were developed for the conterminous United States at a 1/8-degree cell size (approximately 140 square kilometers [$km^2$]) using the National Oceanic and Atmospheric Administration Cooperative network of climate stations, which covers the United States with an average density of about one station per 700 $km^2$.

### Statistically-Downscaled GCM Climate Simulations

For the SERAP study, daily precipitation and maximum/minimum temperature output from three GCMs were statistically downscaled to the Maurer dataset using a Modified Statistical Asynchronous Regression method (Stoner and others, 2012; *http://cida.usgs.gov/climate/hayhoe_projections.jsp*) for the period 1960–2099. This approach was originally proposed by O’Brien and others (2001) and applied by Dettinger and others (2004). The original methodology was modified to improve simulation of extremes and tails of the daily distribution. For precipitation, a mixture model clustering approach was used including nonhomogeneous transition probabilities to model the occurrence and intensity of daily precipitation (Vrac and others, 2007). This dual-downscaling method was applied as part of the NCCWSC effort to provide timely “best science” information and includes retrospective downscaled GCM simulations for the years 1960–1999.

## Hydrologic Model

The USGS Precipitation Runoff Modeling System (PRMS) was used as the hydrologic model in the ACF River Basin. PRMS is a modular, deterministic, distributed-parameter, physical-process-based hydrologic model used to simulate and evaluate the effects of various combinations of precipitation, climate, and land use on the hydrologic cycle. Each hydrologic component used to simulate the generation of streamflow is represented within PRMS by a process algorithm that is based on a physical law or empirical relation with measured or estimated characteristics. The reader is referred to Leavesley and others (1983), Leavesley and Stannard (1995), Leavesley and others (2005), and Markstrom and others (2008) for a complete description of PRMS.

The ACF PRMS model for the SERAP is detailed in LaFontaine and others (2011). The ACF PRMS model was divided into hydrologic response units (HRUs) in which the components of flow (groundwater, subsurface, and surface runoff) are computed in response to precipitation, air temperature, land surface, and subsurface characteristics of the basin. The Maurer dataset of daily maximum and minimum temperature and precipitation on a 1/8-degree grid were used as PRMS inputs for the period 1950–1999. Thirty-five USGS streamflow gages were used for PRMS calibration and evaluation. An automated procedure combined with a nested modeling approach was developed to calibrate the ACF PRMS model (LaFontaine and others, 2011). The resulting PRMS model simulates "natural" flow on a daily time step for the period 1950–1999.

## Stream Temperature Model

The Stream Network Temperature model (SNTemp) was used to predict stream water temperatures based on hydrological, meteorological, topographic, vegetative shading, and stream-channel conditions in the ACF River Basin. SNTemp is a mechanistic, one-dimensional heat transport model developed for branched stream networks that predicts the daily mean and maximum water temperatures as a function of stream distance and environmental heat flux. SNTemp incorporates (1) a heat transport model that predicts the daily-mean water temperature and diurnal fluctuations in water temperature as functions of stream distance, (2) a heat flux model that predicts the energy balance between the water and its surrounding environment, and (3) a shade model that predicts the solar radiation-weighted shading resulting from both topography and riparian vegetation. The reader is referred to Theurer and others (1984) and Bartholow (2000) for a complete description of SNTemp.

The ACF SNTemp model for the SERAP was developed using the same stream network (128 stream segments) and spatial units used in the ACF PRMS model. The ACF SNTemp model was calibrated to long-term mean-monthly (average of all values in a particular month for the period of interest) water temperature statistics developed by Dyar and Alhadeff (1997), which used a harmonic curve-fitting procedure based on data from 198 periodic and 22 daily record stations throughout Georgia for the period 1955–1984. The ACF SNTemp model was coupled with the ACF PRMS model using the USGS P2S software documented in Markstrom (2012).

## Methods

In the following section, the climate, hydrology, and stream temperature outputs in figure 1 (yellow boxes) are evaluated for historical conditions (1960–1999) by comparing simulations based on the Maurer dataset versus those produced from the three statistically downscaled GCMs (CCSM3, Geophysical Fluid Dynamics Laboratory model (GFDL), and PCM), similar to the comparison by Maurer and others (2010) .

Owing to the nature of the statistical downscaling technique, downscaled values that fall within a single GCM grid cell will exhibit high spatial and temporal correlations with each other because the day-to-day variability of the GCM grid cell is shared with every downscaled value that falls within it. To evaluate the ability of the statistically downscaled GCMs to replicate the grid-to-grid correlations between temperatures and precipitation of the Maurer dataset and the propagation of this inflated spatial correlation through the hydrology and stream temperature models, correlation matrices were computed between HRUs for daily output produced from climate and hydrology simulations, and stream segments for output produced from stream temperature simulations.

## Results and Discussion

Figure 3 shows the correlation matrix between HRUs for daily maximum and minimum temperature, and precipitation accumulation for the 1960–1999 period. The 1-to-1 line (correlation=1.0) appears as a thin, diagonal white band on each of the plots. The temperature data for both the Maurer dataset and the GCMs are highly correlated across the basin, generally in the range of 0.9–1.0. The precipitation data for the Maurer dataset display some spatial correlation patterns, but not nearly to the extent of what is shown for the downscaled GCMs. All downscaled GCMs show inflated spatial correlations between HRUs when compared to the Maurer dataset. This inflated spatial correlation appears to be related to GCM grid cell size; of the three GCMs, the CCSM3 has the finest grid cell resolution (1.4 degrees, table 1), and most closely matches the correlation patterns seen in the Maurer dataset, especially for precipitation.

To determine the effects of this inflated correlation on modeled precipitation characteristics, for each day and each dataset, the number of HRUs that were wet (any nonzero precipitation), dry (no precipitation), slightly wet (drizzle; nonzero precipitation less than 0.01 inch [0.254 millimeter]), or extremely wet (precipitation greater than 1 inch) were determined and summarized in figure 4. The Maurer dataset shows a higher variability in the number of HRUs that are concurrently wet and generally fewer HRUs with wet days occurring on the same day when compared with the downscaled GCMs (fig. 4*A*). Dry days are more variable, with GFDL showing a higher number of dry days occurring together than the other datasets (fig. 4*B*). The downscaled GCMs show a larger number of drizzle days occurring concurrently across the HRUs compared to the Maurer dataset (fig. 4*C*). The Maurer dataset and CCSM3 values show the most similar distribution of days with precipitation greater than 1 inch occurring concurrently across the HRUs, with the other downscaled GCMs indicating that precipitation greater than 1 inch occurs throughout the basin more often than measured (fig. 4*D*). In summary, when it is wet/dry somewhere in the basin, a larger portion of the basin will also be wet/dry based on the downscaled GCM results.

A similar analysis was conducted with the temperature data to determine the effects of this higher correlation (figs. 5*A*, *B*) on temperature. For each day and each dataset, the number of HRUs that were below freezing and above 95 degrees Fahrenheit (°F; 35 degrees Celsius [°C]), arbitrary thresholds, were determined and summarized in figure 5. The Maurer dataset shows fewer HRUs concurrently having

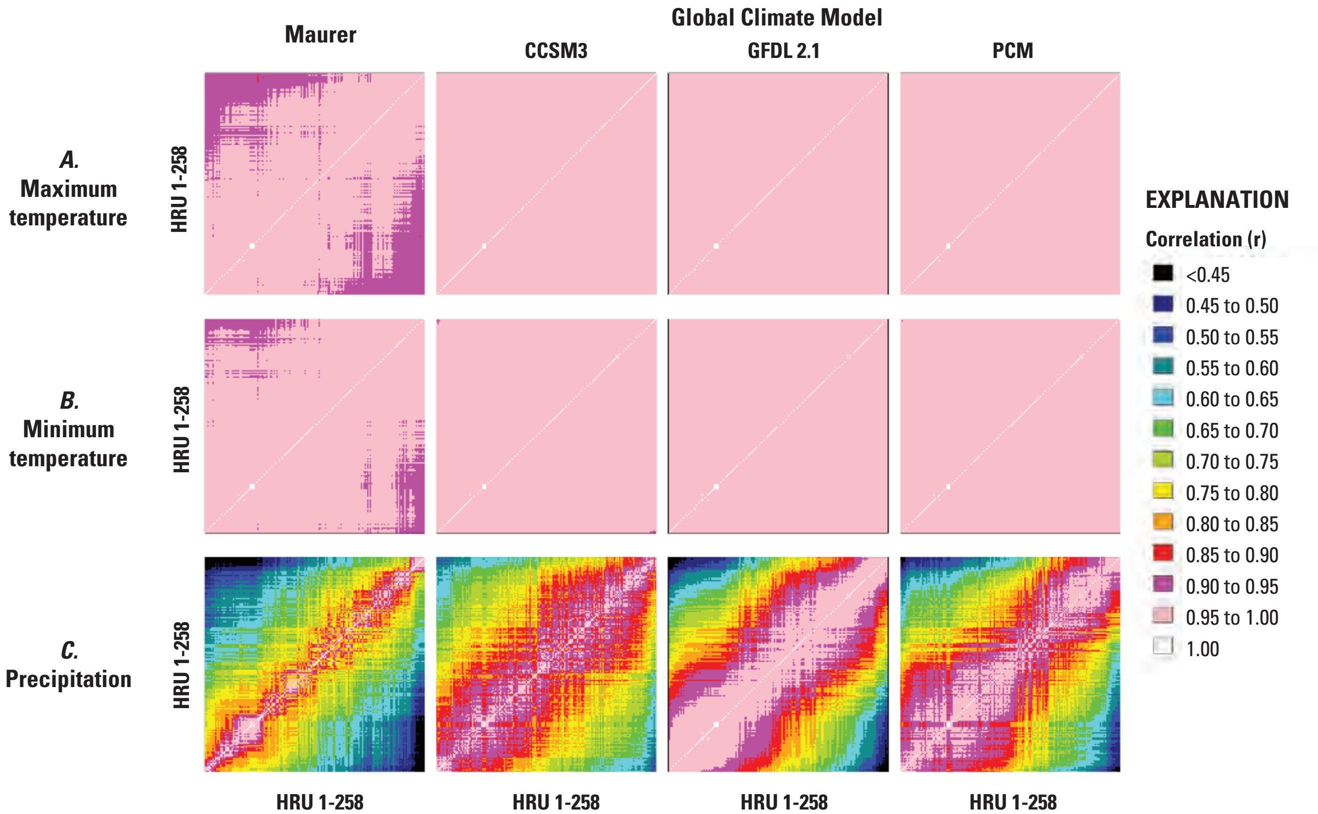


**Figure 3.** Hydrologic response unit (HRU) correlation matrix for *(A)* maximum temperature, *(B)* minimum temperature, and *(C)* precipitation for the Maurer and downscaled Global Climate Models (GCMs) (Community Climate System Model version 3.0 (CCSM3), Geophysical Fluid Dynamics Laboratory model version 2.1 (GFDL), and Parallel Climate Model (PCM)). GCMs are shown in order of increasing grid size from left to right.

**Figure 4.** The number of hydrologic response units (HRUs) that have *(A)* precipitation *(B)* no precipitation, *(C)* drizzle, and *(D)* precipitation greater than 1 inch on a given day. [CCSM3, Community Climate System Model version 3; GFDL, Geophysical Fluid Dynamics Laboratory; PCM, Parallel Climate Model]

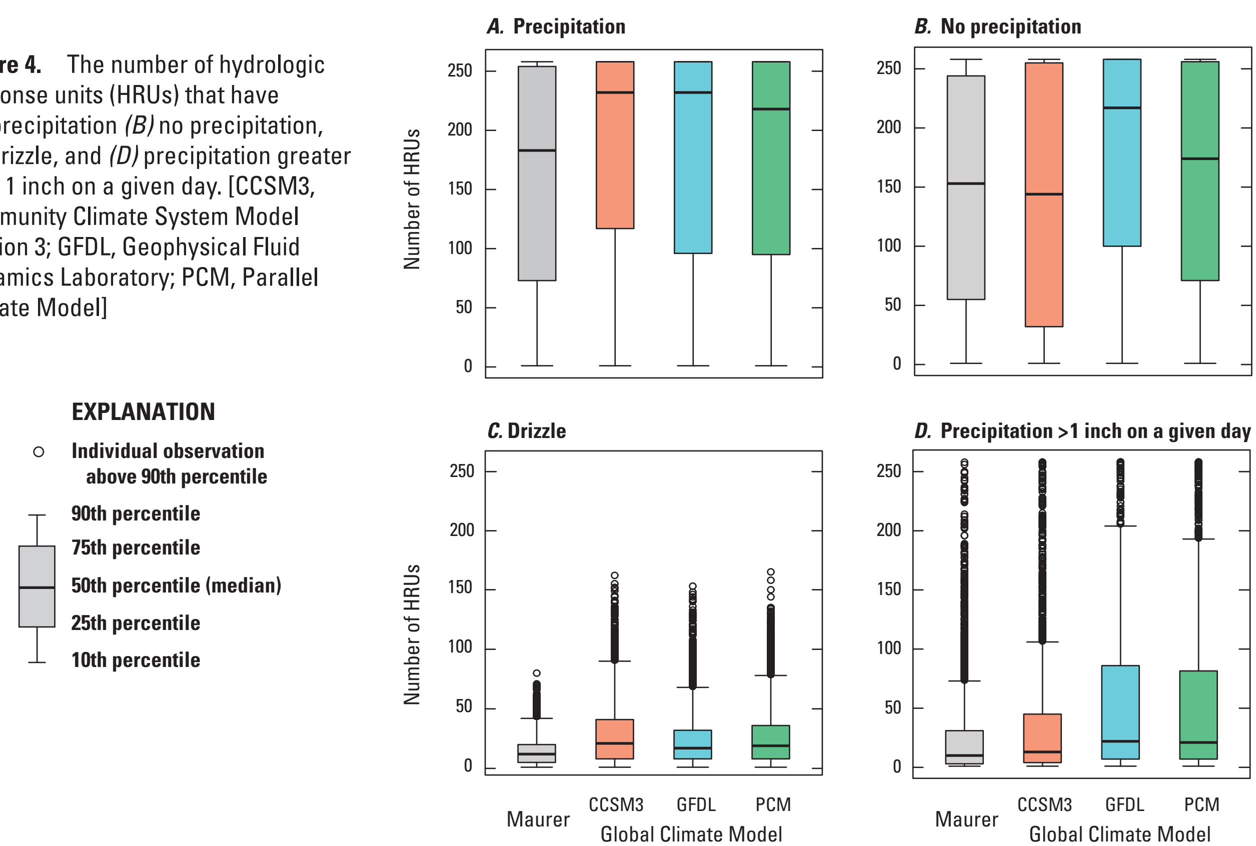

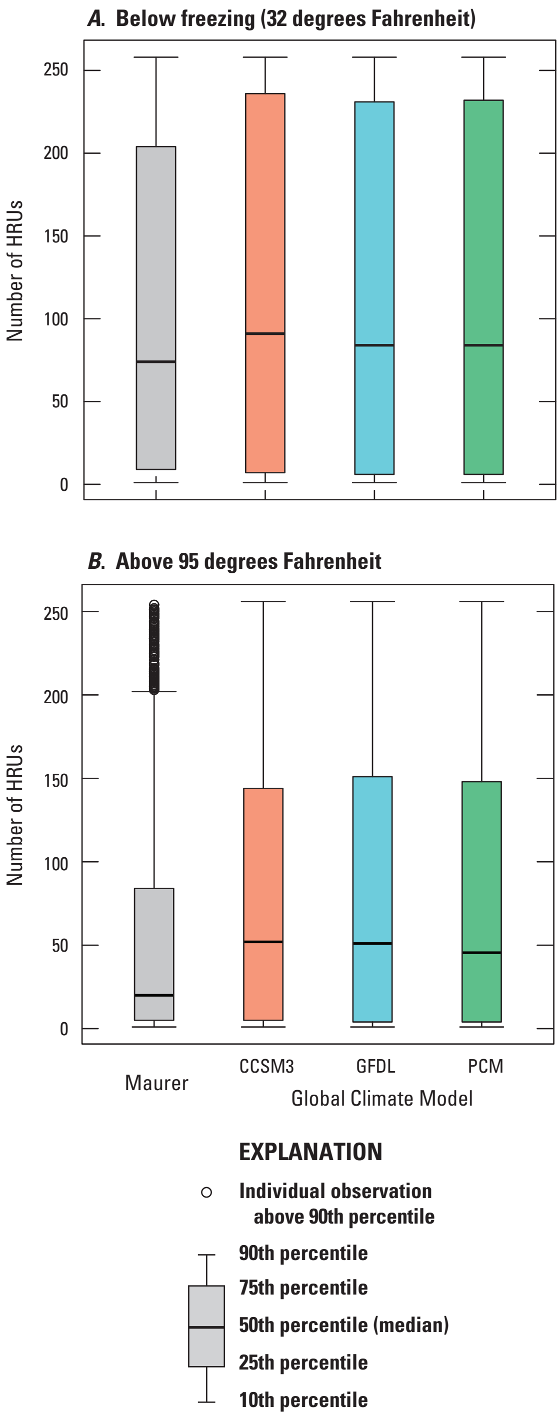


**Figure 5.** The number of hydrologic response units (HRUs) that have temperatures *(A)* below freezing (95 degrees Fahrenheit) and *(B)* above 95 degrees Fahrenheit (35 degrees Celsius) on a given day. [CCSM3, Community Climate System Model version 3; GFDL, Geophysical Fluid Dynamics Laboratory; PCM, Parallel Climate Model]

temperatures below freezing and above 95 °F (35 °C) when compared with the downscaled GCMs. Results from these analyses indicate that cold, hot, and wet days will occur together more often across the basin on any given day with the downscaled results. An interpretation that depends on spatial relations between climate variables (i.e., what percentage of the basin is wet/dry or hot/cold during a given day or season) may have increased uncertainty because of this inflated correlation.

Figure 6 shows the correlation matrix between HRUs for daily total flow and for surface runoff, shallow subsurface, and groundwater flow components output from the ACF PRMS model for the period 1960–1999 using the Maurer dataset and downscaled GCM temperature and precipitation inputs. The correlation matrices for the flow components show much less correlation than the climate correlations in figure 3. The total flow and groundwater correlation matrices (figs. 6*A*, *D*) display similar patterns for the model driven by the Maurer and downscaled GCM datasets. The surface and shallow subsurface correlation matrices display higher correlations for the model driven by the downscaled-GCM driven dataset compared to the Maurer dataset (figs. 6*B*, *C*). As the surface and shallow subsurface components of flow are more sensitive to precipitation events, the higher correlation of precipitation across the basin for the downscaled GCMs and the larger number of wet and drizzle days in the downscaled GCMs may explain the higher correlations for these flow components. The high correlation block of groundwater flow for the lower numbered HRUs in figure 6*D*, which is present in simulations driven by both the Maurer and downscaled GCM datasets, may result from the predominant crystalline aquifer geohydrology (Piedmont physiographic province) that dominates the northern region of the basin (fig. 2).

Figure 7 shows the correlation matrix between stream segments for simulated daily water temperature for the 1960–1999 period. The stream temperature correlation matrices simulated using PRMS hydrologic model results based on inputs from the Maurer dataset and the downscaled GCMs have relatively high correlations throughout much of the ACF River Basin. The correlation differences that were shown in the precipitation and streamflow components have been dampened in the stream temperature results. Because air temperature is highly correlated in the basin and is a significant driver of water temperature, this result is supported by the Maurer dataset/GCM comparison in figure 3. Weaker correlations in the lower-numbered stream segments (which are assigned to the headwater stream segments) are most likely a result of headwaters in the urban area around Atlanta, Georgia, in the northern part of the basin. These urban headwaters are dominated by surface runoff and shallow subsurface flow (caused by impervious surfaces), as opposed to groundwater flow dominating in the rest of the basin. As figures 6*B*, *C* shows, there are significant differences in the correlation matrices between simulations driven by the Maurer dataset and the downscaled GCMs. The dominant source of flow is the most likely driver for the weaker correlations in the lower-numbered stream segments.

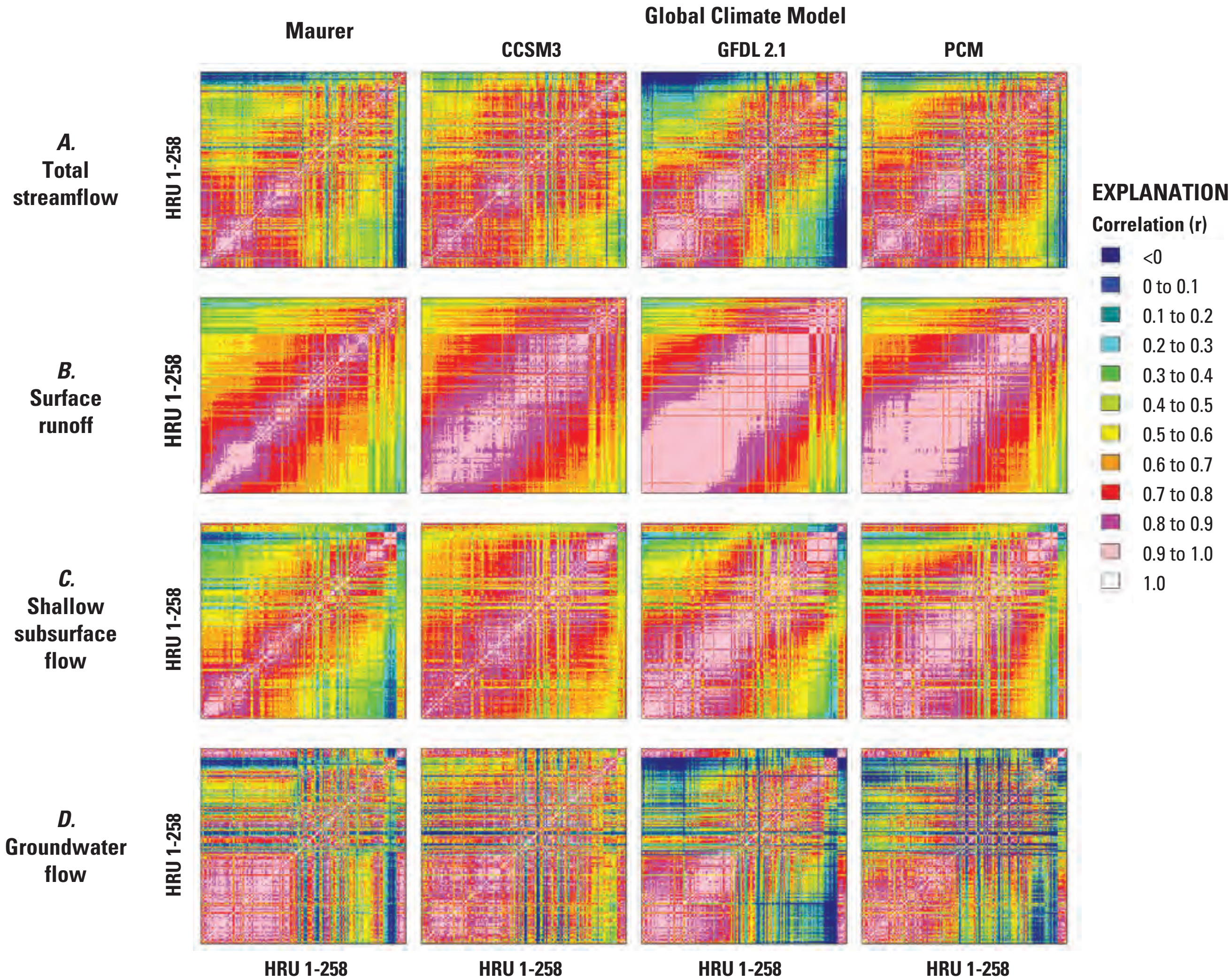


**Figure 6.** Hydrologic response unit (HRU) correlation matrix for *(A)* total, *(B)* surface, *(C)* subsurface, and *(D)* groundwater flow using the Maurer and downscaled Global Climate Model (GCM) (Community Climate System Model version 3.0 (CCSM3), Geophysical Fluid Dynamics Laboratory model version 2.1(GFDL), and Parallel Climate Model (PCM)) climate inputs.

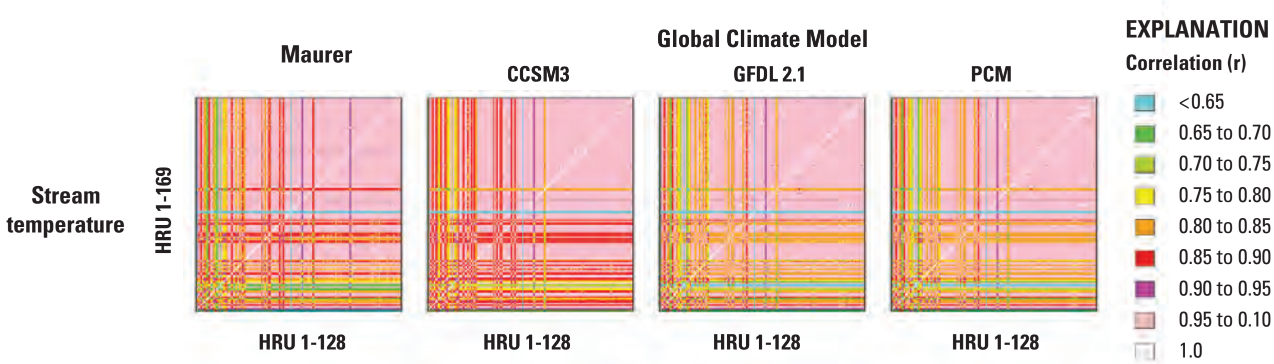


**Figure 7.** Stream segment correlation matrix for water temperature using the Maurer and downscaled Global Climate Model (GCM) (Community Climate System Model version 3.0 (CCSM3), Geophysical Fluid Dynamics Laboratory model version 2.1(GFDL), and Parallel Climate Model (PCM)) climate inputs.

## Summary and Conclusions

As part of the U.S. Geological Survey (USGS) Southeast Regional Assessment Project (SERAP), hydrologic and stream temperature models of the Apalachicola–Chattahoochee–Flint (ACF) River Basin were developed to help environmental resource managers assess potential effects of climate change on ecosystems. The hydrologic model was based on the USGS Precipitation Runoff Modeling System (PRMS) and the stream temperature model was based on the Stream Network Temperature model (SNTemp); these models simulated on a daily timestep and were linked using the USGS P2S software. In an effort to assess the uncertainties associated with using downscaled Global Climate Model (GCM) output in basin-scale applications, climate inputs based on observed data and downscaled GCM simulations were used to drive hydrologic and stream temperature models for the 1960–1999 period.

The scale at which the GCM grid cells were developed is much too coarse for use at the basin scale. The ability to replicate the grid-to-grid correlations between temperature and precipitation using the statistical downscaling approach chosen for SERAP and the implications of inflated correlation (because of GCM grid-cell size) when downscaled results are used as input for hydrological and stream temperature models were examined. Correlation matrices showed that the downscaled GCM climate outputs were more strongly correlated than the dataset based on observations for temperature, precipitation, surface runoff, and shallow subsurface flow. The basin response between measured and downscaled GCM inputs was more similar for total streamflow, groundwater flow, and water temperature. The downscaled GCMs simulated more wet (nonzero precipitation) and drizzle (nonzero precipitation less than 0.01 inch (0.254 millimeter)) days, as well as days with more than 1 inch of precipitation across the model spatial units, Hydrologic Response Units (HRUs), than the dataset based on observed data. The downscaled GCMs also simulated more HRUs having temperatures above 95 degrees Fahrenheit and below freezing than the dataset based on observed data. Despite the inflated correlation in downscaled GCM grid-to-grid temperature and precipitation inputs, however, these do not transfer as much inflated correlation to total streamflow, groundwater flow, or stream temperature as to surface runoff and shallow subsurface flow. As a result, users can have some confidence that the simulations of total streamflow and stream temperature produced using downscaled GCM inputs represent a reasonable basin-wide spatial response. These inflated correlations again are caused by large GCM grid cells, which have a homogenous behavior throughout each cell, being further discretized (downscaled) using finer resolution grids based on observed data. The spatial correlations documented for the climate, hydrology, and stream temperature simulations using downscaled GCMs, PRMS, and SNTemp must be considered when using these results to inform management decisions.

## Selected References

Bartholow, J.M., 2000, The stream segment and stream network temperature models: A self-study course: U.S. Geological Survey Open-File Report 99–112, 270 p.

Dettinger, M.D., Cayan, D.R., Meyer, M.K., and Jeton, A.E., 2004, Simulated hydrologic responses to climate variations and change in the Merced, Carson, and American River basins, Sierra Nevada, California, 1900–2099: Climate Change, v. 62, p. 283–317.

Dyar, T.R., and Alhadeff, S.J., 1997, Stream-temperature characteristics in Georgia: U.S. Geological Survey Water-Resources Investigations Report 96–4203, 150 p.

Fowler, H.J., Blenkinsop, S., and Tebaldi, C., 2007, Linking climate change modelling to impacts studies—Recent advances in downscaling techniques for hydrological modelling: International Journal of Climatology 27, p. 1547–1578.

Hayhoe, K.A., 2010, A standardized framework for evaluating the skill of regional climate downscaling techniques: University of Illinois at Urbana-Champaign, PhD. dissertation, 153 p.

LaFontaine, J.H., Hay, L.E., Viger, R., Markstrom, S., and Regan, R.S., 2011, Simulation of hydrologic response to climate and landscape change using the Precipitation Runoff Modeling System in the Apalachicola–Chattahoochee–Flint River Basin in the southeastern USA, *in* Proceedings of The Fourth Interagency Conference on Research in the Watersheds, September 26–30, 2011, Fairbanks, Alaska: U.S. Geological Survey Scientific Investigations Report 2011–5169, 226 p.

Leavesley, G.H., Lichty, R.W., Troutman, B.M., and Saindon, L.G., 1983, Precipitation-runoff modeling system—User's manual: U.S. Geological Survey Water-Resources Investigations Report 83–4238, 207 p.

Leavesley, G.H., Markstrom, S.L., Viger, R.J., and Hay, L.E., 2005, USGS Modular Modeling System (MMS)—Precipitation-Runoff Modeling System (PRMS) MMS-PRMS, *in* Singh, V.P., and Frevert, D.K., eds., Watershed Models: Boca Raton, Fla., CRC Press, p. 159–177.

Leavesley, G.H., and Stannard, L.G., 1995, The precipitation-runoff modeling system—PRMS, *in* Singh, V.P., ed., Computer models of watershed hydrology: Highlands Ranch, Colo., Water Resources Publications, p. 281–310.

Markstrom, S.L., Niswonger, R.G., Regan, R.S., Prudic, D.E., and Barlow, P.M., 2008, GSFLOW—Coupled ground-water and surface-water flow model based on the integration of the Precipitation-Runoff Modeling System (PRMS) and the Modular Ground-Water Flow Model (MODFLOW-2005): U.S. Geological Survey Techniques and Methods, book 6 chap. D1, 240 p.

Markstrom, S.L., 2012, P2S—Coupled simulation with the Precipitation-Runoff Modeling System (PRMS) and the Stream Temperature Network (SNTemp) Models: U.S. Geological Survey Open-File Report 2012–1116, 19 p.

Maurer, E.P., Wood, A.W., Adam, J.C., Lettenmaier, D.P., and Nijssen, B., 2002, A long-term hydrologically-based data set of land surface fluxes for the conterminous United States: Journal of Climate, v. 15, no. 22, p. 3237–3251.

Maurer, E.P., Hidalgo, H., Das, T., Dettinger, M., and Cayan, D., 2010, The utility of daily large-scale climate data in the assessment of climate change impacts on daily streamflow in California: Hydrology and Earth System Sciences, v. 14, p. 1125–1138, doi:10.5194/hess-14-1125-2010.

O'Brien, T.P., Sornette, D., and McPherro, R.L., 2001, Statistical asynchronous regression: Determining the relationship between two quantities that are not measured simultaneously: Journal of Geophysical Research, v. 106, no. A8, p. 15533–15544.

Stoner, A.M.K, Hayhoe, K.A., Yang, X., and Wuebbles, D.J., 2012, An asynchronous regional regression model for statistical downscaling of daily climate variables: International Journal of Climatology, doi: 10.1002/joc.3603.

Theurer, F.D., Voos, K.A., and Miller, W.J., 1984, Instream water temperature model: U.S. Fish and Wildlife Service Instream Flow Information Paper 16, FWS/OBS-85/15, 316 p.

Vrac, M., Stein, M., Hayhoe, K., 2007, Statistical downscaling of precipitation through nonhomogeneous stochastic weather typing: Climate Research v. 34, p. 169–184.

# Spatial and Temporal Assessment of Back-Barrier Erosion on Cumberland Island National Seashore, Georgia, 2011–2013

By Daniel L. Calhoun and Jeffrey W. Riley


## Abstract

Erosion and accretion processes for seaward zones of coastal barrier islands have been a subject of research for some time. However, a current management concern for Cumberland Island National Seashore is the effects of erosion on the island's resources along the western shoreline, also referred to as the back barrier. Lateral erosion has been estimated recently to be as much as 1 meter annually and currently threatens important terrestrial habitats, historic and prehistoric resources, and modern infrastructure on the island. Prior research aided the National Park Service in identifying the most severely eroded areas and those vulnerable to further loss, but in order to develop effective management actions, additional information is needed to determine the conditions that cause erosion to occur. A 3-year study is in progress to monitor spatial and temporal rates of back-barrier shoreline change at five locations on the island's back barrier (figs. 1 and 2) and to correlate the data with natural and anthropogenic activities and events.

A three-tiered approach is being taken during 2011–2013 wherein (1) initial and final shoreline/margin positional surveys are conducted on four approximately half-kilometer long prioritized segments, (2) erosion pins are installed and distance to margin face is measured over multiple intervals, and (3) photoelectric bank pins (PEEPs; fig. 3) are located at each site providing continuous estimates of specific margin position. In addition, continuous water-surface height and acoustic energy data are collected at each site to provide data on tide and wave height and boat traffic, respectively. Climatological data, such as wind speed, wind direction, and rainfall, provide additional information that help to explain measured estimates of periodic erosion events. These data can be used quantitatively to provide estimates of rates of erosion and possible causative mechanisms at multiple scales and qualitatively to compare the instrumented sites to one another to allow potential prioritization of management options.

Initial results based on data from December 2011 to August 2012 indicate that estimates of erosion obtained from physical measurements of the erosion face of the back-barrier using traditional bank pins are comparable to the continuous measurements of the island margins at specific sites. The continuous estimates of the erosion margin with the PEEPs indicate that the majority of the observed erosion occurs during punctuated events and appear to be associated with climatological factors, such as high winds and wave action


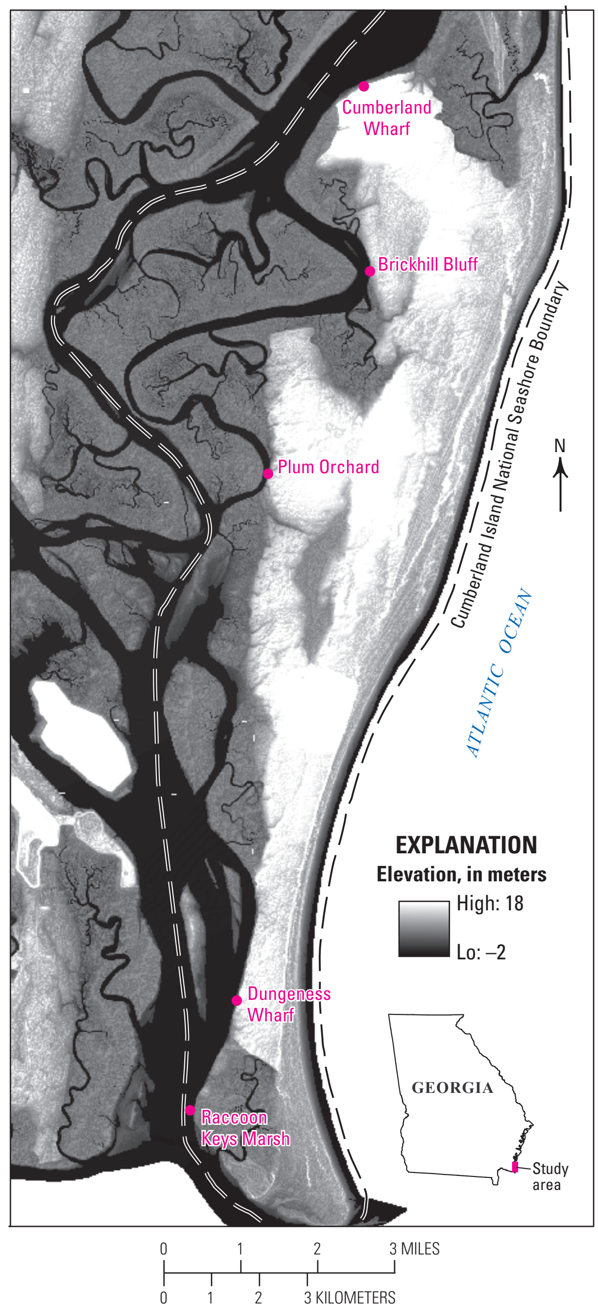


**Figure 1.** Study locations on Cumberland Island National Seashore. Image is a digital elevation model created using Lidar data.

brought about by storms and high tides. As data sets are completed and assembled, the ability to distinguish between the influences of climatological and anthropogenic factors on the measured erosion estimates will be strengthened. Follow-up precise global positioning system surveys of the established studied locations will reveal if the point estimates of shoreline position are representative of the cumulative changes at the individual sites and allow for comparison of the results to previously published remotely sensed estimates of back-barrier erosion at Cumberland Island National Seashore.

**Figure 2.** One of the sites where erosion is being assessed, Brickhill Bluff facing north along the western margin of Cumberland Island National Seashore (photo by Alan M. Cressler, USGS).

**Figure 3.** Photoelectric bankpin (PEEP) used to continuously measure changes in shoreline position (photo by Alan M. Cressler, USGS).

# Using Environmental DNA to Verify the Presence of Imperiled Aquatic Species

By Anna McKee,[1] Daniel Calhoun,[1] William Barichivich,[2] Stephen Spear,[3] Caren Goldberg,[4] and Travis Glenn[5]

## Abstract

Aquatic species often must compete with humans for water resources. Determining the distributions of aquatic species, particularly threatened species, will help facilitate informed decisions about the best approaches for meeting human demands for water while minimizing ecological impacts. Molecular techniques have been used as effective and efficient methods for detecting the presence of species across a range of aquatic systems (Goldberg and others, 2011, Thomsen and others, 2012). The general method is to isolate environmental deoxyribonucleic acid (eDNA) from focal taxa by water filtration and eDNA amplification. The simplicity, cost-effectiveness, and non-invasiveness of molecular techniques for detecting the presence of rare and cryptic species indicates great potential for their incorporation into inventory and monitoring programs of aquatic species (Goldberg and others, 2011; Jerde and others, 2011).

The U.S. Geological Survey, in cooperation with the U.S. Fish and Wildlife Service, developed an eDNA marker for the gopher frog (*Lithobates capito*), an imperiled pond-breeding amphibian species found in Georgia and Florida. This marker was tested under laboratory conditions to determine if eDNA could be a feasible tool for detecting the presence of *L. capito* for inventory and monitoring purposes, as well as to determine if eDNA concentrations differ depending on the volume of water collected.

The eDNA of *L. capito* was isolated in water samples collected from four 100-gallon tadpole-rearing tanks at the Atlanta Botanical Gardens (fig. 1). The number of tadpoles in each tank was approximately 100 individuals. Two replicate samples of differing volumes (15 and 60 milliliter [mL]) were collected from each tank, and a negative control (deionized water) sample was collected concurrently. Each water sample was filtered through a separate 47-millimeter-diameter 0.45-micrometer cellulose nitrate membrane filter to extract eDNA. The eDNA samples were used as templates for quantitative polymerase chain reaction (qPCR), with *L. capito*-specific mitochondrial primers. Three replicate qPCRs were set up for each tank replicate. Amplification of the target mitochondrial region was determined using Applied Biosystems StepOnePlus™ real-time PCR.


**Figure 1.** Collecting water samples from *Lithobates capito* tadpole-rearing tanks at the Atlanta Botanical Gardens in Atlanta, Georgia (photo by Alan M. Cressler, USGS, September 2012).

The qPCR cycle at which fluorescence (that is, amplification, ΔRn) begins to exponentially increase is representative of the relative concentration of DNA in the sample. In general, the DNA concentrations were approximately the same among samples from all four tanks (fig. 2). For a given tank, however, the DNA concentration of the 60-mL sample was almost always slightly greater than that of the 15-mL sample. Although these results are preliminary, we consistently detected *L. capito* DNA in all of the tanks. Water in each tank contained, on average, approximately the same concentration of *L. capito* eDNA, which indicates similar tadpole abundances (Thomsen and others, 2012). The larger volume samples contained slightly higher concentrations of DNA, which indicates that collecting larger volumes of water may enhance detection of eDNA. These results indicate that eDNA may be an efficient and reliable tool for detecting *L. capito*, but additional work is needed before implementation of eDNA protocols can be used for inventory and monitoring purposes. Future research plans include testing this method on natural populations as well as expanding this assay to test for the presence of three additional imperiled amphibian species that are native to Georgia.

[1] U.S. Geological Survey, Georgia Water Science Center, Norcross, Georgia.

[2] U.S. Geological Survey, Southeast Ecological Science Center, Gainesville, Florida.

[3] The Orianne Society, Clayton, Georgia.

[4] University of Idaho, Moscow, Idaho.

[5] University of Georgia, Athens, Georgia.

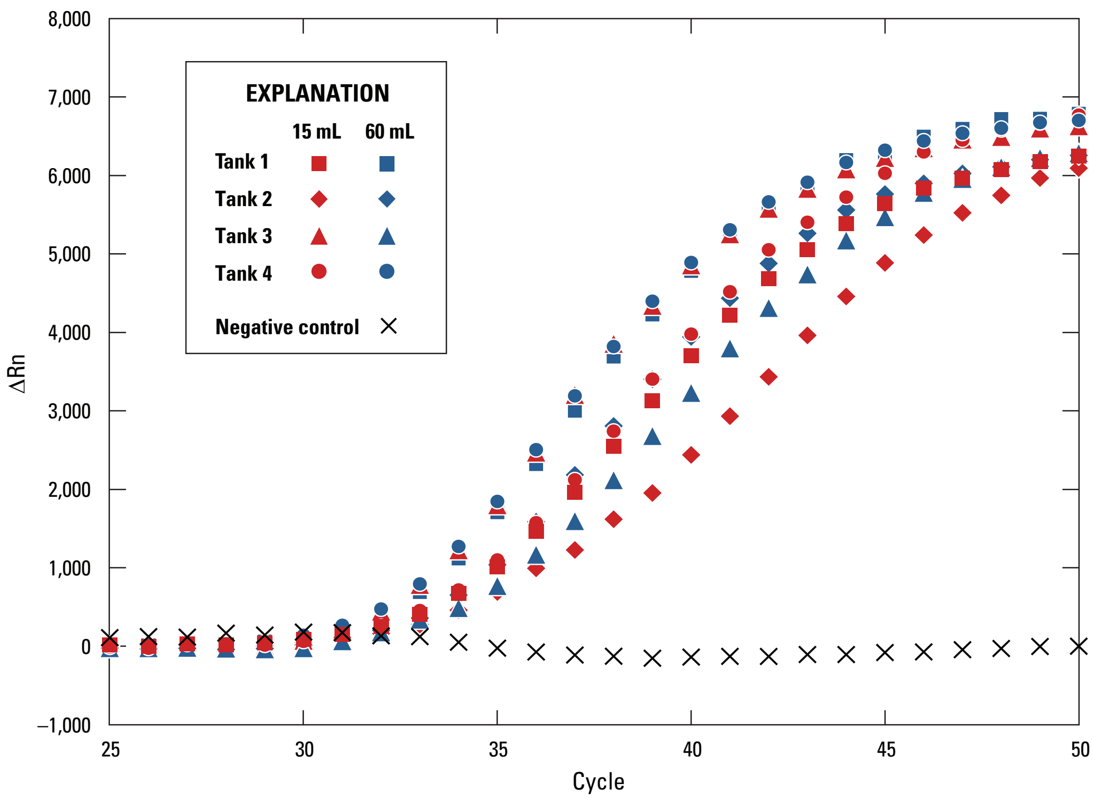


**Figure 2.** Quantitative PCR amplification (ΔRn) curve for a target mitochondrial DNA sequence in *Lithobates capito*. Template DNA for the reaction was isolated in water samples from four tanks containing *L. capito*. [DNA, deoxyribonucleic acid; mL, milliliter; PCR, polymerase chain reaction]

## References Cited

Goldberg, C.S., D.S. Pilliod, R.S. Arkle, and L.P. Waits. 2011. Molecular detection of vertebrates in stream water: A demonstration using Rocky Mountain tailed frogs and Idaho giant salamanders. PLoS one 6:e22746.

Jerde, C.L., A.R. Mahon, W.L. Chadderton, and D.M. Lodge. 2011. "Sight-unseen" detection of rare aquatic species using environmental DNA. Conservation Letters 4:150–157.

Thomsen, P., J. Kielgast, L. Iversen, C. Wiuf, M. Rasmussen, M. Gilbert, L. Orlando, and E. Willerslev. 2012. Monitoring endangered freshwater biodiversity using environmental DNA. Molecular Ecology 21:2565–2573.

# Pond Identification, Classification, and Inundation Dynamics at St. Marks National Wildlife Refuge, Northwest Florida, USA

By Jeffrey W. Riley,[1] Daniel L. Calhoun,[1] and William J. Barichivich[2]

## Abstract

The persistence and resilience of amphibian communities is largely dependent on adequate breeding habitat. This is especially important for threatened and endangered species that may exist as isolated populations and have specific requirements for breeding. The U.S. Geological Survey is conducting a study, in cooperation with the U.S. Fish and Wildlife Service, to investigate the feasibility of a repatriation effort of the striped newt (*Notophthalmus perstriatus*), a federal candidate species, in St. Marks National Wildlife Refuge (SMNWR), Panecea Unit, in northwest Florida (fig. 1). This amphibian species requires ponds that are free of fishes and, therefore, generally chooses ephemeral ponds as breeding sites. The delineation of potential breeding habitat is a first step in selecting candidate areas for repatriation. Although the National Wetland Inventory (NWI) is used to identify and select wetlands for a variety of investigations, often it doesn't include smaller, isolated water bodies that also are important in ecosystem studies. Thus, an alternative approach to wetland identification was taken, based solely on topographical characteristics.

The study area is located in the panhandle of Florida on the gulf coast where sediments overlie limestone bedrock, which is conducive to sinkhole formation. This has given rise to numerous wetlands and ponds. Additionally, SMNWR's close proximity to the gulf coast results in relatively subtle topography (elevation ranges ~11 meters to <0 meters) and requires the use of a high-resolution digital elevation model (DEM) to identify shallow depressions in the landscape. To achieve this, a light detection and ranging (LiDAR)-derived DEM and Topographic Position Index (TPI) classification were used to identify and classify isolated depressions across the landscape. The TPI works by defining a neighborhood shape (for example, circle or annulus) and size and then evaluates the difference in elevation from the central cell to the mean elevation of the neighborhood. Thus, depressions are characterized by negative values on the TPI raster; however, threshold TPI values must be used to determine true depressional ponds from slight depressions that occur on the landscape but do not hold water. These values were determined using a calibration set of ponds. Determining the most useful neighborhood shape and size was an iterative process that was informed by a calibration dataset consisting of 45 field-identified ponds, the perimeters of which were surveyed with a high precision real-time kinematic global positioning system. Twenty-two of these ponds were instrumented with water-level recorders to investigate inundation dynamics across a wide range of hydrologic conditions.

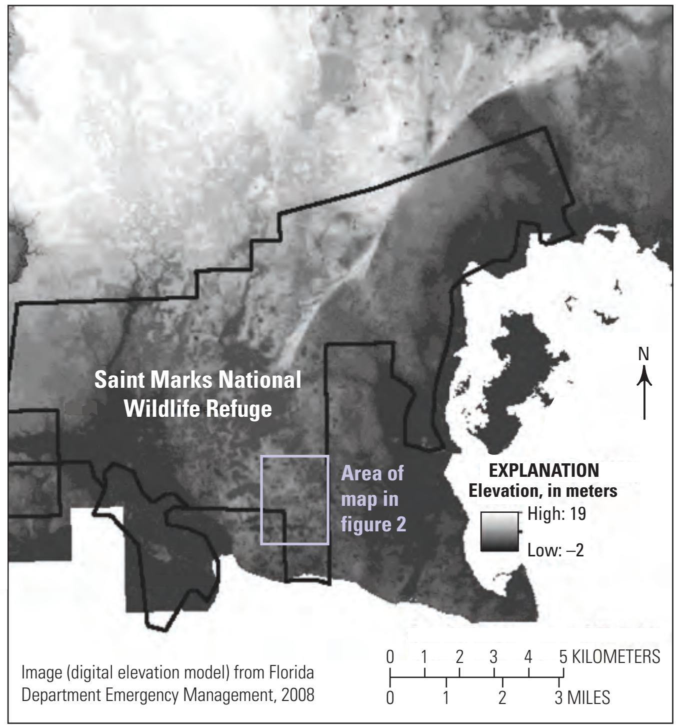


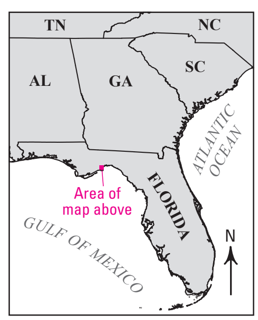


**Figure 1.** Location of the St. Marks National Wildlife Refuge Panacea Unit, northwest Florida.

Preliminary results indicate that the TPI procedure performed reasonably well in relation to the surveyed ponds (fig. 2). Additionally, many smaller depressions were identified that were not in the NWI dataset. Thus far, this approach has yielded useful information regarding pond types and their distribution. However, more study will be required to complete the task of creating a classification framework for relating physical characteristics of ponds and their landscapes to hydroperiods at SMNWR, and ultimately helping to determine potential striped newt repatriation sites.

[1] U.S. Geological Survey, Georgia Water Science Center, Norcross, Georgia.

[2] U.S. Geological Survey, Southeast Ecological Science Center, Gainesville, Florida.

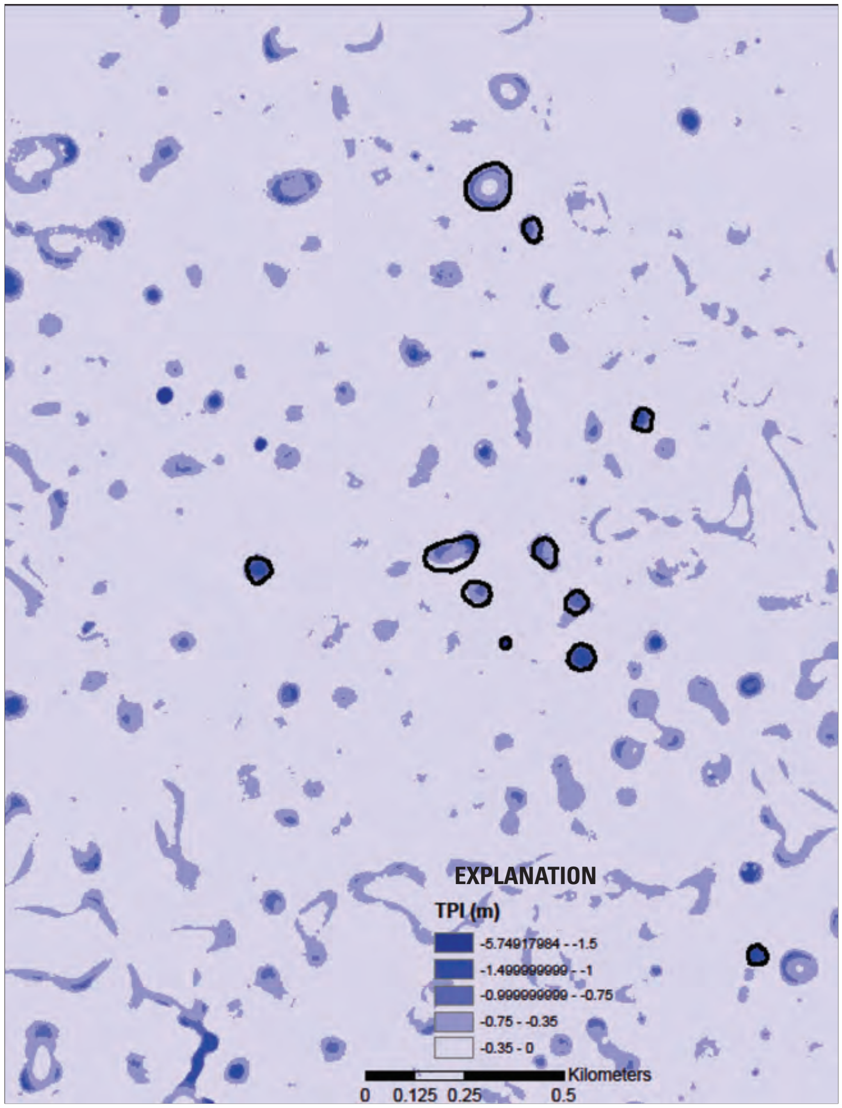


**Figure 2.** Image showing the relation between the modeled ponds from the Topographic Position Index (TPI) classification (blue) and the surveyed margins (black) based on vegetative indicators of mean high water. Note some discrepancies in size occurred where the actual size of the depression is larger than where vegetative indicators occur.

# Brackish and Saline Aquifers—A Potential Alternative Water Source in the Southeastern United States

By Lester J. Williams and Amanda E. Lanning

## Abstract

The U.S. Geological Survey Groundwater Resources Program assessed brackish and saline groundwater resources in two regional aquifer systems in the southeastern United States to determine their potential for supplementing existing freshwater supplies in the area (fig. 1). These resources were mapped in terms of their dissolved-solids concentrations, estimated mostly from borehole geophysical logs, and supplemented with water-quality data collected from wells with known open intervals. Maps and cross sections were constructed for each of the major hydrogeologic units that depict salinity variations in four zones: (1) the freshwater zone, containing dissolved-solids of less than 1,000 milligrams per liter (mg/L); (2) the brackish-water zone, containing between 1,000 and 10,000 mg/L of dissolved solids; (3) the salinity transition zone, containing between 10,000 and 35,000 mg/L of dissolved solids; and (4) the saline-water zone, containing between 35,000 and 100,000 mg/L of dissolved solids. The brine zone, containing greater than 100,000 mg/L of dissolved solids, was not differentiated from the saline-water zone.

The results of the study indicate brackish groundwater resources are present in a variety of clastic and carbonate rock aquifers ranging in depth from a few hundred feet to several thousand feet or more. Brackish zones were mapped in two aquifers of the Southeastern Coastal Plain aquifer system (the Chattahoochee River aquifer and Black Warrior River aquifer) and two aquifers of the Floridan aquifer system (the Upper and Lower Floridan aquifers) (Miller, 1986; Renken, 1996) (fig. 2). Because of differences in permeability, proximity to recharge areas, and the local presence of relict seawater or brine that has not been fully flushed out of the freshwater flow system, vertical and lateral salinity variations in successively deeper aquifers can be complex. A cross section through southeastern Georgia demonstrates the varying extents of brackish water zones in the Southeastern Coastal Plain and Floridan aquifer systems (fig. 3).

Regionally, the shallowest and most accessible brackish groundwater resources are present in the Upper Floridan aquifer, mostly in coastal areas of Georgia, Alabama, South Carolina, and throughout most of the coastal areas in Florida. Deeper, less accessible aquifers containing brackish groundwater resources are present throughout much of the Southeastern Coastal Plain aquifer system in Georgia, Alabama, and South Carolina.

Additional study will be needed to assess the extent, water quality, and potential of using brackish- and saline-water resources to supplement existing freshwater supplies. Major considerations for development include the depth and cost of drilling into these deeper zones, alternatives for brine disposal that may be associated with treatment of brackish water, and the potential yield of these aquifers.

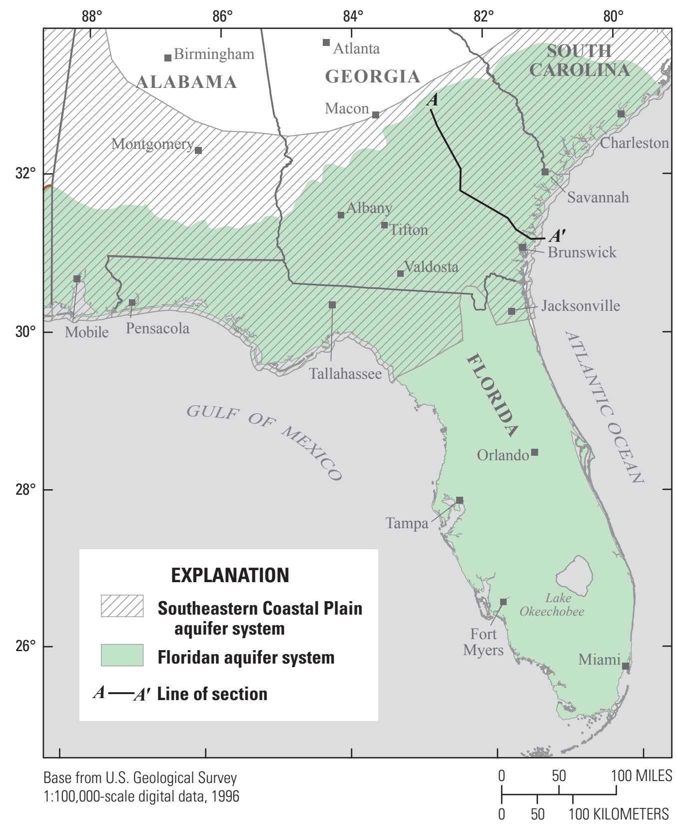


**Figure 1.** Location of study area showing the extent of regional aquifer systems and cross section location, southeastern United States.

## Referenced Cited

Miller, J.A., 1986, Hydrogeologic framework of the Floridan aquifer system in Florida and in parts of Georgia, Alabama, and South Carolina: U.S. Geological Survey Professional Paper 1403–B, 91 p.

Renken, R.A., 1996, Hydrogeology of the Southeastern Coastal Plain aquifer system in Mississippi, Alabama, Georgia, and South Carolina: U.S. Geological Survey Professional Paper 1410–B, 101 p., 142 pls p.

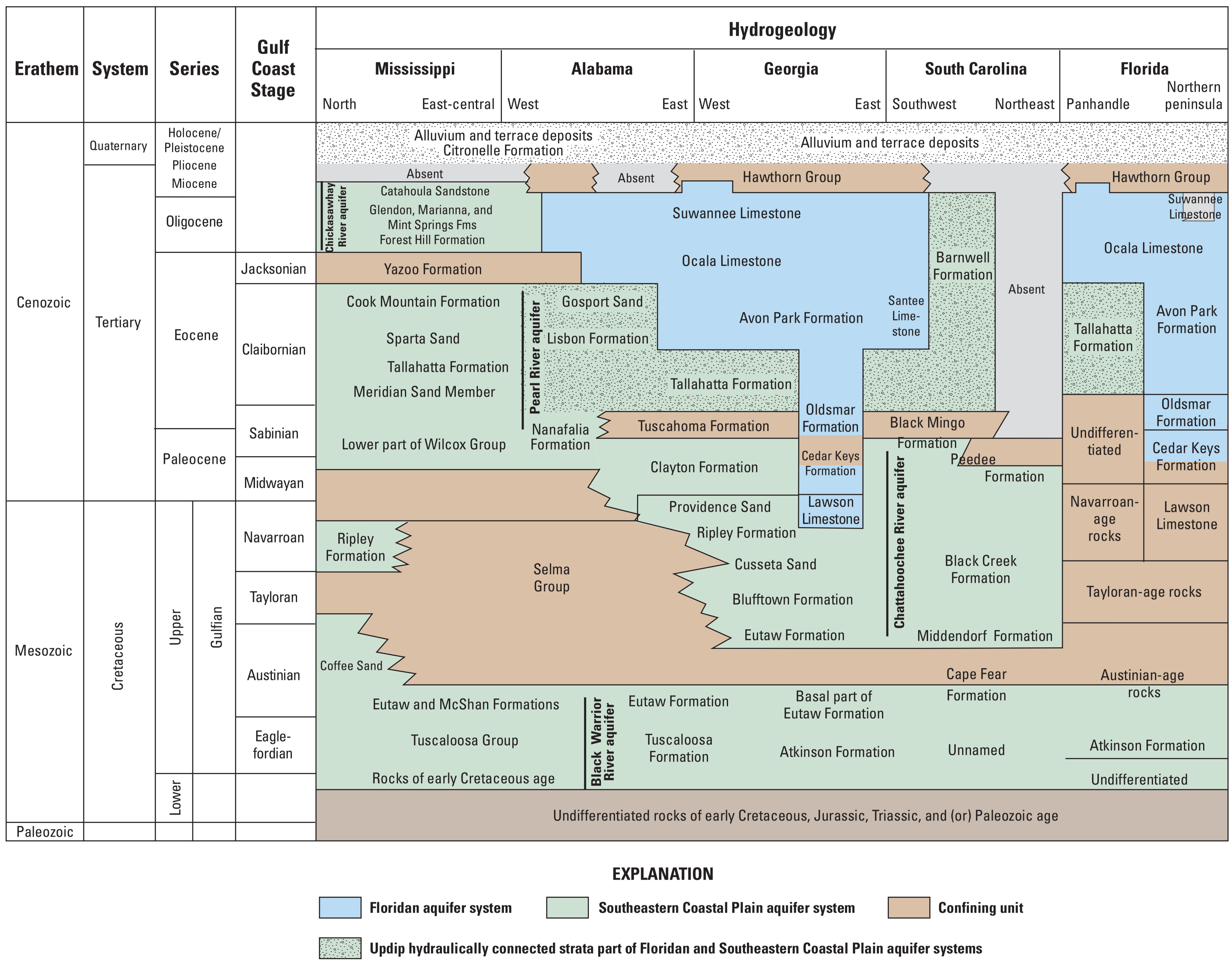


**Figure 2.** Generalized correlation chart showing stratigraphic units and hydrogeologic units, of the Floridan and Southeastern Coastal Plain aquifer systems. (modified from Renken, 1996)

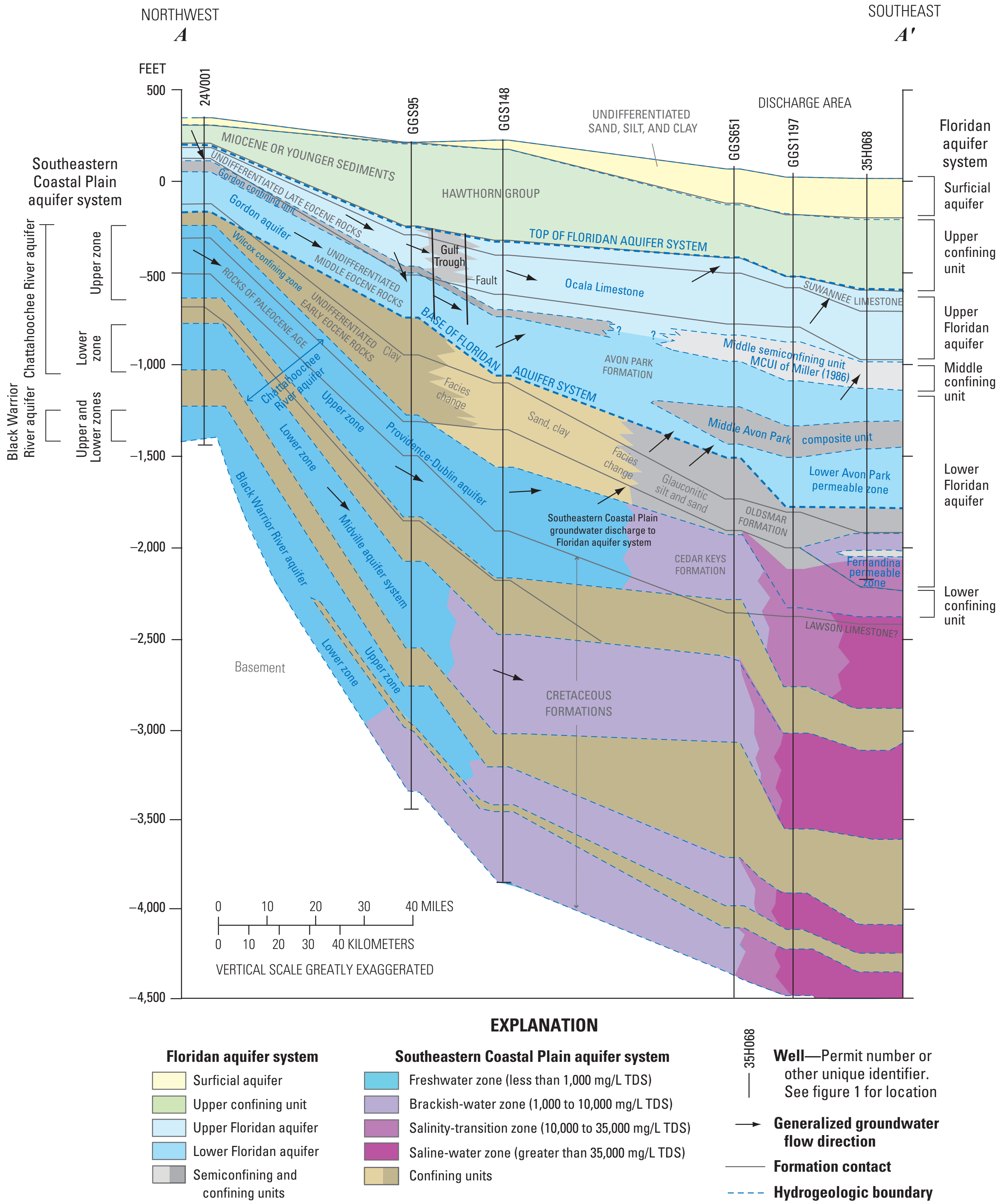


**Figure 3.** Generalized hydrogeologic cross section *A–A′* from Johnson County to Glynn County, Georgia. Line of section shown on figure 1. [mg/L, milligrams per liter; TDS, total dissolved solids]

# Groundwater Modeling to Evaluate Interaquifer Leakage in the Floridan Aquifer System in Coastal Georgia

By Gregory S. Cherry

## Abstract

A regional groundwater-flow model was used to determine the influence of pumping the Lower Floridan aquifer (LFA) on the volume of leakage from the Upper Floridan aquifer (UFA) at three sites in coastal Georgia. Steady-state simulations were performed representing a pumping rate of about 1 million gallons per day at newly constructed production wells tapping the LFA at Hunter Army Airfield (HAAF), Fort Stewart, and the City of Pooler to evaluate the long-term effects of pumping on the Floridan aquifer system. Separate models were developed for each of the three sites to simulate drawdown response and to quantify interaquifer leakage from the UFA into the LFA near each production well. Model grid resolution, hydrogeologic-unit depth and thickness, and hydraulic properties were adjusted based on new field data from each of the sites. Results of simulations indicate that interaquifer leakage from the UFA into the LFA accounted for 48 percent of the flow to the well at HAAF and 98 percent of the flow at each of the sites at Fort Stewart and Pooler. Sensitivity analysis of hydraulic properties within the largest zone, which includes HAAF and Pooler, indicates that simulated heads are most sensitive to changes in horizontal and vertical hydraulic conductivity of the UFA and LFA, and that varying hydraulic properties changed the groundwater model inflows and outflows through the general and specified-head boundaries, but maintained the interaquifer leakage between the UFA and LFA at 98 percent of the pumping rate.

## Introduction

The Upper Floridan aquifer (UFA) is the principal source of freshwater in the coastal area of Georgia (fig. 1). Because pumping in Georgia may affect saltwater intrusion at Hilton Head, South Carolina, the Georgia Environmental Protection Division (GaEPD) capped permitted groundwater withdrawals from the UFA at 2004 rates in Chatham County and parts of adjacent counties and encouraged the development of alternative water sources, including the Lower Floridan aquifer (LFA). Pumping from the LFA increases head gradients locally between the UFA and LFA, induces groundwater leakage from the UFA to the LFA, and lowers water levels in the UFA. GaEPD guidelines (Nolton Johnston, Georgia Environmental Protection Division, written commun., January 28, 2003) stipulate that permit applicants for new LFA wells must determine any adverse effects pumping the LFA might have on the UFA, and determine an appropriate pumping reduction (offset) in the UFA that will result in “no net negative impact.”

To assess the hydrogeology and water quality of the Floridan aquifer system and the effects of pumping the LFA on the UFA in coastal Georgia, the U.S. Geological Survey (USGS), in cooperation with the U.S. Department of the Army, conducted investigations at Hunter Army Airfield (HAAF) and Fort Stewart during 2009–2010 and performed a similar study for the City of Pooler during 2011. Field investigations at the three study sites included the construction of test wells in the UFA and LFA, geophysical logging, flowmeter surveys, water sampling and analysis, hydraulic analysis of core, packer tests, and 24- and 72-hour (hr) aquifer tests. This paper describes results of simulations that incorporated field data from the 72-hr aquifer tests at the three sites into a modified regional groundwater flow model of coastal Georgia. Simulations determined the amount of drawdown in the UFA and LFA and quantified the amount of interaquifer leakage and flow from model boundaries when adding a new LFA production well at each site. In addition, results of a sensitivity analysis to assess model response to specific changes in calibrated horizontal and vertical hydraulic-conductivity ($K_h$ and $K_v$, respectively) values in the vicinity of HAAF and Pooler are described.

## Regional Groundwater-Flow Model and Modifications

A regional groundwater-flow model (Payne and others, 2005) for the coastal region of Georgia and adjacent parts of South Carolina and Florida was modified and used to simulate the effects of pumping from the LFA at HAAF, Fort Stewart, and Pooler, Georgia. Modifications to the regional model are described in detail in Clarke and others (2010, 2011) and Cherry and Clarke (2013). A brief discussion is included here.

The regional groundwater-flow model covers an area of 42,155 square miles ($mi^2$) and uses the finite-difference code MODFLOW-2000 (Harbaugh and others, 2000) to simulate steady-state groundwater flow during predevelopment, 1980, and 2000. The model includes seven model layers, listed in order of descending depth (fig. 2):

- Layer 1: Confined upper and lower water-bearing zones of the surficial aquifer system;
- Layer 2: Brunswick aquifer system confining unit;
- Layer 3: Upper and lower Brunswick aquifers, which compose the Brunswick aquifer system;
- Layer 4: Upper Floridan confining unit;

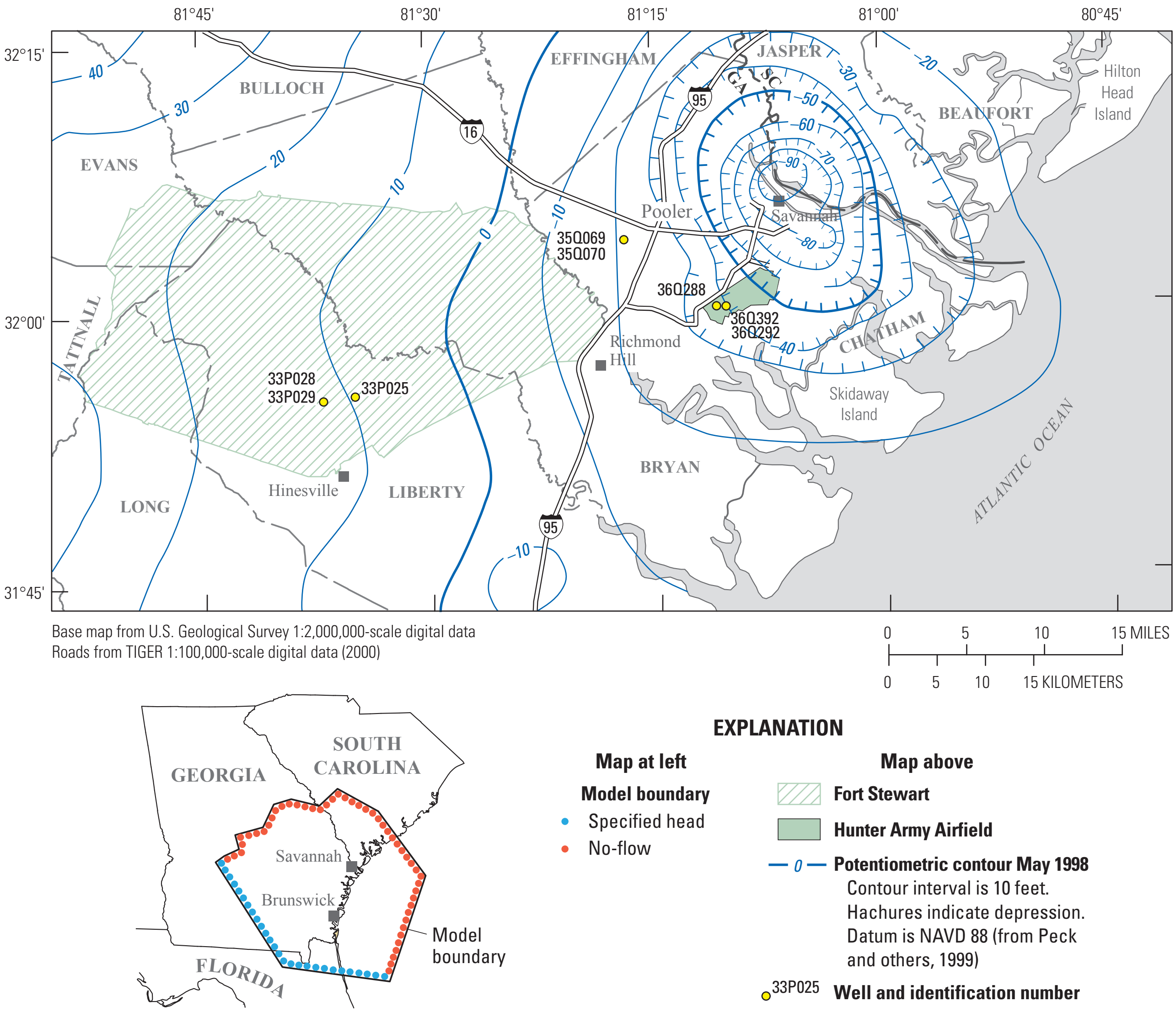


**Figure 1.** Locations of the study area, potentiometric surface contours for the Upper Floridan aquifer, groundwater-flow model boundaries and wells near Hunter Army Airfield, Fort Stewart, and Pooler in coastal Georgia.

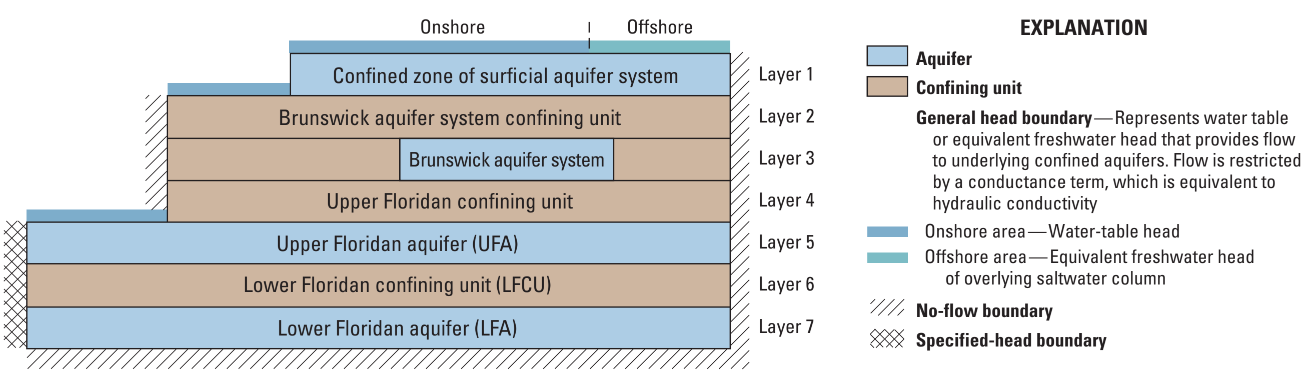


**Figure 2.** Schematic diagram showing model layers and boundary conditions (from Payne and others, 2005).

- Layer 5: Upper Floridan aquifer (UFA);
- Layer 6: Lower Floridan confining unit (LFCU); and
- Layer 7: Lower Floridan aquifer (LFA).

Lateral model boundaries for all layers were designated as no flow except the southern and southwestern sides of layers 5, 6, and 7 (UFA, LFCU, and LFA, respectively; fig. 1), which were designated as specified-head because the Floridan aquifer system extends beyond the boundaries of the model in these areas. Heads assigned to specified-head cells were based on estimates of UFA head derived from the potentiometric-surface map for 1998 (Peck and others, 1999). The lowermost boundary was designated as no flow, and the uppermost boundary was designated as a general head boundary representing the unconfined zone of the surficial aquifer system above model layer 1 (fig. 2). The general head boundary also was applied to the top active aquifer cells in model layers 2 and 5 corresponding to unit outcrop or recharge areas. For the offshore area, a general head boundary condition was applied to the top of active model cells in layer 1.

To enable more detailed simulation of flow gradients and leakage in the vicinity of new LFA wells, three separate models were developed with smaller grid cells. Grid resolution was changed from variably spaced cell sizes ranging from approximately 4,000×5,000 feet (ft; 0.7 $mi^2$) to 16,500×16,500 ft (9.8 $mi^2$) in the Payne and others (2005) model to a variably spaced grid with cell sizes ranging from 10×10 ft near the new LFA well to a maximum spacing of about 16,200×16,300 ft away from the pumping well in each of the revised models.

Results of field investigations at HAAF (Clarke and others, 2010; Williams, 2010), Fort Stewart (Clarke and others, 2011; Gonthier 2011), and Pooler (Cherry and Clarke 2013; Gonthier, 2012) provided the basis for $K_h$ and $K_v$ values in newly established hydraulic-property zones in the revised steady-state models. The addition of new hydraulic-property zones were used to accommodate results from first the HAAF study, followed by the Fort Stewart study, and then most recently the Pooler study. New hydraulic-property zones were added as follows (fig. 3):

- UFA (layer 5)—Zone F13 was added at HAAF, zone F14 was added at Fort Stewart, and then F13 was enlarged to include Pooler.
- LFCU (layer 6)—Zone LFC2 was added at HAAF, zone LFC3 was added at Fort Stewart, and then LFC2 was enlarged to include Pooler.
- LFA (layer 7)—Zone LF2 was added at HAAF, zone LF3 was added at Fort Stewart, and then LF2 was enlarged to include Pooler.

The model at Pooler incorporates modifications to hydraulic-property zones completed for the HAAF and Fort Stewart models, and includes the expansion of zones F13, LFC2, and LF2 from an area of 114 $mi^2$ in the HAAF model to an area of 221 $mi^2$ in the Pooler model (fig. 3). The revised models were run to simulate steady-state groundwater flow during 2000. At a regional scale, year-2000 simulated head and water budgets for the revised models were similar to those of the original model (Payne and others (2005)), indicating that revisions did not cause substantial regional changes to the original model.

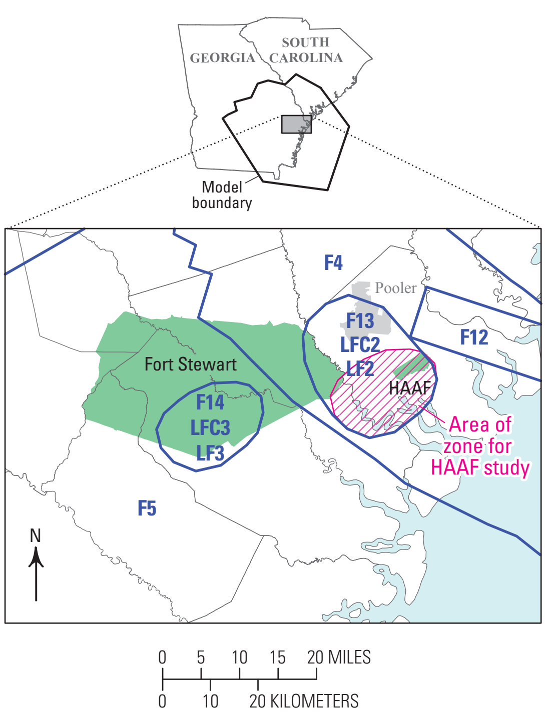


[$K_h$, horizontal hydraulic conductivity; $K_v$, vertical hydraulic conductivity; ft/d, foot per day; T, transmissivity; $ft^2$/d, foot squared per day; —, not applicable; Note: zones LFC1 and LF1 cover areas outside zones LFC2, LFC3, LF2, and LF3]

| Unit | Layer | Payne and others (2005) | | | Cherry and Clarke (2013) | | | |
|---|---|---|---|---|---|---|---|---|
| | | Hydraulic-property zone | $K_h$ (ft/d) | $K_v$ (ft/d) | Hydraulic-property zone | $K_h$ (ft/d) | $K_v$ (ft/d) | T ($ft^2$/d) |
| | | F4 | 70 | 70 | F4 | 70 | 70 | — |
| | | F5 | 394 | 394 | F5 | 394 | 394 | — |
| UFA | 5 | F12 | 25 | 25 | F12 | 25 | 25 | — |
| | | — | — | — | F13 | 90 | 90 | 44,000 |
| | | — | — | — | F14 | 398 | 398 | 100,000 |
| | | n/a | 0.02 | 0.02 | LFC1 | 0.02 | 0.02 | — |
| LFC | 6 | | | | LFC2 | 2.0 | 0.20 | — |
| | | | | | LFC3 | 10 | 0.20 | — |
| | | n/a | 10 | 10 | LF1 | 10 | 10 | — |
| LFA | 7 | | | | LF2 | 87 | 10 | 4,600 |
| | | | | | LF3 | 15.8 | 1.6 | 5,000 |

**Figure 3.** Revised hydraulic-property zones for model layers 5–7, Pooler area groundwater model (modified from Payne and others, 2005; Cherry and Clarke, 2013).

## Simulated Results and Sensitivity Analysis

Long-term changes in water levels and water budget caused by increased pumping in the LFA at HAAF, Fort Stewart, and Pooler were simulated using the revised models. The steady-state water budget was evaluated by using the MODFLOW postprocessor ZONEBUDGET (Harbaugh, 1990), which sums simulated inflows and outflows in a designated area of the model domain. The year 2000 “base case” condition was used for comparisons of changes in net flows along general and specified-head boundaries, interaquifer leakage between the UFA and LFA, and flow between individual model layers for each simulation.

### Hunter Army Airfield Well 36Q392

At HAAF, a new LFA well (36Q392) was assigned a pumping rate of 748 gallons per minute (gal/min) or 1.08 million gallons per day (Mgal/d). Simulated steady-state drawdown in the LFA was 36.2 ft, which closely matched the observed maximum drawdown of 36.3 ft during a 72-hr aquifer test (Clarke and others, 2010; table 1). Observed maximum drawdown values of 0.76 ft in UFA observation well 36Q292 and 0.43 ft in UFA observation well 36Q288 during the 72-hr aquifer test were less than the simulated steady-state drawdown values of 2.03 and 1.9 ft, respectively (Clarke and others, 2010). The match of simulated steady-state drawdown in the LFA to observed maximum drawdown during the 72-hr aquifer test is reasonable because test data indicated that water levels had nearly stabilized at the end of the 72-hr pumping period, whereas test data from the two UFA observation wells indicated that water levels had not stabilized at the end of the 72-hr pumping period. Simulated steady-state drawdown in the UFA as a result of interaquifer leakage through the LFCU was greater than 1 ft over a 141-$mi^2$ area surrounding LFA well 36Q392 (Clarke and others, 2010; table 1). Simulated flow to well 36Q392 was derived from increased inflow and decreased outflow (net inflow) from the general head boundary above layer 1 and specified-head boundary in layer 5, which indicated 48 percent of flow moving from the UFA through the LFCU into the LFA. The remaining flow (52 percent) was derived from increased lateral flow in the LFA (simulated as decreased flow from layer 7 to layer 6) and from increased net inflows from the specified-head boundary in layer 7. Sixty-five percent of the simulated interaquifer leakage from the UFA to the LFA occurs within a 1-mile (mi) radius of the pumped well, reflecting the steeper head gradient between the two aquifers near to the well (Clarke and others, 2010).

### Fort Stewart Well 33P028

At Fort Stewart, LFA well 33P028 was assigned a pumping rate of 740 gal/min (1.07 Mgal/d), and the simulated steady-state drawdown of 38.6 ft closely matched the observed maximum drawdown of 38.8 ft from a 72-hr aquifer test (Clarke and others, 2011; table 1). Observed maximum drawdown in two UFA observation wells (33P029 and 33P025) was 0.4 and 0.3 ft, respectively, compared with simulated steady-state drawdown of 1.12 and 0.81 ft, respectively (Clarke and others, 2011). As in the HAAF simulations, the good match of simulated (steady-state) to observed (72-hr maximum) LFA drawdown and the higher simulated than observed UFA drawdown could be expected in that these results reflect differences in the time required for the UFA and LFA to reach steady-state conditions. Simulated steady-state drawdown in the UFA resulting from interaquifer leakage through the LFCU was greater than 1 ft over a 1.4-$mi^2$ area surrounding well 33P028 (Clarke and others, 2011; table 1). Simulated interaquifer leakage from the UFA through the LFCU to the LFA occurred over a smaller area near Fort Stewart than at HAAF because Kh in the LFCU near Fort Stewart of 10 feet per day (ft/d) was 50-times greater than at the original hydraulic-property zone established at HAAF, and transmissivity of the UFA was 100,000 feet squared per day ($ft^2/d$; fig. 3) as opposed to 37,000 $ft^2/d$ in the HAAF area. Simulated flow to well 33P028 was derived from the UFA and overlying layers (98 percent)

**Table 1.** Simulated drawdown in the Upper and Lower Floridan aquifers and interaquifer leakage at Hunter Army Airfield, Fort Stewart, and Pooler, Georgia.

[HAAF, Hunter Army Airfield; LFA, Lower Floridan aquifer; UFA, Upper Floridan aquifer; gal/min, gallon per minute; ft, foot; $mi^2$, square mile]

| Facility | LFA well | LFA pumping rate, in gal/min | UFA drawdown | | LFA drawdown | | Interaquifer leakage, in percent | Leakage within a 1-mile radius of pumping well, in percent |
|---|---|---|---|---|---|---|---|---|
| | | | Maximum, in ft | Area of 1-foot contour, in $mi^2$ | Maximum, in ft | Area of 1-foot contour, in $mi^2$ | | |
| HAAF | 36Q392 | 748 | 2.03 | 141 | 36.2 | 146 | 48 | 65 |
| Fort Stewart | 33P028 | 740 | 1.12 | 1.4 | 38.6 | 4.4 | 98 | 80 |
| City of Pooler | 35Q069 | 780 | 2.52 | 163 | 52.1 | 163 | 98 | 81 |

transmitted through the LFCU, with 80 percent of the interaquifer leakage occurring within a 1-mi radius (Clarke and others, 2011). The remaining 2 percent of flow was derived from lateral flow from specified-head boundaries in the LFA.

## Pooler Well 35Q069

At Pooler, LFA well 35Q069 was assigned a pumping rate of 780 gal/min (1.12 Mgal/d), and the simulated steady-state drawdown of 52.1 ft closely matched the observed maximum drawdown of 52.0 ft during a 72-hr aquifer test (Cherry and Clarke, 2013; table 1). Observed maximum drawdown in the UFA observation well (35Q070) was 0.9 ft compared with a simulated steady-state drawdown of 2.52 ft. Simulated steady-state drawdown in the UFA resulting from interaquifer leakage through the LFCU was greater than 1 ft over a 163-$mi^2$ area surrounding well 35Q069 (Cherry and Clarke, 2013; table 1). The $K_h$ and $K_v$ in the LFCU for the expanded hydraulic-property zone (LFC2), which includes Pooler and HAAF, was 10-times greater than the smaller original zone established at HAAF, and transmissivity of the UFA (F13) increased from 37,000 to 44,000 $ft^2$/d in the expanded zone (fig. 3). The transmissivity of the LFA (LF2) in the expanded hydraulic-property zone decreased slightly from 5,200 to 4,600 $ft^2$/d. Similar to well 33P028 at Fort Stewart, simulated steady-state flow to well 35Q069 at Pooler was derived from the UFA and overlying layers (98 percent) with 81 percent of the interaquifer leakage occurring within a 1-mi radius (Cherry and Clarke, 2013). The remaining 2 percent of flow was derived from lateral flow from specified-head boundaries in the LFA.

To provide insight into the sensitivity of simulated steady-state head and water-budget components to modified hydraulic property zones in the revised model at Pooler, a series of model simulations were run whereby the LFA was pumped at a rate of 780 gal/min (1.12 Mgal/d) and $K_h$ and $K_v$ were varied by factors of 0.1, 0.5, 1.0, 2.0, and 10.0 (Cherry and Clarke, 2013). Properties of the UFA were varied in the area of hydraulic-property zone F13, of the LFA in the area of zone LF2, and of the LFCU in the area of zone LFC2 (fig. 3). The plots shown in figure 4 document changes in the maximum simulated steady-state drawdown in the LFA pumping well and in the UFA using the multiplier for selected hydraulic model parameters in model layers 5 through 7. The analysis indicates the model is most sensitive to changes in $K_h$ and $K_v$ of the UFA in zone F13 (fig. 4*B*), followed by similar changes within the LFA in zone LF2 (fig. 4*A*). The model is relatively insensitive to changes in the $K_h$ and $K_v$ of the LFCU in zone LFC2 (fig. 4*C*). In general, maximum drawdowns increase when $K_h$ and $K_v$ decrease with the exception of drawdown in the UFA, which decreases when $K_h$ and $K_v$ of the LFCU decrease in zone LFC2 (fig. 4*C*). The evaluation of water budgets using ZONEBUDGET (Harbaugh, 1990) indicated minor changes to groundwater flow that enters and leaves the model area through the general and specified-head boundaries in model layers 1 and 5, but the relative contribution through interaquifer leakage from the UFA through the LFCU into the LFA is maintained at 98 percent.

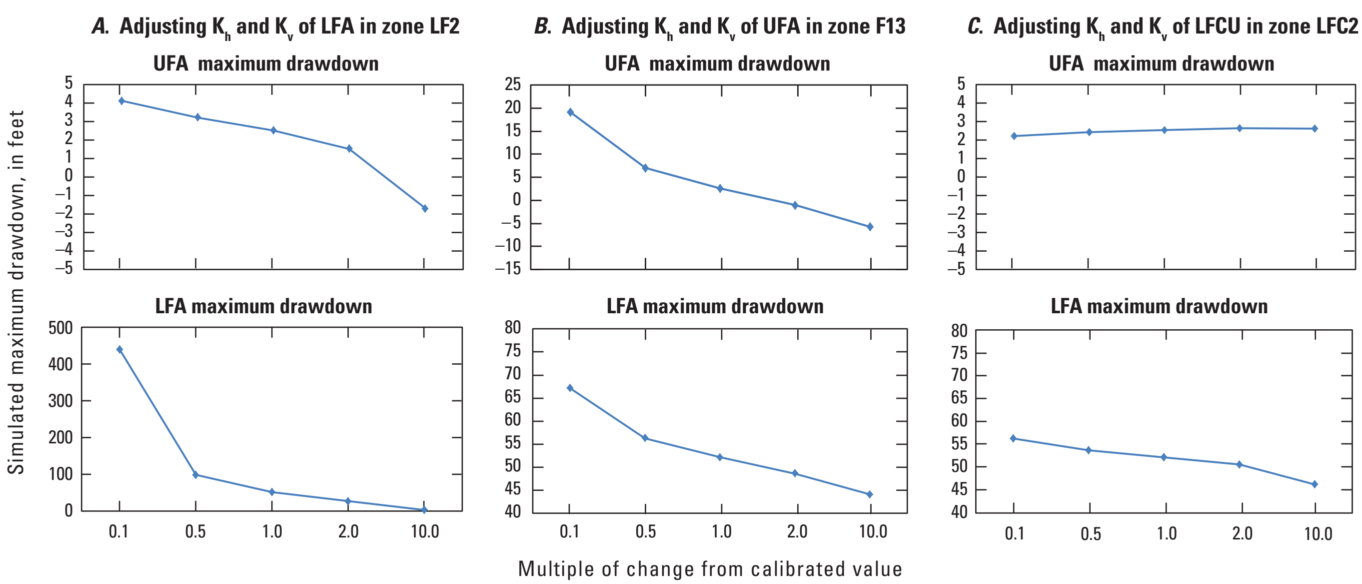


**Figure 4.** Sensitivity of simulated maximum drawdown in the Upper and Lower Floridan aquifers (UFA and LFA) to changes in horizontal and vertical hydraulic conductivity of the *(A)* LFA in hydraulic-property zone LF2, *(B)* UFA in zone F13, and *(C)* Lower Floridan confining unit (LFCU) in zone LFC2 (see figure 3 for locations of hydraulic-property zones).

## Discussion

Results of model simulations at three sites in coastal Georgia indicate that pumping the LFA at a rate of about 1 Mgal/d in wells 36Q392, 33P028, and 35Q069 results in downward leakage from the UFA and overlying units that provide from 48 to 98 percent of the flow. ZONEBUDGET (Harbaugh, 1990) analysis indicates between 65 to 81 percent of the interaquifer leakage occurs within 1-mi of the pumped well. The remainder of flow to the LFA well is provided by lateral flow from specified-head boundaries. Results of a sensitivity analysis indicate that $K_h$ and $K_v$ of the UFA and LFA are the most important parameters in model simulations. Errors in these values affect simulated maximum drawdown and associated drawdown offset computations. Increasing or decreasing the $K_h$ and $K_v$ of hydrogeologic units had little effect on net inflows from general and specified-head boundaries and on interaquifer leakage. $K_h$ and $K_v$ values of the LFCU had little effect on simulated interaquifer leakage and groundwater levels. Simulation results have improved regional characterization of the Floridan aquifer system, which will assist State officials in evaluating requests for groundwater withdrawal from the LFA.

## References

Cherry G.S., and Clarke, J.S., 2013, Simulated effects of Lower Floridan aquifer pumping on the Upper Floridan aquifer at Pooler, Chatham County, Georgia: U.S. Geological Survey Scientific Investigations Report 2013–5004, 46 p., available at *http://pubs.usgs.gov/sir/2013/5004/*.

Clarke, J.S., Williams, L.J., and Cherry, G.S., 2010, Hydrogeology and water quality of the Floridan aquifer system and effect of Lower Floridan aquifer pumping on the Upper Floridan aquifer at Hunter Army Airfield, Chatham County, Georgia: U.S. Geological Survey Scientific Investigations Report 2010–5080, 56 p., available at *http://pubs.usgs.gov/sir/2010/5080/*.

Clarke, J.S., Cherry, G.S., and Gonthier, G.J., 2011, Hydrogeology and water quality of the Floridan aquifer system and effects of Lower Floridan aquifer pumping on the Upper Floridan aquifer at Fort Stewart, Georgia: U.S. Geological Survey Scientific Investigations Report 2011–5065, 59 p., available at *http://pubs.usgs.gov/sir/2011/5065/*.

Gonthier, G.J., 2011, Summary of hydrologic testing of the Floridan aquifer system at Fort Stewart, Liberty County, Georgia: U.S. Geological Survey Open-File Report 2011–1020, 40 p., available at *http://pubs.usgs.gov/of/2011/1020/*.

Gonthier, G.J., 2012, Hydrogeology and water quality of the Floridan aquifer system and effect of Lower Floridan aquifer pumping on the Upper Floridan aquifer, Pooler, Chatham County, Georgia, 2011–2012: U.S. Geological Survey Scientific Investigations Report 2012–5249, 62 p., available at *http://pubs.usgs.gov/sir/2012/5249/*.

Harbaugh, A.W., 1990, A computer program for calculating subregional water budgets using results from the U.S. Geological Survey modular three-dimensional finite-difference ground-water flow model: U.S. Geological Survey Open-File Report 90–392, 46 p.

Harbaugh, A.W., Banta, E.R., Hill, M.C., and McDonald, M.G., 2000, MODFLOW-2000, The U.S. Geological Survey modular ground-water model—User guide to modularization concepts and the ground-water flow process: U.S. Geological Survey Open-File Report 00–92, 121 p., available at *http://pubs.er.usgs.gov/publication/ofr200092*.

Payne, D.F., Abu Rumman, Malek, and Clarke, J.S., 2005, Simulation of ground-water flow in coastal Georgia and adjacent parts of South Carolina and Florida—Predevelopment, 1980, and 2000: U.S. Geological Survey Scientific Investigations Report 2005–5089, 91 p., available at *http://pubs.usgs.gov/sir/2005/5089/*.

Peck, M.F., Clarke, J.S., Ransom, Camille, III, and Richards, C.J., 1999, Potentiometric surface of the Upper Floridan aquifer in Georgia and adjacent parts of Alabama, Florida, and South Carolina, May 1998, and water-level trends in Georgia, 1990–98: Georgia Geologic Survey Hydrologic Atlas 22, 1 sheet.

Williams, L.J., 2010, Summary of hydrologic testing of the Floridan aquifer system at Hunter Army Airfield, Chatham County, Georgia: U.S. Geological Survey Open-File Report 2010–1066, 30 p., available at *http://pubs.usgs.gov/of/2010/1066/*.

# Characterization of Groundwater Contribution and Water Quality in Multi-Screened Wells Using Flowmeter and Water-Sampling Data, Waynesboro, Georgia, 2011

By Gerard J. Gonthier


## Abstract

In the Georgia Coastal Plain, production wells usually are completed with multiple screens in clastic sediments. Determination of the relative yield and water quality of each screened interval is useful for estimating the hydraulic properties and water quality of different hydrogeologic units. Flowmeter-survey and caliper-log data are used to provide flow rates at different depths within a wellbore and can be used to determine the contribution of flow coming from each hydrogeologic unit. Water samples collected within the wellbore above contributing intervals during the pumping can be analyzed for water quality. Each water sample is a composite of flow contributed from all screened intervals below the sample-collection point. A mixing equation, the wellbore flow rate and concentrations of major ions and total dissolved solids or values of specific conductance in water samples collected at different depths can be used to determine the constituent concentrations or values in water from each hydrogeologic unit. This information can be used to determine water quality of the aquifers contributing to the well and to identify zones within the aquifer system that contribute water of less-than-desirable quality to the well.


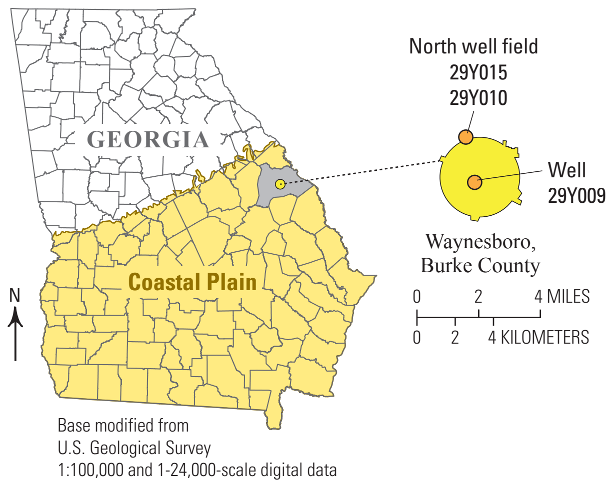


**Figure 1.** Location of wells in the north well field 1.5 miles north of downtown Waynesboro in Burke County, Georgia, 2011.

## Introduction

The Dublin and Midville aquifer systems are the principal sources of groundwater in the northern Coastal Plain of east-central Georgia (Ga.; fig. 1; Clarke and others, 1985). The City of Waynesboro in Burke County, Ga., relies on groundwater from the Dublin and Midville aquifer systems for most of its water supply. Waynesboro is located within an area characterized by dissolved iron concentrations in the Dublin and Midville aquifer systems in excess of 300 micrograms per liter (µg/L; Clarke and others, 1985, p. 46). The presence of iron in drinking water is objectionable because of its taste, staining capacity, and encrusting property (U.S. Environmental Protection Agency, 1976).

At Waynesboro, groundwater is supplied by two wells open to the Dublin and Midville aquifer systems. Well 29Y009 is located within the city limits and was a water-supply well as of September 7, 2012. Well 29Y010 is 1.5 miles north of downtown in what is referred to as the north well field. Supply well 29Y010 was constructed during 1994 and was gradually taken out of service by 2006 because of lost productivity when iron-oxide clogged the well screens (Reggie Hanton, Waynesboro Water Department, oral commun., September 7, 2012). The city currently (October 2012) is investigating ways of increasing its water supply at the north well field by in-stalling and testing a replacement well (29Y015) located 42 feet (ft) northwest of well 29Y010 (herein referred to as old production well 29Y010).

The U.S. Geological Survey (USGS), in cooperation with the City of Waynesboro, performed site investigations during April through August 2011 to assess the hydrogeology and water quality of the Dublin and Midville aquifer systems. The assessment provided a more detailed regional characterization of the two aquifer systems. Aquifers were characterized using data from a flowmeter survey and water-quality sampling of the replacement well and a flowmeter survey of the old production well 29Y010 at Waynesboro, Ga. Water-quality data for all analyzed constituents are presented, with an emphasis on manganese and iron concentrations.

## Hydrogeologic Description

The Waynesboro, Burke County, area is underlain by Coastal Plain strata consisting mostly of unconsolidated layers of Upper Cretaceous to lower Miocene sand and clay and some layers of limestone. The Coastal Plain strata attain a maximum thickness of about 985 ft (Falls and others, 1997). These sediments constitute the following three major aquifer systems, in order of descending depth:

- Floridan aquifer system, consisting of the Upper Three Runs and Gordon aquifers;
- Dublin aquifer system, consisting of the Millers Pond and upper and lower Dublin aquifers; and
- Midville aquifer system, consisting of the upper and lower Midville aquifers.

## Methods of Study

Flowmeter surveys were performed using an electromagnetic flowmeter to determine the relative contribution of flow from screens in wells 29Y010 and 29Y015 that are open to the Dublin and Midville aquifer systems. A pump operated above the screens and flowmeter survey to produce upward flow in the screened sections of the wellbore. The pumping rate at well 29Y010 was 300 gallons per minute (gal/min) in April 2011, and 1,000 gal/min at well 29Y015 during a 24-hour aquifer test in August 2011. The flowmeter measured the upward flow velocity at different depths within the multi-screened wells. Caliper-log data were used to refine the well construction (figs. 2, 3) and confirm the wellbore diameter within the wells. The flow velocity and wellbore diameter were used to determine the upward flow rate in the well at different depths. An increase in upward flow rate from one depth to a shallower depth indicates a contribution of flow from the interval.

Water samples were collected using a wireline grab sampler just above five of the seven screens in pumped well 29Y015. Sample collection began after the completion of a flowmeter survey about 9 hours into the 24-hour aquifer test. Each water sample was a composite of flow contributed from all screens below the sample-collection point.

Samples were analyzed for total dissolved solids, specific conductance, pH, and alkalinity (reported as calcium carbonate); and for major ions, including sodium, potassium, magnesium, calcium, manganese, iron, fluoride, chloride and sulfate. Water was assumed to flow through screens from adjacent hydrogeologic units and completely mix before reaching the collection point. A simple mixing equation, the known flow contribution from screens (from the flowmeter survey), and composite water-sample constituent concentrations were used to determine the sample-interval constituent concentrations, where sample intervals are between sample-collection points. The mixing equation from Kendall and Caldwell (1998) was applied to sample intervals in the wellbore as follows:

$$Q_{T,n}\,C_{T,n} = Q_{T,n-1}\,C_{T,n-1} + Q_{I,n}\,C_{I,n} \qquad (1)$$

where

$Q_{T,n}$ is the composite discharge at sample-collection point $n$, contributed to or flowing up the wellbore from all screened intervals below sample-collection point $n$, in gallons per minute;

$C_{T,n}$ is the concentration of a specific conservative constituent in discharge water $Q_{T,n}$, expressed in a linear-unit value that varies with each constituent but represents the mass of the constituent per volume of water;

$Q_{T,n-1}$ is the composite discharge at sample-collection point $n-1$, contributed to or flowing up the wellbore from all screened intervals below sample-collection point $n-1$, in gallons per minute;

$C_{T,n-1}$ is the concentration of a specific conservative constituent in discharge water $Q_{T,n-1}$, expressed in a linear-unit value that varies with each constituent but represents the mass of the constituent per volume of water;

$Q_{I,n}$ is the discharge entering the well from the interval between sample-collection points $n$ and $n-1$, in gallons per minute; and

$C_{I,n}$ is the concentration of a specific conservative constituent in discharge water $Q_{I,n}$, expressed in a linear-unit value that varies with each constituent but represents the mass of the constituent per volume of water.

Equation 1 can be rearranged to solve the concentration, $C_{I,n}$, of a conservative constituent occurring in water discharging to the well between the two sample-collection points $n$ and $n-1$ ($Q_{I,n}$):

$$C_{I,n} = \frac{Q_{T,n}C_{T,n} - Q_{T,n-1}C_{T,n-1}}{Q_{I,n}} \qquad (2)$$

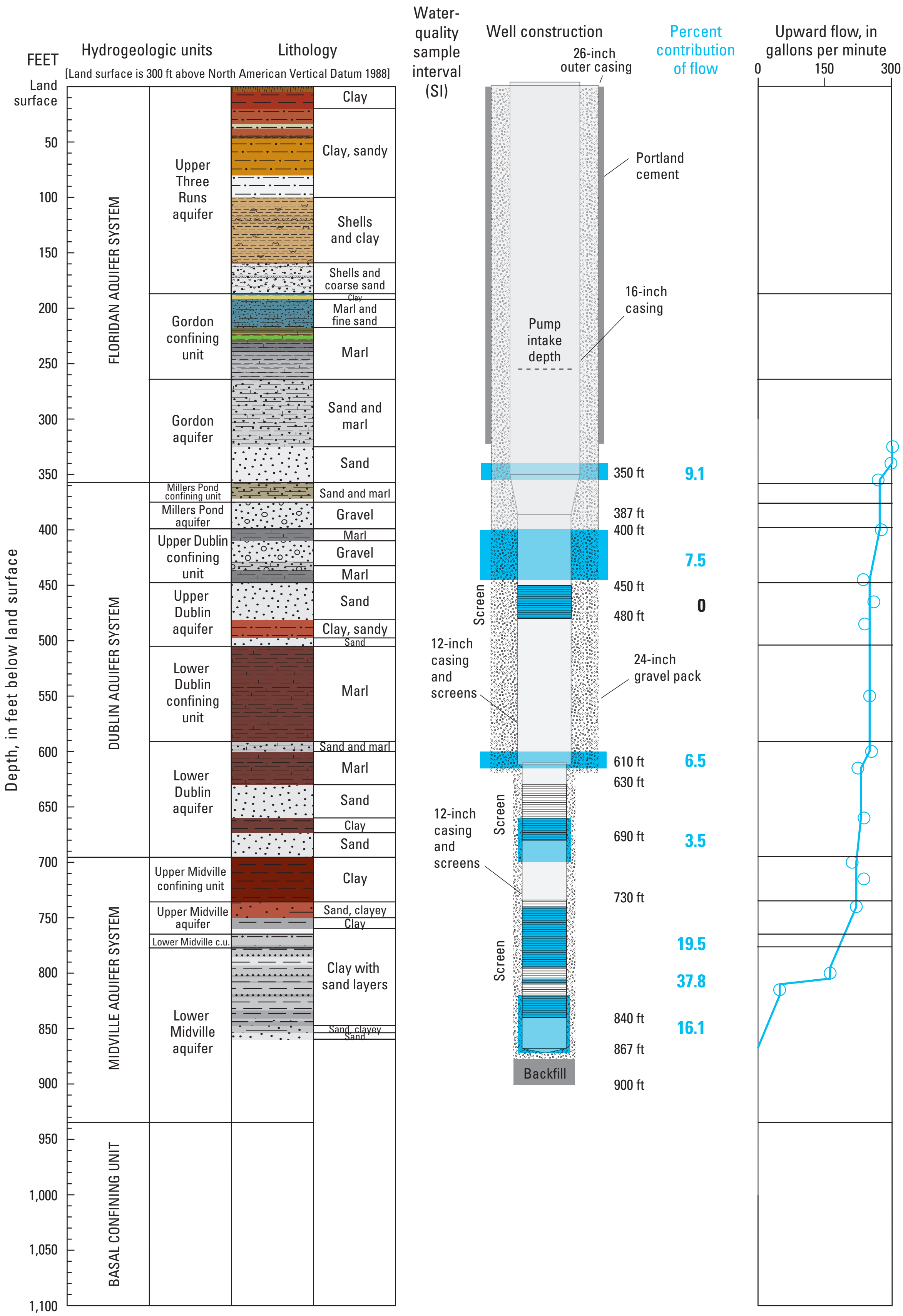


**Figure 2.** Construction and flowmeter survey results for well 29Y010 near Waynesboro, Georgia, April 2011. [c.u., confining unit]

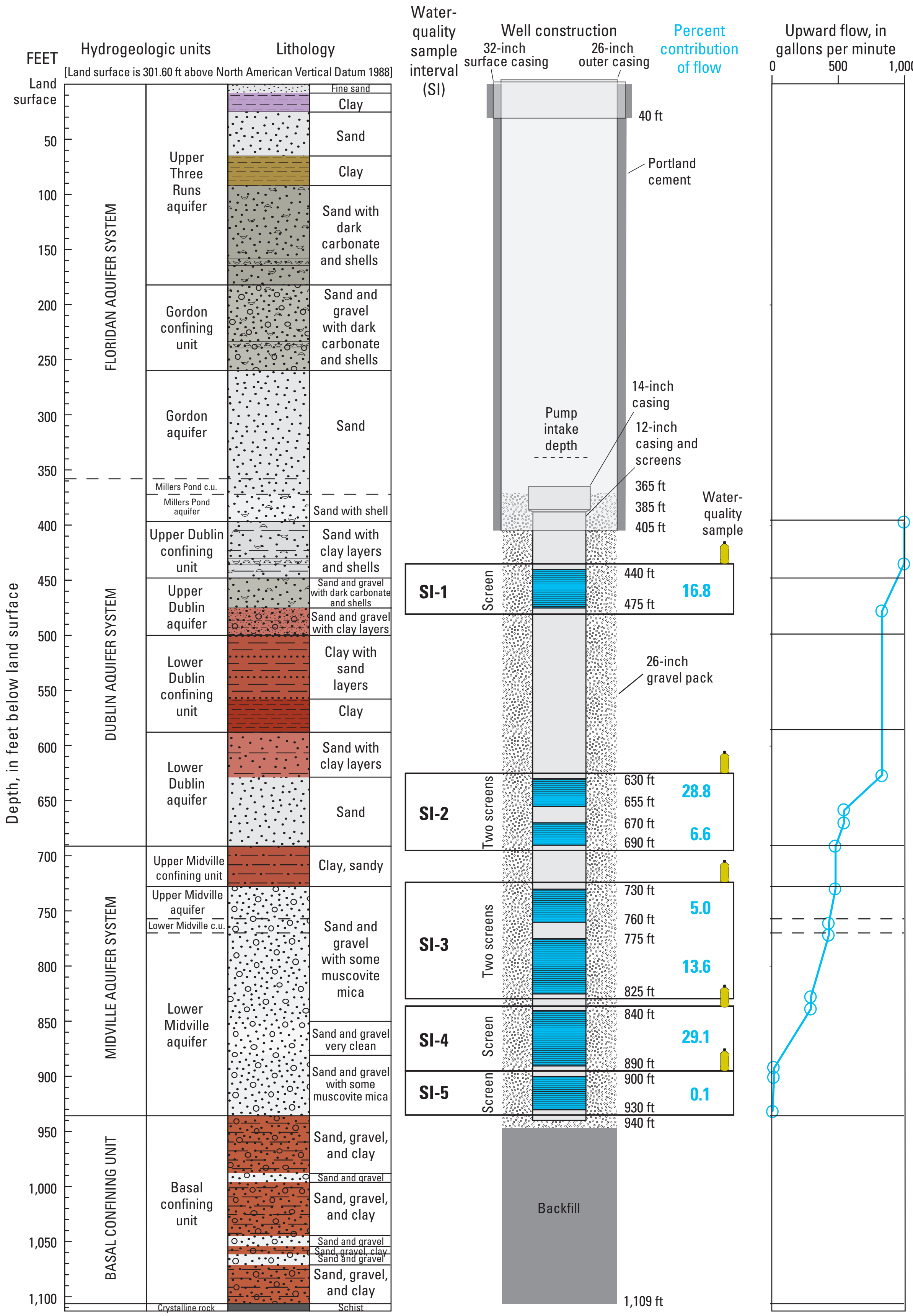


**Figure 3.** Construction, flowmeter survey results, and water-quality sample intervals for well 29Y015 near Waynesboro, Georgia, August 2011. [c.u., confining unit]

## Wellbore Flow

The flowmeter-survey data indicated that well 29Y010 was in a compromised condition that precluded the use of its water-level data in the analysis of the 24-hour aquifer test at well 29Y015 in August 2011. The flowmeter survey of well 29Y010 indicated leaks in the casing and clogged screens, with 73.4 percent of the flow to the well derived from the Midville aquifer system below a depth of 730 ft (fig. 2). The remaining 26.6 percent of flow was contributed by leaks in the well at 350, 400–450, and 610 ft (23.1 percent) and at the well screen at 690 ft (3.5 percent). No measurable flow came from the screened interval open to the upper Dublin aquifer at 450–480 ft deep.

The flowmeter-survey data provided information that could be used with the 24-hour aquifer-test data to assess the hydraulic properties of the Dublin and Midville aquifer systems. The flowmeter survey of well 29Y015 indicated that 52.2 percent of the well discharge came from the three screens open to the Dublin aquifer system; the remaining 47.8 percent came from the four screens open to the Midville aquifer system (fig. 3). This information allowed for a broader assessment of hydraulic properties from the 24-hour aquifer-test data. The deepest screened interval at 900–930 ft deep contributed less than 0.1 percent of the total flow at this well.

## Water Quality in Well 29Y015

Manganese and iron concentrations increased with increasing depth. Therefore, manganese and iron concentrations were greater in water sampled from the Midville aquifer system (26.1 and 419 µg/L), respectively) than in water sampled from the Dublin aquifer system (9.4 and 218 µg/L, respectively). Within sample intervals manganese concentrations increased from 6.5 to 59.1 µg/L (fig. 4*H*); iron concentrations increased from 130 to 1,160 µg/L (fig. 4*I*). Manganese and iron concentrations from the lower part of the lower Midville aquifer (900–930 ft deep, SI-5) exceeded secondary water-quality standards of 50 and 300 µg/L, respectively (U.S. Environmental Protection Agency, 2011). Concentrations of iron in sample intervals SI-4 and SI-3, which represent almost all of the water from the Midville aquifer system, and total flow from both the Dublin and Midville aquifer systems exceeded the secondary water-quality standard of 300 µg/L. Because SI-5 contributed only 0.1 percent of the total flow, the total load of manganese and iron coming from this sample interval had little effect on the total concentration coming from both the Dublin and Midville aquifers. Based on the mixing equation, excluding the contribution of SI-4 (clean, clay-free interval within the lower Midville aquifer at a depth of 840–890 ft) would result in an iron concentration below the secondary water-quality standards in the total flow from the other sample intervals. The resulting flow from both aquifer systems, assuming an original flow of 1,000 gal/min, would be reduced by 29.1 percent to 709 gal/min. Other major ions varied less than iron and manganese (fig. 4) and did not exceed water-quality standards for general drinking-water purposes (U.S. Environmental Protection Agency, 2011).

## Conclusions

Flowmeter-survey results provided crucial information in the study of the Dublin and Midville aquifer systems. Specifically, flowmeter-survey results indicated that the old production well was in a compromised condition that precluded the use of its water-level data in the analysis of the 24-hour aquifer test at well 29Y015 in August 2011. The flowmeter survey of new replacement well 29Y015 provided information that could be used with the 24-hour aquifer-test data to assess the hydraulic properties of the Dublin and Midville aquifer systems. Three screens open to the Dublin aquifer system contributed slightly more (52.2 percent) water than four screens open to the Midville aquifer system (47.8 percent). The lower part of the lower Midville aquifer contributed very little water to the well. Both manganese and iron concentrations increase with depth in replacement well 29Y015. Thus, manganese and iron concentrations were greater in the deeper Midville aquifer system (26.1 and 419 µg/L, respectively) than in the shallower Dublin aquifer system (9.4 and 218 µg/L, respectively). While water from the lower part of the lower Midville aquifer had a relatively high iron concentration, the small contribution to flow in the well had little effect on the total concentration coming from both the Dublin and Midville aquifer systems. Water from the Midville aquifer system has iron concentrations that exceed the secondary water-quality criteria. Assuming a pumping rate of 1,000 gal/min, sealing off the interval open to the clean, clay-free interval within the lower Midville aquifer (840–890 ft deep) would cause the iron concentration in water produced by the well to be below the secondary water-quality criteria while reducing the flow about 29 percent.

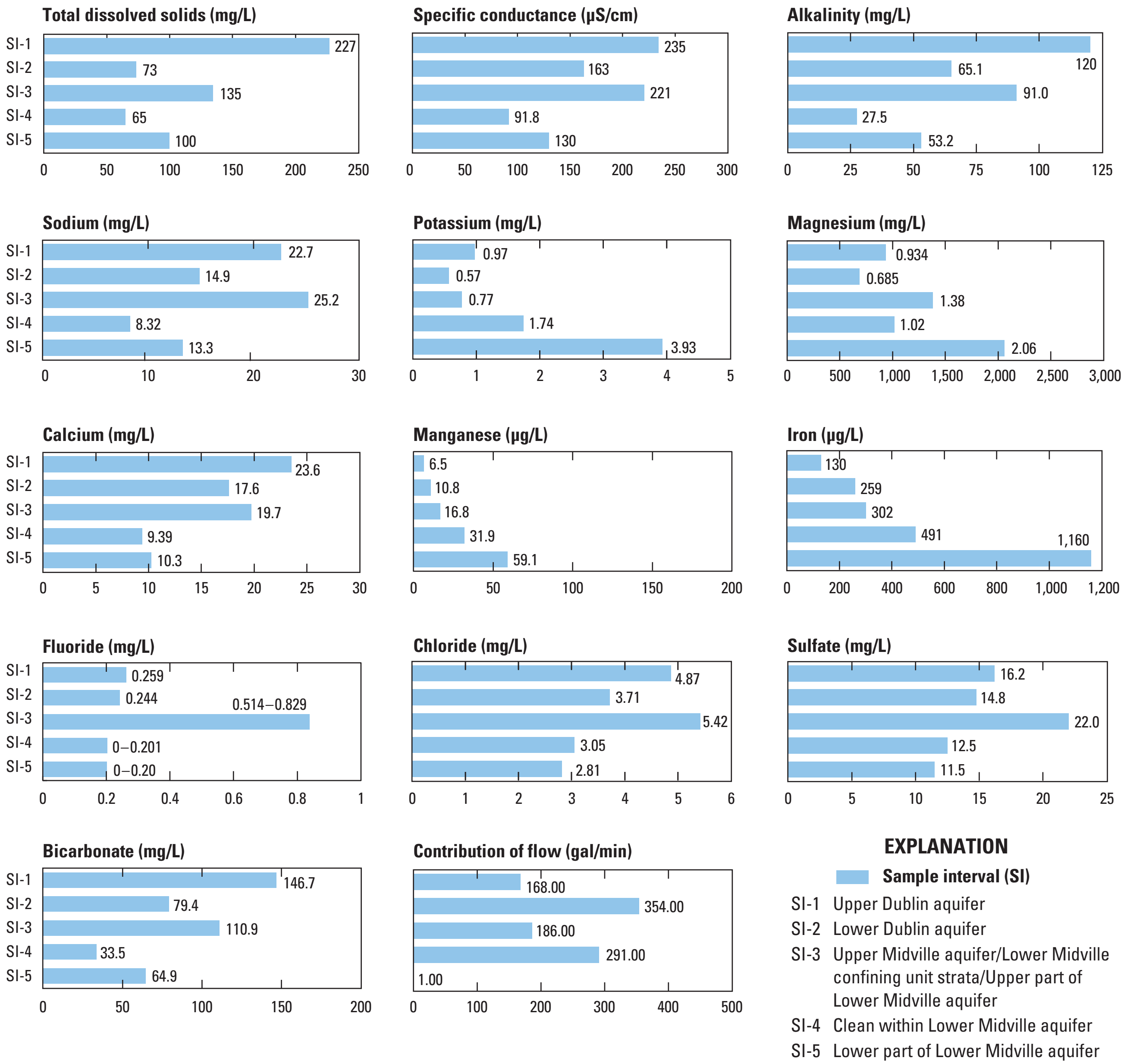


**Figure 4.** Water-quality values by sample interval. Sample interval locations are shown in figure 3. Ranges for fluoride in sample intervals are due to censored values in composite samples. [µS/cm, microsiemens per centimeter at 25 degrees Celsius; mg/L, milligrams per liter; µg/L, micrograms per liter]

## References


Clarke, J.S., Brooks, Rebekah, and Faye, R.E., 1985, Hydrogeology of the Dublin and Midville aquifer systems of east-central Georgia: U.S. Geological Survey Information Circular 74, 62 p.

Falls, W.F., Baum, J.S., Harrelson, L.G., Brown, L.H., and Jerden, J.L., Jr., 1997, Geology and hydrogeology of Cretaceous and Tertiary strata, and confinement in the vicinity of the U.S. Department of Energy Savannah River site, South Carolina and Georgia: U.S. Geological Survey, Water-Resources Investigations Report 97–4245, 125 p.

Kendall, Carol, and Caldwell, E.A., 1998, Fundamentals of isotope geochemistry, *in* Kendall, Carol, and McDonnell, J.J., eds., 1998, Isotope tracers in catchment hydrology: Amsterdam, The Netherlands, Elsevier Science B.V., 839 p.

U.S. Environmental Protection Agency, 1976, Quality criteria for water: Washington, D.C., EPA PB-263 943, 501 p.

U.S. Environmental Protection Agency, 2011, 2011 Edition of the drinking water standards and health advisories: Washington, D.C., EPA 820-R-11-002, 12 p.

# Geostatistical Estimation of Growing Season Irrigation Rates Using Monthly Metered Data, Middle-to-Lower Chattahoochee–Flint River Basin, Southwestern Georgia

By Lynn J. Torak and Jaime A. Painter

## Abstract

Metered irrigation-water-use data collected monthly during the 2012 growing season from a 100-site monitor network operated by the Georgia Soil and Water Conservation Commission were analyzed in a geostatistical framework to estimate irrigation depth in the middle-to-lower Chattahoochee–Flint River basin of southwestern Georgia. Kriging and conditional simulation yielded monthly irrigation-depth estimates within the basin on a regular orthogonal grid consisting of about 8,100 – 8,800 locations, depending on monthly data distributions. Spatial and temporal variabilities of irrigation depth were evidenced in the distinct patterning of simulated and measured monthly values and by their statistical moments. Estimation uncertainty related to monthly irrigation-depth estimates was assessed from the covariance of the kriging error resulting from conditional simulation. Geostatistical analysis enhanced understanding of the patterning and amount of irrigation water use at metered and non-metered sites in the basin and may help water managers develop efficient resource and conservation strategies statewide.

## Introduction

Since 2008, the U.S. Geological Survey (USGS), in cooperation with the Georgia Soil and Water Conservation Commission (Commission), has been investigating the spatial variability and patterning of agricultural irrigation in Georgia through the analysis of metered irrigation-water-use data. The Commission received a legislative mandate in June 2003 to "[implement] a program of measuring farm uses of water in order to obtain clear and accurate information on the patterns and amounts of such use, which information is essential to proper management of water resources by the state and useful to farms for improving the efficiency and effectiveness of their use of water… and [for] improving water conservation" (Georgia General Assembly, 2003). This paper describes how spatial and temporal patterns of irrigation water use were identified from geostatistical analysis of monthly meter readings collected during March to October 2012 at a monitor network of 100 irrigation sites located in the middle-to-lower Chattahoochee–Flint River basin of southwestern Georgia (fig. 1) and concludes with a discussion of the application of geostatistical methods to estimate irrigation water use statewide.

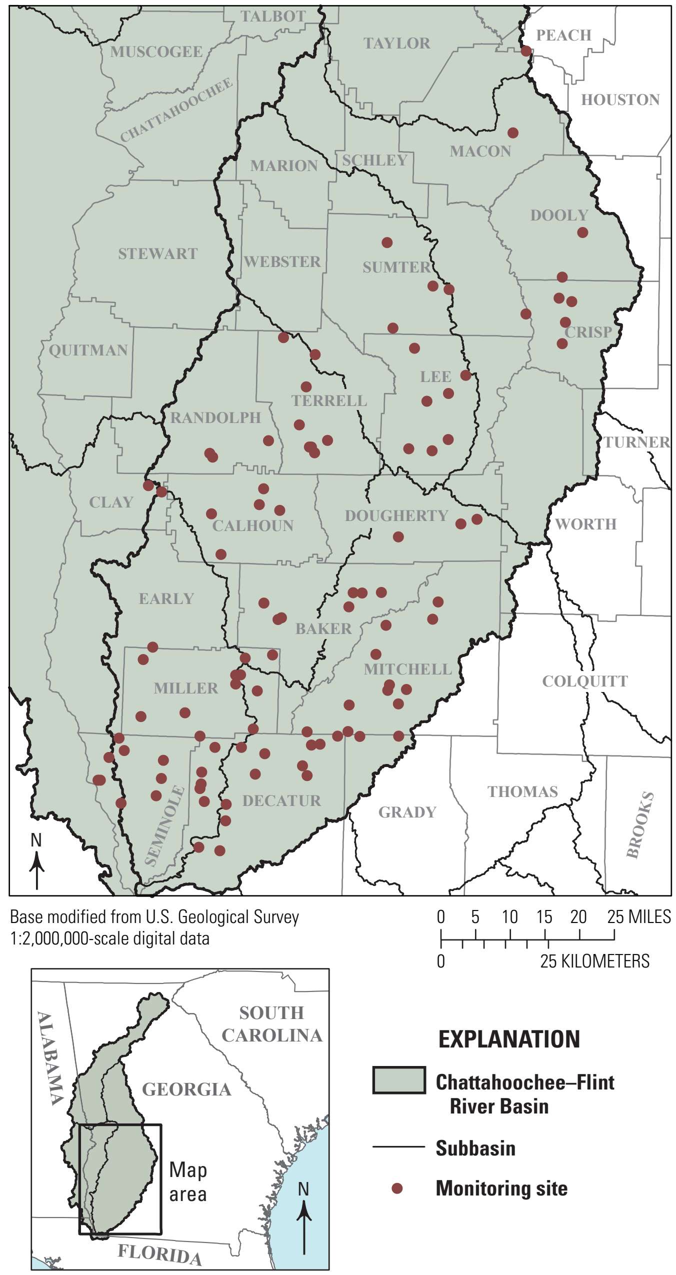


**Figure 1.** Location of metered irrigation network, subbasin boundaries, and counties contained in the middle-to-lower Chattahoochee–Flint River basin, southwestern Georgia.

Geostatistics is a collection of statistical techniques for the analysis of spatial data (Journel and Huijbregts, 1989). The statewide irrigation metering network established by the Commission generates a typical spatial dataset consisting of meter readings at permitted irrigation sites (Torak and Painter, 2011). Complex variations and processes related to soil, climate, crop pattern, and type of irrigation system all contribute to spatial variation of irrigation and introduce uncertainty in knowing specific details about irrigation water use at every agricultural field. Many of the water-related variables are spatial functions presenting complex variations that cannot be effectively described by simple deterministic functions. Geostatistics recognizes these difficulties and provides the statistical tools for calculating the most accurate predictions (estimation); quantifying the accuracy of these predictions; and selecting the parameters to be measured and where and when to measure them (Rouhani, 1989).

## Data Analysis

Monthly data from irrigation-water meters underwent a regimen of statistical analysis and normalization to render the meter readings suitable for use in geospatial models that estimated basinwide irrigation water use. Irrigated acres were factored from (divided into) meter readings of irrigation volume, measured in acre-inches, to obtain monthly values of “per-acre” irrigation depth, in inches. The irrigation-depth values were unaffected by field size, volume pumped, or water source (groundwater, including well-to-pond systems, and surface water), thus mitigating disparities among the various irrigation systems in operation at network metered sites and their corresponding water-use data. Statistical moments (mean, variance, skewness, and kurtosis) of the raw (non-transformed) and log-transformed irrigation-depth data identified monthly variations in irrigation water use at the network metered sites (table 1) and identified the utility of log transformation in normalizing the skewed irrigation-depth distributions prior to geostatistical analysis.

Spatial correlation and estimation of monthly irrigation depth were evaluated in a framework of geostatistical modeling involving structural analysis, variogram development, interpolation (kriging), and conditional simulation (Journel and Huijbregts, 1989). A description of these geostatistical techniques is given in Torak and Painter (2011), where these techniques were applied successfully to annual metered irrigation-depth data in the study area for the 2007 growing season. These geostatistical techniques were applied in the same manner to the 2012 growing season to analyze and estimate monthly irrigation depth for the 2012 growing season.

Structural analysis involved assessing the statistical structure of the normalized monthly irrigation-depth data through an evaluation of the first two statistical moments of the data, namely the mean and covariance (or the semivariogram)

**Table 1.** Statistics for monthly metered irrigation depth, middle-to-lower Chattahoochee–Flint River basin, southwestern Georgia, March–October 2012.

[minimum, maximum, and mean irrigation depth in inches; variance in inches squared; skewness and kurtosis, dimensionless]

| Statistic | March | April | May | June | July | August | September | October |
|---|---|---|---|---|---|---|---|---|
| N (values) | 38 | 44 | 74 | 77 | 81 | 64 | 33 | 26 |
| Raw (non-transformed) irrigation depth | | | | | | | | |
| Minimum | 0.20 | 0.11 | 0.19 | 0.17 | 0.22 | 0.19 | 0.10 | 0.06 |
| Maximum | 4.13 | 5.20 | 11.97 | 9.92 | 10.71 | 3.74 | 5.68 | 5.35 |
| Mean | 1.19 | 1.41 | 2.54 | 1.99 | 3.33 | 1.46 | 1.42 | 1.15 |
| Variance | 0.98 | 1.42 | 5.16 | 2.97 | 3.08 | 0.84 | 2.13 | 1.84 |
| Skewness | 1.31 | 1.37 | 1.76 | 2.34 | 1.05 | 0.69 | 1.53 | 2.12 |
| Kurtosis | 0.77 | 1.37 | 3.29 | 7.11 | 2.89 | −0.34 | 1.57 | 3.79 |
| Log-transformed irrigation depth | | | | | | | | |
| Mean | −0.13 | −0.00 | 0.57 | 0.38 | 1.03 | 0.15 | −0.15 | −0.42 |
| Variance | 0.60 | 0.78 | 0.78 | 0.65 | 0.44 | 0.55 | 1.14 | 1.13 |
| Skewness | 0.30 | −0.20 | −0.19 | −0.19 | −1.36 | −0.59 | −0.08 | −0.06 |
| Kurtosis | −0.83 | −0.52 | −0.24 | −0.02 | 2.55 | −0.25 | −0.77 | −0.56 |

(American Society of Civil Engineers Task Committee on Geostatistical Techniques in Geohydrology, 1990). Monthly irrigation-depth data ($Z$) are spatially correlated based on the separation distance ($h$) between pairs of data ($z_i$ and $z_{i+h}$, which are elements of $Z$) and their difference ($z_i - z_{i+h}$), where "$i$" indexes each irrigation-depth value. The semivariance, $\gamma(h)$, accounts for the difference in values ($z_i - z_{i+h}$) between all $N(h)$ data pairs in the distance-class interval $h$ as

$$\gamma(h) = \frac{\sum_{i=1}^{n}(z_i - z_{i+h})^2}{2N(h)}$$

A plot of average semivariance by average separation distance for each distance class of monthly irrigation-depth data constituted the experimental semivariogram (fig. 2), which represents the spatial-correlation structure of the irrigation-depth data.

Structural analysis was completed by fitting a simple mathematical function (exponential curve in figure 2) to each monthly experimental semivariogram to produce a variogram model. Strong spatial correlation exists between monthly irrigation-depth data that are separated by distances that correspond with the curved part of the variogram model. The range represents the maximum separation distance between irrigation-depth pairs that maintain spatial correlation, determined graphically from the variogram model (fig. 2, table 2). Conversely, no spatial correlation exists between irrigation-depth data that are separated by distances corresponding with the horizontal part of the variogram model or by distances larger than the range.

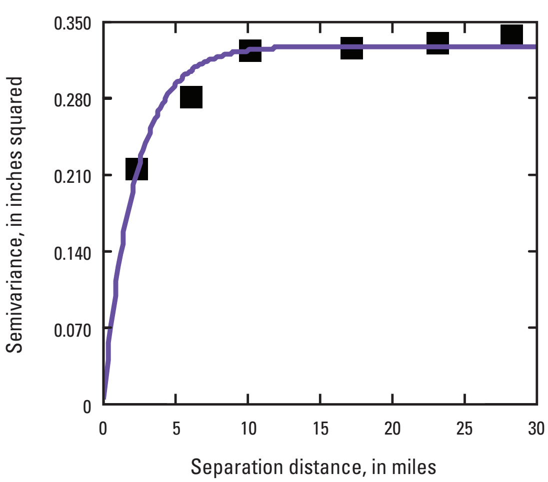


**Figure 2.** Experimental variogram (solid squares) and exponential variogram model (curve) for normalized July 2012 irrigation-depth values, middle-to-lower Chattahoochee–Flint River basin, southwestern Georgia.

**Table 2.** Geostatistical characteristics of monthly irrigation-depth data, middle-to-lower Chattahoochee–Flint River basin, southwestern Georgia, March–October 2012.

[ft, foot; Cov, kriging error, covariance of the kriging error derived from conditional simulation; ft$^2$, foot squared]

| Month | Variogram model | Range (ft) | Cov, kriging error (ft$^2$) |
|---|---|---|---|
| March | Exponential | 30,500 | 0.3211 |
| April | Exponential | 26,000 | 0.3886 |
| May | Spherical | 49,300 | 7.171 |
| June | Exponential | 25,400 | 1.018 |
| July | Exponential | 35,400 | 3.514 |
| August | Exponential | 31,500 | 0.8783 |
| September | Spherical | 30,200 | 1.353 |
| October | Spherical | 59,400 | 3.544 |

Monthly variogram models of irrigation depth from the 100-site monitor network were used in a linear-interpolation process (kriging) to estimate irrigation depth within the study area for the 2012 growing season. Kriging provided unbiased estimates for the expected values of the spatial variable (for example, irrigation depth) as a weighted sum of the measured data having minimum estimation variance (American Society of Civil Engineers Task Committee on Geostatistical Techniques in Geohydrology, 1990). Conditional simulation utilized the exact interpolation properties of kriging with the monthly variogram models to produce synthetic spatial distributions of irrigation depth over the study area (fig. 3). Monthly distributions of irrigation depth were calculated on a square grid containing about 8,100–8,800 points, depending on the distribution of the monthly data.

Measured values of irrigation depth at the monitor-network sites were used along with estimates derived from conditional simulation to analyze the uncertainty inherent to estimating the spatial distribution of irrigation depth in the middle-to-lower Chattahoochee-Flint River basin. The exact interpolation properties of kriging used in conditional simulation allowed the "simulated" values at the monitor-network sites to equal the measured values at those sites. For many realizations performed during conditional simulation—in this case, 1,000 simulations at each location on the interpolation grid—the covariance of the simulated monthly irrigation depths equaled the covariance of the kriging error (Journel and Huijbregts, 1989) (table 2). In this manner, a measure of the estimation accuracy, or uncertainty, is obtained from the covariance derived from conditional simulation of monthly irrigation depth.

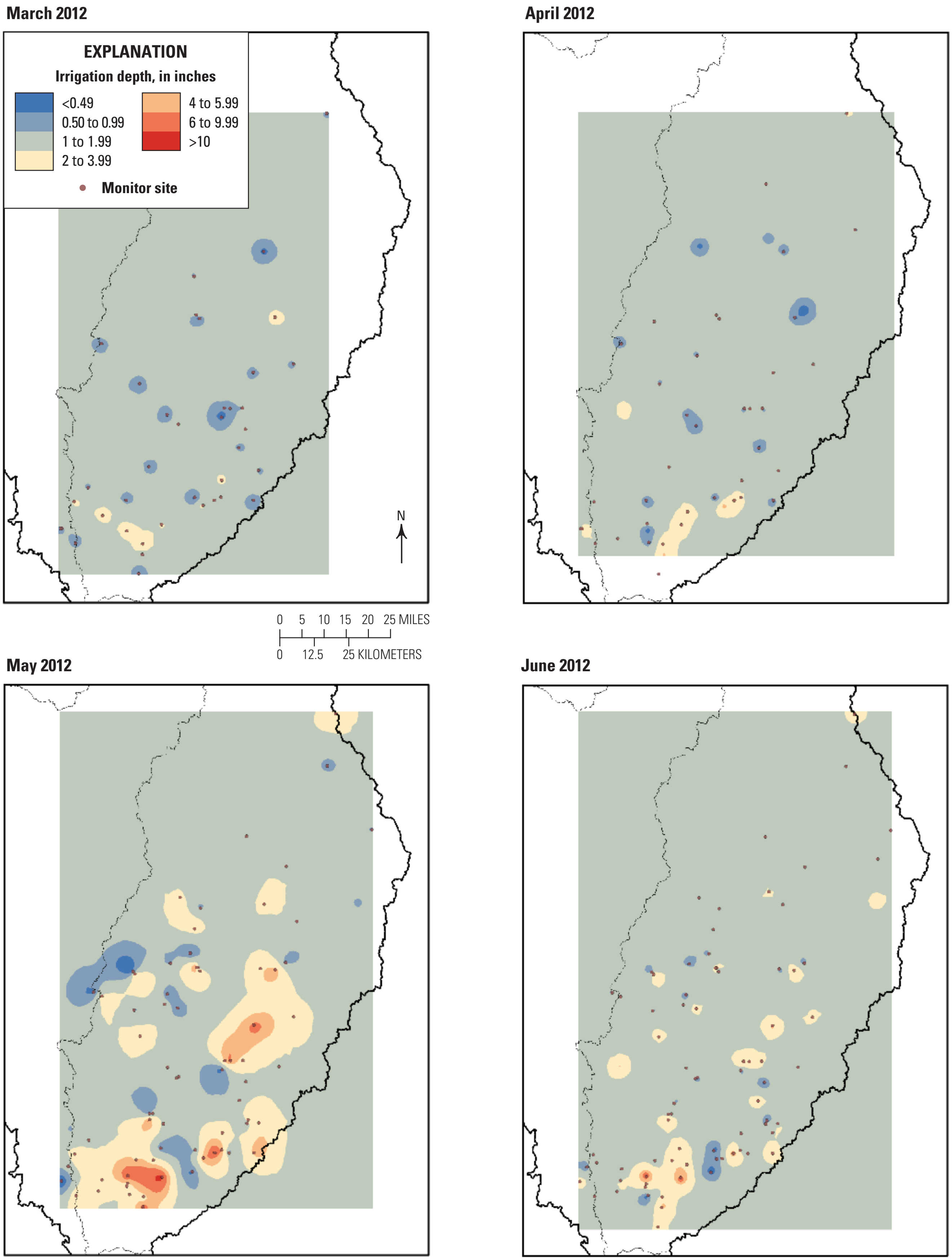


**Figure 3.** Estimated irrigation-depth for the 2012 growing season from conditional simulation based on monthly meter data and variogram models for the middle-to-lower Chattahoochee–Flint River basin, southwestern Georgia.

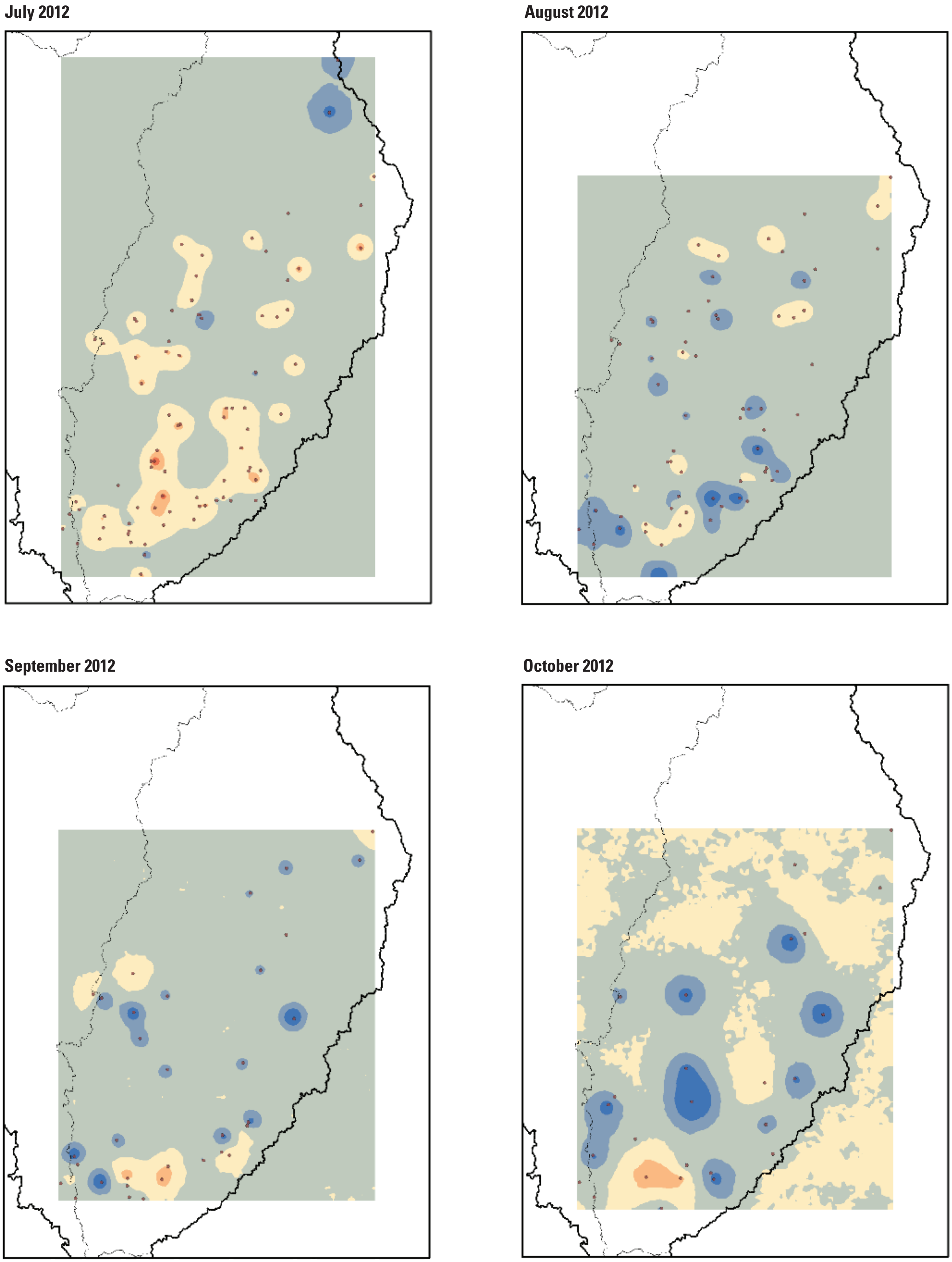


**Figure 3.** Estimated irrigation-depth for the 2012 growing season from conditional simulation based on monthly meter data and variogram models for the middle-to-lower Chattahoochee–Flint River basin, southwestern Georgia.—Continued

## Monthly Irrigation Depth During 2012 Growing Season

Basinwide maps showing monthly estimates of irrigation depth derived from conditional simulation and monthly variogram models (fig. 3) provide a means to identify spatial patterning of irrigation that is not possible when using classical statistical evaluation. Simple comparisons of mean estimated irrigation depths during the growing season (fig. 4) cannot address spatial variability in monthly patterning of irrigation water use; the mean values contain no measure of spatial relevance. Furthermore, the narrow range of average monthly irrigation-depth values for the basin during the 2012 growing season—1.33 to 1.77 inches—implies that irrigation water use is fairly constant within the basin; however, spatial patterning of irrigation depth evident on the monthly maps proves otherwise. Changes in patterns of irrigation water use in the basin during the growing season indicate irrigation of specific crops, such as high irrigation of corn during May and June. The migration of high irrigation rates within the basin during the growing season could indicate high irrigation of other crops or delayed harvesting of corn due to delayed planting, for example.

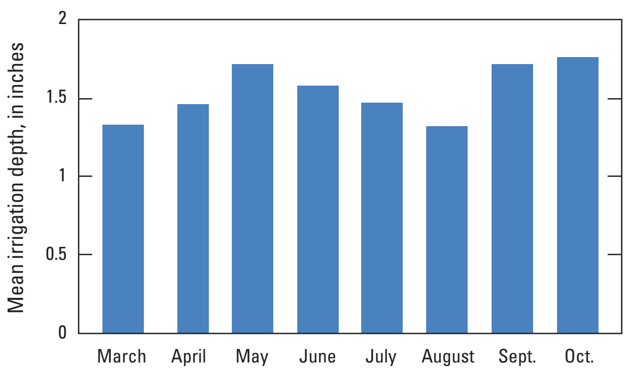


**Figure 4.** Mean irrigation depth by growing season month, derived from conditional simulation, middle-to-lower Chattahoochee–Flint River basin, 2012

## Conclusions

Geostatistical analysis can enhance understanding of the patterning and amount of irrigation water use derived from the statewide network of metered irrigation data collected by the Georgia Soil and Water Conservation Commission. Variogram modeling can be used to identify statistical structure within the irrigation-depth data and can be used to measure the spatial correlation between monitor-network locations, which is a necessary prerequisite for interpolation (estimation) of irrigation depth at non-metered irrigation sites. Insight gained from structural analysis can help water managers design efficient monitor networks that achieve accurate representation of irrigation water use with a minimum number of observations. Detailed distributions of metered and unmetered irrigated acres for a specific agricultural region can be combined with a corresponding distribution of irrigation-depth estimates obtained from conditional simulation to estimate irrigation volume and water use. Knowledge of the patterning and amount of irrigation water use made possible through geostatistical analysis of metered irrigation-water-use data may contribute valuable insight toward assessing Georgia's water resources and may assist water managers and scientists in developing future resource and conservation strategies.

## References

American Society of Civil Engineers Task Committee on Geostatistical Techniques in Geohydrology, 1990, Review of geostatistics in geohydrology—I. Basic concepts: Journal of Hydraulic Engineering, v. 116, no. 5, p. 612–632.

Georgia General Assembly, 2003, Georgia General Assembly HB579—Water resources; farm uses; water-measuring device, Atlanta, Georgia, accessed March 23, 2010, at *http://www.legis.state.ga.us/legis/2003_04/search/hb579.htm*.

Journel, A.J., and Huijbregts, C.J., 1989, Mining geostatistics: New York, NY, Academic Press, 600 p.

Rouhani, Shahrokh, 1989, Geostatistics in water resources, *in* Hatcher, K.J., ed., Proceedings of the 1989 Georgia Water Resources Conference, May 16 and 17, 1989, The University of Georgia, Athens, Georgia, p. 169–171.

Torak, L.J., and Painter, J.A., 2011, Summary of the Georgia Agricultural Water Conservation and Metering Program and evaluation of methods used to collect and analyze irrigation data in the middle and lower Chattahoochee–Flint River basins, 2004–2010: U.S. Geological Survey Scientific Investigations Report 2011–5126, 26 p.

# Using Conventional Borehole Geophysical Logs to Map Salinity Variations in Carbonate-Rock Aquifer Systems of the Southeastern United States

By Lester J. Williams and Jessica E. Raines

## Abstract

Conventional borehole geophysical logs, collected mostly from oil and gas test wells, are often the only means available for mapping regional salinity variations in an aquifer system. When geophysical log calculations are made to estimate total dissolved solids in a single well, the results are of interest locally, but when applied to a larger number of wells such calculations can be a valuable tool to help establish salinity patterns in a regional aquifer system and for mapping the approximate position of freshwater/saltwater interface. In 2012, the U.S. Geological Survey completed a mapping study using approximately 550 wells to assess brackish-water resources in the southeastern United States (fig. 1). Challenges in using well logs to estimate salinity include (1) understanding which intervals along the log should be used to calculate total dissolved solids; (2) estimating missing porosity values; (3) determining lithologic influences on the log response; (4) selecting appropriate coefficients for the most common types of equations used and computing the formation-water resistivity; and (5) computing and correcting formation-water resistivity to account for local variations in geothermal gradients and water chemistry (fig. 2).

Although different approaches to log analysis were used during the study, for mapping purposes in carbonate-rock aquifers, the overall log response was reviewed to focus analysis on intervals where a freshwater-to-saltwater profile needed to be defined. In the example log (fig. 3), a gradual decrease in the deep-reading resistivity curve (ILD) between 600 and 750 feet below land surface is an indication of increasing salinity with depth in the carbonate rocks of the Floridan aquifer system. After identifying the approximate interval for analysis, a limited number of values were tabulated along the logs to define the salinity profile (table 1). Indiscriminate selection of resistivity and porosity values were avoided because poor hole condition (washed out intervals) and thin resistive beds in carbonate-rock aquifers commonly produce erroneous results in calculations of total dissolved solids (see thin-bed effect on “quick-look” total dissolved-solids curve, fig. 3). Adjusting values for lithologic effects and selection of values for the cementation factor, m, and for tortuosity, a, were important considerations in the quantitative analysis but did not significantly affect the position of the overall transition zone from fresh to saline water on a regional scale. Once the depths of the various concentrations levels were mapped in each borehole, maps were produced depicting the altitude of the 10,000-milligram-per-liter boundary and other boundaries needed to define brackish-water resources in the southeastern United States.

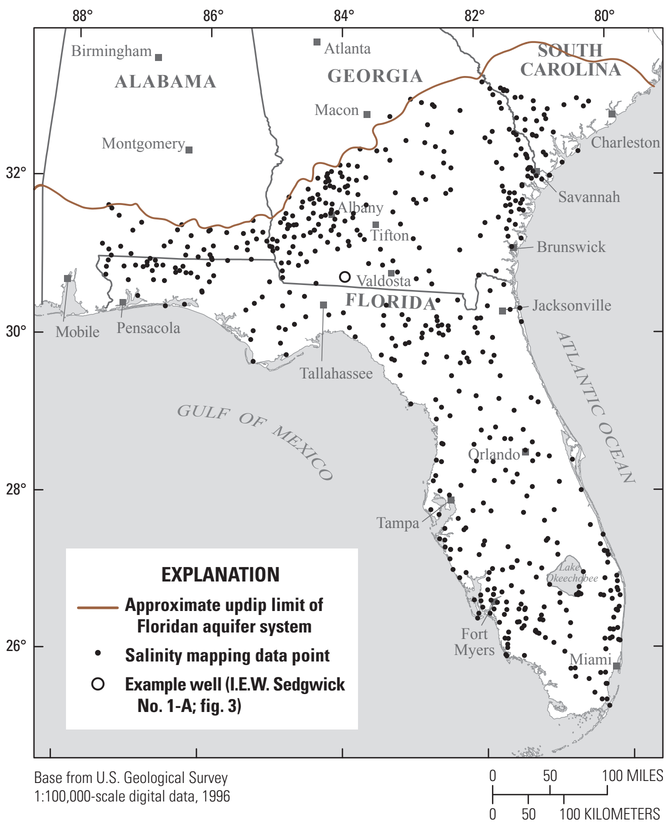


**Figure 1.** Location of wells used to map salinity variations in the Floridan aquifer system, southeastern United States.

## Referenced Cited

Archie, G.E., 1942, The electrical resistivity log as an aid in determining some reservoir characteristics: American Institute of Mining and Metallurgical Engineers Transactions, v. 146, p. 54–62.

Arps, J.J., 1953, Technical Note 195: Journal of Petroleum Geology, v. sec. 1, p. 18.

Asquith, G. and Krygowski, D., 2004, Basic Well Log Analysis for Geologists, AAPG Methods in Exploration Series, No. 16, 2nd ed.: The American Association of Petroleum Geologists, Tulsa, Oklahoma.

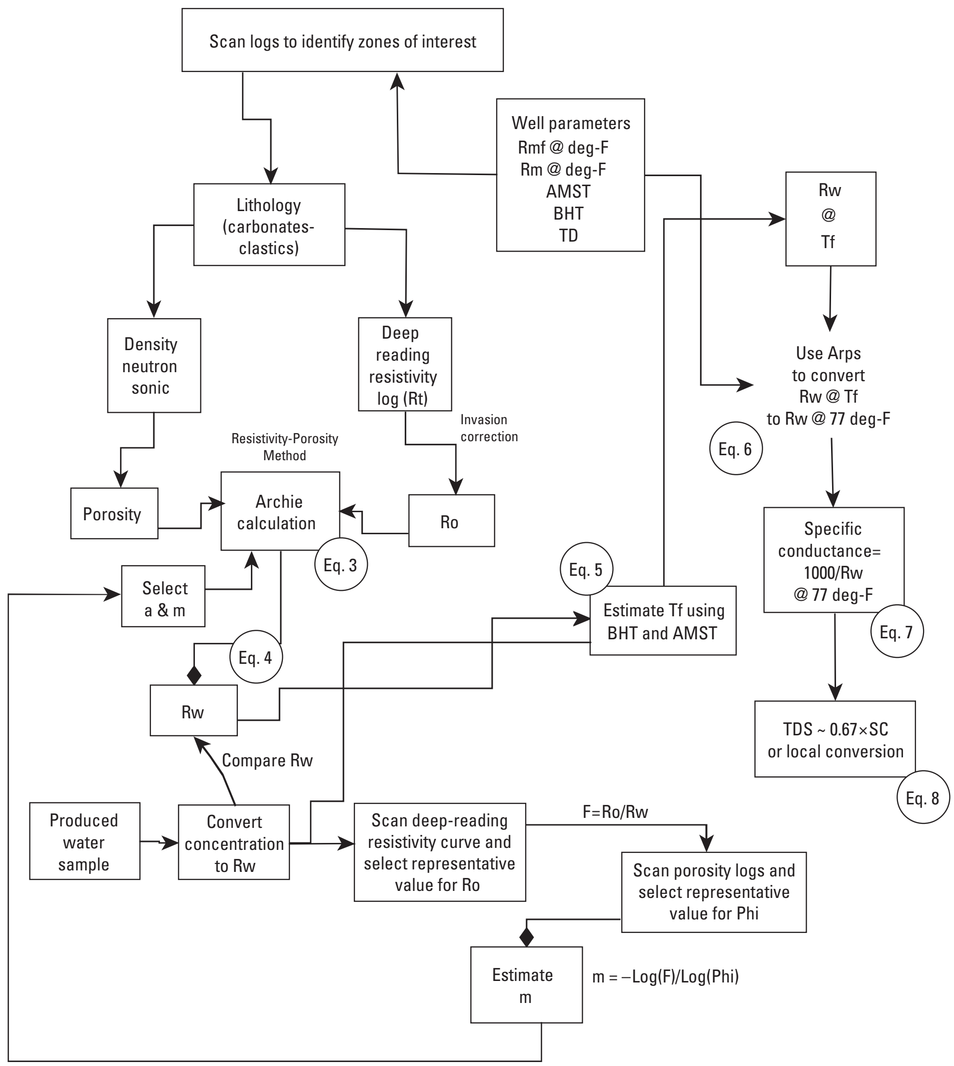


## EXPLANATION

**Abbreviations used**

a, tortuosity
m, cementation factor
F, formation factor
Rt, deep reading resistivity value
Ro, true resistivity
Rw, resistivity of the formation water
SC, specific conductance
Phi, porosity
deg-F, degrees Fahrenheit
Tf, formation temp
Rmf, resistivity of mud filtrate
Rm, resistivity of mud
AMST, annual mean surface temperature
BHT, bottom hole temperature
TD, total depth
TDS, total dissolved solids
Arps, arps equation (see equation 6)
Eq., refers to equations on facing page

Note: Equations 1 and 2 (facing page) are the general forms of Archie's Law and are not shown on the flow chart

**Figure 2.** Flow chart showing general process of conducting log analysis using the resistivity-porosity method (equations on facing page).

Notes:

Archie (1942) defines the formation resistivity factor (formation factor) as the ratio of the formation resistivity (from logs) and the resistivity of the water contained in the formation

$$F = \frac{R_0}{R_w} \ , \qquad (1)$$

Where
- $F$ is formation resistivity factor (dimensionless),
- $R_o$ is resistivity of the water-saturated formation (ohmmeters), and
- $R_w$ is resistivity of the formation water occupying pores (ohmmeters).

↓

The formation factor also is related to the physical properties of the rock. Coefficients *m* and *a* are usually selected from previously published values. If a produced water sample from a known interval is provided then the value of *m* can be calculated by setting the value of *a* to 1.

$$F = \frac{a}{\Phi^m} \ , \qquad (2)$$

Where
- $m$ is cementation factor (dimensionless), which varies with grain size and grain-size distribution;
- $a$ is tortuosity (dimensionless), which describes the complexity of the paths in the pores as the ratio of actual path length to straight path length; and
- $\Phi$ is porosity, which is given in percent.

↓

Select appropriate coefficients (see table at right) to calculate formation factor, insert value of porosity from available logs. If porosity is not available estimate the value from nearby wells.

$$F = \frac{1.0}{\Phi^{2.0}} \ , \qquad (3)$$

Coefficients used to calculate formation factor (F). (Modified after Asquith and Krygowski, 2004)

| *a* | *m* | Comments |
|---|---|---|
| 1 | 2 | Carbonates |
| 0.81 | 2 | Consolidated sandstones |
| 0.62 | 2.15 | Unconsolidated sands (Humble formula) |
| 1.45 | 1.54 | Average sands |
| 1.65 | 1.33 | Shaly sands |
| 1.45 | 1.7 | Calcareous sands |
| 0.85 | 2.14 | Carbonates |
| 1 | $\Phi^{(2.05-\Phi)}$ | Clean granular formations |

↓

Divide resistivity values obtained from geophysical log by the formation factor to estimate Rw. The resulting values are "apparent" water resistivity that is further adjusted for formation temperature.

$$R_w = \frac{R_o}{F} \ , \qquad (4)$$

↓

Estimate the formation temperature (Tf) using bottom hole temperature (BHT) and annual mean surface temperature (AMST). The BHT is obtained from the log header or from a nearby well. AMST is determined from climatic data.

$$T_f = \left(\frac{BHT - AMST}{TD} \times FD\right) + AMST \ , \qquad (5)$$

Where
- $T_f$ is formation temperature (degrees Fahrenheit [deg-F]),
- $BHT$ is bottom hole temperature (deg-F),
- $AMST$ is annual mean surface temperature (deg-F),
- $TD$ is total depth (feet), and
- $FD$ is formation depth (feet).

↓

Calculate the adjusted water resistivity using the Arps equation (Arps, 1953)

$$Rw_{77} = \frac{R_0(T_f + 6.77)}{77 + 6.77} \ , \qquad (6)$$

↓

Convert Rw77 to specific conductance

$$SC = \frac{10{,}000}{Rw_{77}} \ , \qquad (7)$$

↓

Estimate total dissolved solids by multiplying specific conductance by a local or regional factor. A factor of 0.67 can be used for rocks of the Southeastern Coastal Plain (see graph at right)

$$TDS = (0.67 \times SC) \qquad (8)$$

Relation of specific conductance and total dissolved solids Southeastern Coastal Plain aquifer system (258 well samples)

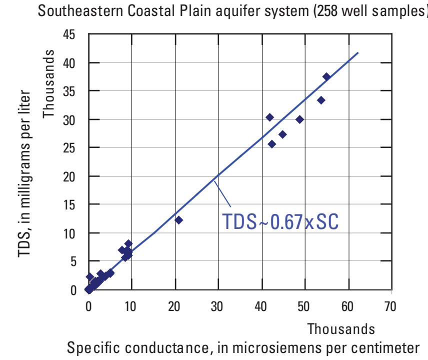

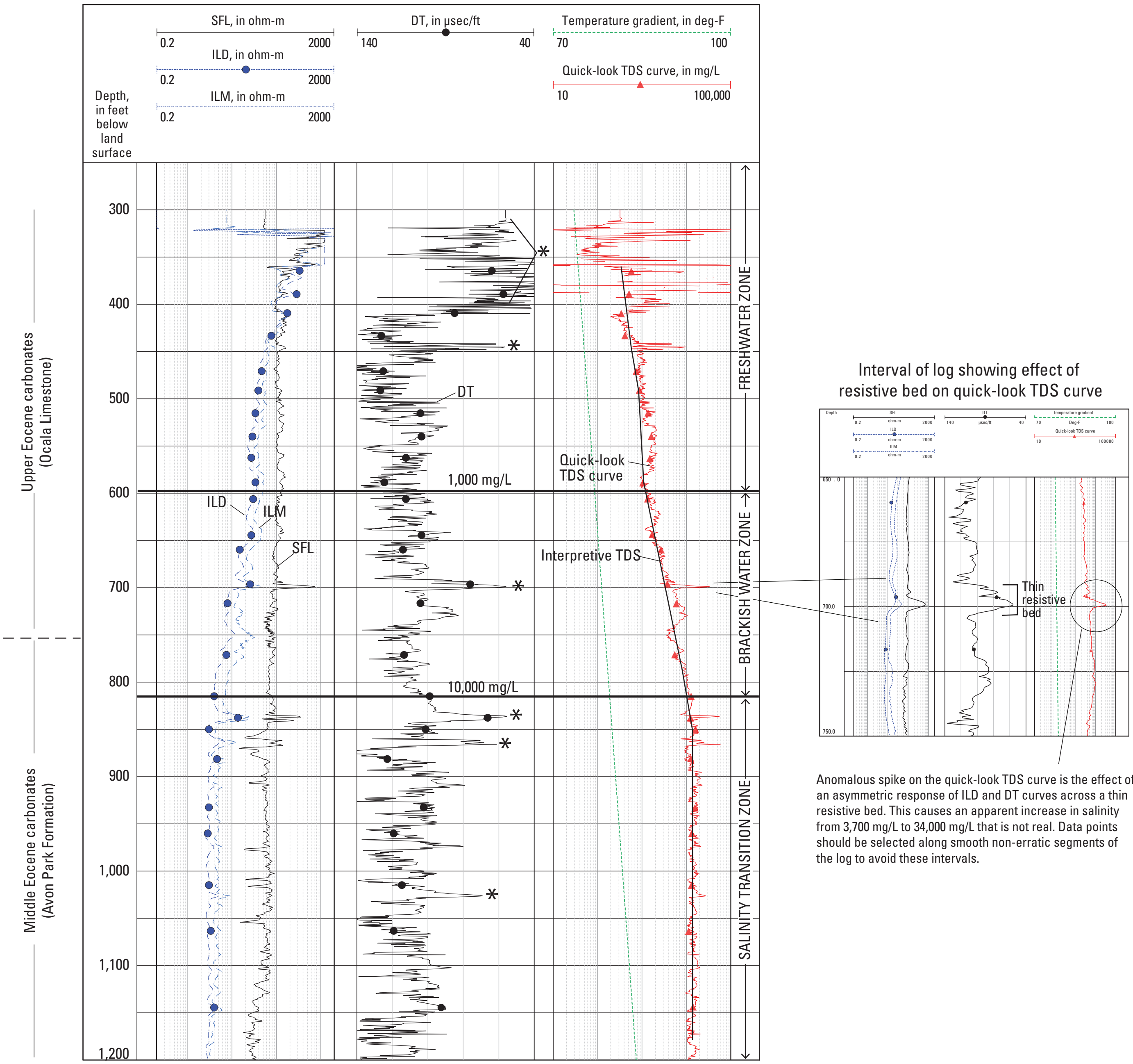


**EXPLANATION**

- **Deep induction resistivity value selected**
- **DT value selected**
- **Calculated TDS for selected induction resistivity and DT values**
- **Thin resistive (low-porosity) bed**

**Figure 3.** Example calculation of estimated total dissolved solids in well I.E.W. Sedgwick No.1-A in Thomas County, Georgia. [See fig. 1 for location; DT, interval transit time; ILD, induction log deep; ILM, induction log medium; SFL, spherically focused log; TDS, total dissolved solids concentration; mg/L, milligrams per liter; ohm-m, ohm-meters; µs/ft, microseconds per foot, Deg-F, degrees Fahrenheit]

**Table 1.** Calculation of formation factor and estimated total dissolved solids from well-log data, I.E.W. Sedgwick No.1-A, Thomas County, Georgia.

[ft bls, feet below land surface; ILD, deep induction resistivity; SPHI, sonic porosity; F, formation factor; Rw, formation water resistivity; Tf, formation temperature; Rw77, formation water resistivity adjusted to 77 degrees Fahrenheit; SC, specific conductance; TDS, total dissolved solids; ohm-m, ohm meter; deg-F, degrees Fahrenheit; µS/cm, microsiemens per centimeter at 25 degrees Celsius; mg/L, milligrams per liter]

| Depth (ft bls) | Log data | | Eq. 3 | Eq. 4 | Eq. 5 | Eq. 6 | Eq. 7 | Eq. 8 |
|---|---|---|---|---|---|---|---|---|
| | ILD (ohm-m) | SPHI (percent) | F | Rw (ohm-m) | Tf (deg-F) | Rw77 (ohm-m) | SC (µS/cm) | TDS (mg/L) |
| 365 | 333 | 0.15 | 32.03 | 10.40 | 79.0 | 10.7 | 939 | 569 |
| 389 | 286 | 0.17 | 24.82 | 11.51 | 79.3 | 11.8 | 846 | 505 |
| 410 | 176 | 0.26 | 10.98 | 16.07 | 79.5 | 16.5 | 605 | 339 |
| 433 | 77 | 0.38 | 5.65 | 13.72 | 79.7 | 14.2 | 706 | 408 |
| 471 | 47 | 0.38 | 5.70 | 8.19 | 80.2 | 8.5 | 1,177 | 732 |
| 491 | 39 | 0.38 | 5.61 | 6.99 | 80.4 | 7.3 | 1,375 | 868 |
| 515 | 34 | 0.33 | 7.32 | 4.60 | 80.6 | 4.8 | 2,084 | 1,356 |
| 540 | 29 | 0.33 | 7.39 | 3.90 | 80.9 | 4.1 | 2,448 | 1,606 |
| 563 | 27 | 0.35 | 6.54 | 4.16 | 81.2 | 4.4 | 2,288 | 1,496 |
| 589 | 34 | 0.38 | 5.73 | 5.87 | 81.4 | 6.2 | 1,618 | 1,036 |
| 606 | 30 | 0.35 | 6.54 | 4.58 | 81.6 | 4.8 | 2,067 | 1,344 |
| 644 | 27 | 0.33 | 7.39 | 3.68 | 82.1 | 3.9 | 2,560 | 1,683 |
| 660 | 15 | 0.36 | 6.41 | 2.34 | 82.2 | 2.5 | 4,025 | 2,690 |
| 696 | 26 | 0.22 | 14.97 | 1.72 | 82.6 | 1.8 | 5,461 | 3,677 |
| 717 | 7.9 | 0.33 | 7.32 | 1.08 | 82.8 | 1.2 | 8,625 | 5,852 |
| 771 | 7.5 | 0.35 | 6.45 | 1.16 | 83.4 | 1.2 | 8,006 | 5,426 |
| 815 | 4.0 | 0.32 | 7.98 | 0.50 | 83.9 | 0.5 | 18,601 | 12,709 |
| 838 | 14 | 0.16 | 26.35 | 0.52 | 84.2 | 0.6 | 17,843 | 12,189 |
| 850 | 3.0 | 0.32 | 7.67 | 0.39 | 84.3 | 0.4 | 23,311 | 15,947 |
| 881 | 2.9 | 0.38 | 5.83 | 0.50 | 84.6 | 0.5 | 18,411 | 12,579 |
| 933 | 3.0 | 0.33 | 7.54 | 0.40 | 85.2 | 0.4 | 22,687 | 15,518 |
| 960 | 2.9 | 0.37 | 6.04 | 0.47 | 85.5 | 0.5 | 19,197 | 13,119 |
| 1,015 | 3.0 | 0.36 | 6.36 | 0.48 | 86.1 | 0.5 | 18,948 | 12,948 |
| 1,064 | 3.3 | 0.37 | 6.04 | 0.55 | 86.6 | 0.6 | 16,255 | 11,097 |
| 1,144 | 4.0 | 0.29 | 9.08 | 0.44 | 87.5 | 0.5 | 20,348 | 13,910 |

Approved November 20, 2013

Prepared by the USGS Science Publishing Network
Raleigh Publishing Service Center
Illustrations and layout by Caryl J. Wipperfurth

For more information concerning this report, contact:
Director
U.S. Geological Survey
Georgia Water Science Center
1770 Corporate Drive, Suite 500
Norcross, Georgia 30093
dc_ga@usgs.gov

or visit our Web site at:
http://ga.water.usgs.gov/

Clarke and Dalton—**Hydrologic Monitoring and Selected Hydrologic and Environmental Studies by the U.S. Geological Survey in Georgia, 2011–2013**—Open-File Report 2013–1278

ISSN 2331-1258 (online)
*http://dx.doi.org/10.3133/ofr20131278*